SIMULATION OF RUNOFF AND FLOOD INUNDATION IN KOSI RIVER BASIN USING HYDROLOGICAL MODELS, ANN, REMOTE SENSING AND GIS

A THESIS SUBMITTED IN PARTIAL FULFILLMENT OF THE
REQUIREMENTS FOR THE DEGREE OF

Master of Technology (Research)

In

Civil Engineering

By

RAY SINGH MEENA

Under the guidance of

Dr. Ramakar Jha

Dr. K.K. Khatua

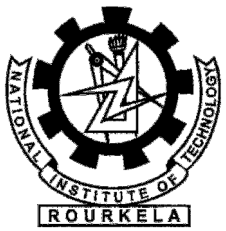

Department of Civil Engineering
National Institute of Technology
Rourkela-769008
October-2012

National Institute of Technology Rourkela

Rourkela-769008

CERTIFICATE

This is to certify that the thesis entitled, "**Simulation of Runoff and Flood Inundation in Kosi River Basin using Hydrological models, ANN, Remote Sensing and GIS" s**ubmitted by **Shree RAY SINGH MEENA** a part of requirements for the award of **Master of Technology (Research)** Degree in Civil Engineering at the National Institute of Technology, Rourkela is an authentic work carried out by him under our supervision and guidance.

To the best of our knowledge, the matter embodied in the thesis has not been submitted to any other University/ Institute for the award of any Degree or Diploma.

Date:

Place: Rourkela

(Dr. Ramakar Jha)
Professor
Department of Civil Engineering
National Institute of Technology
Rourkela-769008

(Dr. K. K. Khatua)
Associate Professor
Department of Civil Engineering
National Institute of Technology
Rourkela-769008

ACKNOWLEDGEMENT

I would like to express my sincere gratitude to Prof. Ramakar Jha and Prof. K. K. Khatua for their invaluable inputs, guidance, cooperation and constant encouragement during the course of the project. I truly appreciate their esteemed guidance and encouragement from beginning to the end of the thesis, their knowledge and company at the time of crisis would be remembered lifelong.

I am extremely grateful to Prof. S. K. Sarangi, our esteemed Director for blessing me with all the facilities in M.Tech (Research) programme.

I am also grateful to Prof. M. Panda, Dean (SRICC) for providing me all facilities during data collection for project work.

I am grateful to Prof. N. Roy, Head of the Civil Engineering Department, National Institute of Technology, Rourkela for providing all kinds of help and support.

I express my deep sense of gratitude to the member of my Master Scrutiny Committee Prof. A. Kumar and Prof. K.C. Biswal of Civil Engineering Department and Prof R. K. Singh of Chemical Engineering Department. I am thankful to Prof. K.C. Patra, Prof. S.P. Singh, Prof. S.K. Sahu, Prof. S.K. Das, Prof. M.R. Barik, Prof. C.R. Patra and all the professors of Civil Engineering Department for their valuable suggestions and instructions and encouragements at various stages of work. I am also thankful to my friends, Laboratory Assistants and other staff of Civil Engineering Department N.I.T., Rourkela for their helping hands during the project.

Lastly, I would like to express my heedful gratitude to my parents and family members for their ever support for their loving son in all respect.

Date:

Place: Rourkela

(RAY SINGH MEENA)
(Roll No. - 609CE301)
Department of Civil Engineering
National Institute of Technology
Rourkela-769008

TABLE OF CONTENTS

LIST OF FIGURES

LIST OF TABLES

LIST OF ABBREVIATIONS

Particular	Description
1-D	One Dimensional
2-D	Two Dimensional
3-D	Three Dimensional
AMC	Antecedent Moisture Condition
ANN	Artificial Neural Network
AWiFS	Advanced Wide Field Sensor
BFGS	Broyden-Fletcher-Goldfarb-Shanno
CWC	Central Water Commission
DEM	Digital Elevation Model
DMD	Disaster Management Department
DTM	Digital Terrain Model
ESRI	Environmental Systems Research Institute
FMIS	Flood Management Information System
GFCC	Ganga Flood Control Commission
GIS	Geographic Information System
GeoHMS	Geospatial Hydrologic Modelling System
GeoRAS	Geospatial River Analysis System
HEC	Hydrologic Engineering Center
HMS	Hydrologic Modelling System
IMD	Indian Metrological Department
ISRO	Indian Space Research Organization
km	Kilometer
m	Meter
MLP	Multilayer Perceptron
msl	Mean Above Sea Level
NBSS &LUP	National Bureau of Soil Survey and Land Use Planning
NOAA	National Oceanic and Atmospheric Administration
NRSA	National Remote Sensing Agency
NRCS	Natural Resources Conservation Service
RAS	River Analysis System
RBF	Radial Basis Function
SCS-CN	Soil Conservation Service-Curve Number
SOS	Sum of Squares
SRTM	Shuttle Radar Topography Mission
TRMM	Tropical Rainfall Measuring Mission
USGS	United State Geological Survey
WRD	Water Resources Department

ABSTRACT

Floods are probably the most recurring, widespread, disastrous and frequent natural hazards of the world. India is one of the worst flood-affected countries. In India the Himalayan Rivers account for maximum flood damage in the country. The problem of flood in the state of Bihar is well known and every year it becomes a recurring problem to the entire region. The plains of north Bihar are some of the most susceptible areas in India, prone to flooding. Flood forecasting & flood warning, flood hazard mapping and flood risk zoning are quite effective non-structural procedures in managing floods that decreases the risks and disasters floods may cause.

In view of this an attempt has been made in the present work to simulate runoff and flood inundation for Kosi River Basin in Bihar, India. This study introduces about the parameterization of hydrologic and hydraulic modelling for simulation of runoff and flood inundated area mapping. Time series analysis of hydrological data has been done to look for the rainfall and runoff behaviour in Kosi Basin and their cross-correlation. SRTM-DEM of 90m resolution is used to generate the various maps (DEM) of Kosi Basin. Hydrological and hydraulic models HEC-HMS, HEC-RAS, SCS-CN in addition to ANN models are used for runoff and floodplain inundation modelling. Results indicated that for Kosi catchment, the empirical runoff prediction approach (ANN technique), in spite of requiring much less data, predicted daily runoff values more accurately than semi-distributed conceptual runoff prediction approach (SCS-CN method). The flood inundation simulation for the Kosi River floodplain is carried out using HEC-RAS 1-D hydrodynamic model indicates promising results. Further, linear/non-linear regression models were developed to estimate the flood inundation area provides best results.

Keywords: Rainfall, Runoff, DEM, HEC-HMS, HEC-RAS, ANN, Flood Inundation.

CHAPTER~01
INTRODUCTION

1.1 General

Water is an essential ingredient of life. However, since the beginning of the existence of mankind, drought and floods have affected human activities throughout the world. Flood is an unusually high stage in a river, normally the level at which the river overflows its banks and inundates the adjoining area (Subramanya, 2008). In the past, structural and non-structural measures have been adopted for the flood control and flood management. Non-structural measures used to estimate the floods and their proper management has been accelerated in the last couple of decades throughout the globe in comparison to expensive structural measures. Non-structural measure includes evaluation of impact of rainfall on runoff of a catchment, return period of different magnitudes/frequency of floods and flood inundated areas, and socio-economic aspects of floods. In the following section approaches based non-structural flood management have been discussed, which are integral part of the present research work.

1.2 Time Series Analysis

Prior to the application of rainfall-runoff modeling, time series analysis is important to understand the distribution trend of rainfall and runoff data over entire basin. This includes (a) making time-series plots and carry out primary data validation for any abrupt data entry or outliers, (b) possible trend and seasonality analysis in each data set, (c) inter-station cross-correlation among rainfall data, (d) rainfall-runoff relationship (linear and non-linear) for different discharge data, and (e)

rainfall-runoff relationship (linear and non-linear) for different combinations using mean rainfall over the basin obtained by arithmetic, isohyetal and thiessen polygon methods.

1.3 Rainfall-Runoff Modelling

The rainfall-runoff relationship is an important issue in hydrology and a common challenge for hydrologists. Due to the tremendous spatial and temporal variability of Himalayan basin characteristics such as snow pack, Land use/ land cover, soil moisture, hydraulic conductivity, topography (relief), erratic rainfall, in India, Nepal and Tibet, the impact of rainfall on runoff becomes more intensive and their proper estimate is essential for flood management.

Since the middle of the 19th century, different methods have been demonstrated by hydrologists to assess the impact of rainfall on runoff whereupon many models have attempted to describe the physical processes involved in it (Daniel, 1991; Smith and Eli, 1995; Harun et al., 1996; Dawson and Wilby, 1998; Tokar and Markus, 2000; Elshorbagy et al., 2000; Idris, 2000; Gautam et al., 2000; Imrie, 2000; Demuth and Beale, 2001; Dastorani and Wright, 2001; Garcia-Bartual, 2002; Zhang and Govindaraju, 2003; Bessaih et al., 2003; Rajurkar et al., 2004; Kumar et al., 2005; Sahoo et al., 2006; Leahy et al., 2006; Dawson et al., 2006). These rainfall-runoff models generally fall into black box or system theoretical models, conceptual models and physically-based models. Black box models normally contain no physically based input and output transfer functions and therefore, are considered to be purely empirical models. Conceptual rainfall-runoff models usually incorporate interconnected physical elements with simplified forms, and each element is used to represent a significant or dominant constituent hydrologic process of the rainfall-runoff transformation (O'Connor, 1997; Sanaga and Jain, 2006). Physically based model are distributed models consists a large number of parameters as input to the model.

1.4 Flood Inundation Modelling

As floods occurrence and their serious consequences are common in many parts of the world, it has raised public, political and scientific awareness for proper flood control and management (Becker et al., 2003). Using non-structural techniques, assessment and management of flood inundated area for different magnitudes of floods is very essential. Various hydrologic models have been developed in the past to simulate flood inundation in the basin area (Iwasa and Inoue, 1982; Samules, 1985; Gee et al., 1990. These models consider overland and river flows. Also, these models are applied either only in test catchments or in some small flat areas with hypothetical conditions. Only a few models are available to simulate flood inundation in a river basin for real flood events considering all the spatial heterogeneity of physical characteristics of topography such as HEC-GeoHMS, HEC-GeoRAS, MIKE BASIN, MIKE-11, MIKE-FLOOD and other models.

1.5 Objective of the Study

In the present work, HEC-GeoHMS and HEC-GeoRAS models have been used for rainfall-runoff modeling and to obtain the flood inundated areas in Kosi Basin. Further, different ANN algorithms were used for rainfall-runoff modeling, and different linear/non-linear models were used for flood inundation modelling. The objectives of the present research work are.

- **i.** Time series analysis of rainfall-runoff data to develop linear and non-linear relationship.
- **ii.** Remote sensing data analysis using ERDAS-Imagine and Arc-GIS to obtain input data sets for rainfall-runoff and flood inundation modelling.
- **iii.** Rainfall-Runoff modelling using hydrological models (HEC-GeoHMS with SCS-CN method) and ANN models.
- **iv.** Flood inundated area assessment using HEC-GeoRAS and non-linear regression models.

v. Performance evaluation using error statistics of results obtained during calibration, testing and validation of the data.

1.6 Thesis Outline

- **Chapter 1** is introduction part of the research work.
- **Chapter 2** Describe literature reviews related to time series analysis of rainfall-runoff data, rainfall-runoff modeling, and flood inundation modeling.
- **Chapter 3** Describe the study area Kosi River Basin, topographic information, rainfall, temperature, soil characteristic and land use pattern, various input data collected for the HEC-HMS, ANN, HEC-RAS and non-linear models setup.
- **Chapter 4** Presents the detailed procedures followed for time series analysis of rainfall-runoff data, rainfall-runoff modeling, flood inundation modeling for Kosi Basin, and performance evaluation using error statistics.
- **Chapter 5** Represents the result and discussion part, in which the results of time series analysis, rainfall-runoff modeling, flood inundation modeling, liner/non-linear modeling are discussed in detail. Performance evaluation using error statistics of results obtained during calibration, testing and validation of the data is also done in this chapter.
- **Chapter 6** Provides the conclusion based on the analysis of rainfall-runoff data using STATISTICA, rainfall-runoff modeling using HEC-HMS & ANN, flood inundation modeling using HEC-GeoRAS, and their linear/nonlinear relationship.
- **Chapter 7** References

CHAPTER~02
LITERATURE REVIEW

In the present chapter literature survey has been done for various aspect of the present work including time series analysis, rainfall-runoff modelling using HEC-HMS, ANN applications in rainfall-runoff modelling and Flood inundation modelling.

2.1 Time Series Analysis of Rainfall-Runoff Data

Singh et al. (1976) developed relationships between statistical parameters of annual rainfall and those of annual runoff obtained using a single linear reservoir and a single non-linear reservoir transformation of rainfall data.

Ramasastri and Nirupama (1987) carried out statistical analysis of monthly and annual rainfall data of Belgaum district to identify the presence of any trend and to study the phenomenon of low rainfall.

Ramamurthy et al. (1987) studied the long term variation in the rainfall over upper Narmada catchment. Monthly, seasonal and annual rainfalls of 38 stations in the upper Narmada catchment for the period of 1901 to 1980 were analysed.

Shahin et al. (1993) described that the main aim of time series analysis is to detect and describe quantitatively each of the generating processes underlying a given sequence of observations. Galkate et al. (1999) analysed of monthly, monsoon, non-monsoon and annual rainfall data for Sagar division. They found the distribution of rainfall in the region was nearly normal. They studied the linear and non-liner trend in the seasonal and annual rainfall data.

Burn et al (2002) studied the spatial differences in trends, which can occur as a result of spatial differences in the changes in rainfall and temperature and spatial differences in the catchment characteristics that translate meteorological inputs into hydrological response.

Adeloye and Montaseri (2002) most statistical analyses of hydrologic time series at the usual time scale encountered in water resources studies are based on the following fundamental assumptions: the series is homogenous, stationary, and free from trends and shifts, non-periodic with no persistence.

Guero (2006) has done statistical analysis of daily and monthly rainfall data for Munster Blackwater Catchment, Ireland. Detailed analysis of spatial and temporal variation over the catchment was examined.

Ahlawat (2010) analyzed the existing hydrological and meteorological data with the help of SPSS, GIS and MS-Excel software for Betwa river basin. Correlation and regression coefficients were derived using flow data at different locations.

2.2 Rainfall-Runoff Modelling

The origins of rainfall-runoff modelling in the broad sense can be found in the middle of the 19th century. In 1932, Sherman introduced the "unit-graph" or unit hydrograph technique. It was the first attempts to predict an entire hydrograph instead of just the peak flow and time to peak.

Early in the 20th century, hydrologists tried to improve the applicability of the rational method to large catchments with heterogeneity in rainfall and catchment characteristics (Todini, 1988).

The real breakthrough came in the 1950s when hydrologists became aware of system engineering approaches used for the analysis of complex dynamic systems (Todini, 1988). This was the period when conceptual linear models originated (Nash, 1958).

The 1960s brought the introduction of computers into hydrological modelling. The first comprehensive hydrologic computes model, the Stanford Watershed Model, was developed at Stanford University (Crawford and Linsley, 1966).

In the late 1960s, HEC-1 was developed by the Hydrological Engineering Centre, U.S. Army Corps of Engineers. Later, with addition of user interface and spatial data input and analysis features, HEC-1 was renamed as HEC-HMS.

During the 1960's and 1970's were the times of developing models with parameters having a physical interpretation.

One of the most widely used techniques for estimating direct runoff depths from storm rainfall is the United States Department of Agriculture (USDA) Curve Number (CN) method (SCS 1972, 1985).

Many researchers (Blanchard 1975; Jackson et al. 1977; Ragan et al. 1980; Slack et al. 1980; Bondelid et al. 1982; Hill et al. 1987; White 1988; Muzik 1988; Stuebe & Johnston 1990; Tiwari et al. 1991, 1997; Das et al. 1992) used land use/land cover information derived from satellite data of Landsat, SPOT, & IRS Satellite and integrated them with GIS to estimate SCS CNs and runoff.

Jain and Ramsastry (1990) successfully used HEC-1 model for modelling rainfall-runoff response of Hemavati river basin up to Sakleshpur within the constraints of data availability. Kottegoda et al. (2000) presented a simple statistical daily streamflow generator with simulated rainfall input where losses were obtained from an equivalent curve number, CN, related to the total rainfall of the event.

Chatterjee et al. (2001) used HEC-1 package and Nash model. They concluded that in general, the performance of the HEC-1 package and Nash IUH model for estimation of the DSRO hydrograph for the catchment under study was comparable.

Anderson et al. (2002) coupled HEC-HMS with an atmospheric model for prediction of watershed runoff in Sierra Nevada Mountains of California, USA.

Zhan and Huang (2004) applied ArcCN-Runoff tool (an extension of ESRI's ArcGIS software) to determine CNs and to calculate runoff or infiltration from a rainfall event for a watershed in Lyon County and Osage County, KS, USA.

Knebl et al. (2005) successfully integrated the NEXARD data and HEC-HMS and HEC-RAS to determine the flood polygons in San Antonio river basin. They provided a tool for hydrological forecasts of flooding on a regional scale.

Jain et al. (2006) developed an enhanced version of the SCS-CN based Mishra-Singh model (Mishra and Singh 1999) incorporating the storm duration and a nonlinear relation for initial abstraction (Ia).

Mishra et al. (2007) used SCS-CN method for computation of direct runoff from long duration rains for five Indian watersheds. They derived curve numbers from long-term daily rainfall-runoff data and Antecedent Moisture Condition (AMC) related with antecedent duration.

Chen et al. (2008) used SCS-CN method and Green-Ampt method to simulate hydrologic responses in the Meilin watershed. They found that the Green-Ampt method obtained better results especially on the simulation of peak streamflow as compared to these with SCS curve number method.

Patil et al. (2008) estimated runoff using curve number techniques (ISRE-CN) and validated with recorded data for the period from 1993 to 2001 of Banha catchment in Damodar valley,

Jharkhand, India. They observed that the application of the modified CN I method in the un-gauged watersheds that were hydrologically similar to the Banha watershed would result in an accurate surface runoff estimation.

Ranaee et al. (2009) had done flood routing in a two branches of ZOSHK river using HEC-GeoHMS, HEC-HMS and MIKE 11 software. They used HEC-GeoHMS software to prepare required statistics for rainfall-runoff modelling in HEC-HMS. Later on, they used the output information of HEC-HMS model as input data for flood routing modeling in MIKE11 software. Finally, they calibrated computed statistics of MIKE 11 software in compare with observed data in hydrometric station which was located in that river outlet. They suggested a suitable procedure for flood routing in rivers which are similar to this case study with uncompleted initial and boundary conditions.

Bhadra et al. (2010) developed SCS-CN and ANN model for Kangsabati catchment, situated in the western part of West Bengal with satisfactory results. They used Monsoon data of 1996 to 1999 for calibration of the models another four years (1987, 1989, 1990, and 1993) monsoon data for validation. In this study they found ANNs result more satisfactory than SCS-CN method for Kangsabati catchment.

Gajbhiye et al. (2012) determined the runoff depth using NRSC-CN method with Remote Sensing and GIS and the effect of slope on runoff generation for Bamhani catchment located in Mandla district of Madhya Pradesh. They determined the Effect of slope on CN values and runoff depth. The result showed that the CN unadjusted value are lower in comparison to CN adjusted with slope. Remote sensing and GIS is very reliable technique for the preparation of most of the input data required by the SCS curve number model.

Akbari et al. (2012) studied about the practical use of public domain satellite data and GIS based hydrologic model. They used SRTM elevation data at 30m cell size for watershed delineation TRMM (V6) and raingauge rainfall data for rainfall-runoff process. The SCS-CN approach was used for losses and kinematic routing method employed for hydrograph transformation through the reaches. They concluded that TRMM estimates do not give adequate information about the storms as it can be drawn from the rain gauges. Event-based flood modelling using HEC-HMS proved that SRTM elevation dataset has the ability to obviate the lack of terrain data for hydrologic modelling where appropriate data for terrain modelling and simulation of hydrological processes is unavailable.

Artificial Neural Network application in rainfall-runoff modelling

The relationship of rainfall-runoff is known to be highly non-linear and complex and difficult problem involving many variables, which are interconnected in a very complicated way.

Daniel (1991) introduced the application of ANNs in water resource and hydrologic modelling to the water resource community, he used ANNs to predict monthly water consumption and to estimate flood occurrence.

A number of researchers (Zhu et al. 1994; Dawson and Wilby 1998; Tokar and Johnson 1999; Coulibaly et al. (2000) have investigated the potential of using neural networks in modelling watershed runoff based on rainfall inputs.

Kumar et al. (2004) have studied the performance of MLP and RBF type neural network models developed for rainfall-runoff modelling of two Indian River basins.

Harun et al. (2002) simulated daily runoff using rainfall as input nodes for ANN model in Lui catchment (Selangor, Malaysia). Results were compared with HEC-HMS model, they found

ANN show a good generalization of rainfall-runoff relationship and better than HEC-HMS model.

Rajurkar et al. (2002) studied the application of artificial neural network (ANN) methodology for modelling daily flows during monsoon flood events for a large size catchment of the Narmada River in Madhya Pradesh, India. They found that a linear multiple-input single-output (MISO) model coupled with the ANN provided a better representation of the rainfall-runoff relationship in such large size catchments compared with linear and nonlinear MISO models.

Jain and Srinivasulu (2004); Rajurkar et al. (2004); De Vos and Rientjes (2005); Ahmad and Simonovic (2005); Tayfur and Singh (2006) found acceptable performance of Artificial Neural Networks (ANNs) in rainfall-runoff modelling.

Kumar et al. (2005) developed MLP and RBF type neural network models for rainfall-runoff modelling of two Indian River basins. The performance of both the MLP and RBF network models were comprehensively evaluated in terms of their generalization properties, predicted hydrograph characteristics, and predictive uncertainty. Merits and limitations of networks of both models were discussed.

Solaimani (2009) developed Artificial Neural Network (ANN) to modelling the rainfall-runoff relationship in a catchment area located in a semiarid region of Iran. The applications of the feed forward back propagation for the rainfall forecasting with various algorithms with performance of multilayer perceptions has been illustrated in this study.

2.3 Flood Inundation Modelling

By 1976, the methods used for solving the Saint-Venant equations appeared to be satisfactory with mathematical models found to be adequate for large number of applications (Priessmann, 1976).

Bates et al. (1997) mention the further development of two-dimensional finite element models of river flood flow. They applied the two-dimensional finite element model to the Missouri river, Nebraskan with integration of hydraulic modelling and remote sensing.

Han et al. (1998) and Chang et al. (2000) have also reported 1-D, 2-D coupled modelling of river flood plain flow. The models have used a full dynamic equation for the channel flow and for the two-dimensional flood plain flow; a diffusion wave approximation is utilized.

Anderson (2000), Robayo et al. (2004) and Knebl et al. (2005) discussed that flood inundation modelling involves hydrologic modelling to estimate peak flows from storm events, hydraulic modelling to estimate water surface elevations, and terrain analysis to estimate the inundation area.

Wright et al. (2008) presented a methodology for using remotely sensed data to both generate and evaluate a hydraulic model of floodplain inundation for a rural case study in the United Kingdom-Upton-upon-Severn.

Zheng et al. (2008) developed a distributed model for simulating flood inundation integrating with rainfall-runoff processes using SRTM-DEM data and some remote sensing data sets in the environment of GIS for Maruyama River basin, Japan. Simulated results in the Maruyama River basin demonstrate an acceptable agreement with the flooded area observed.

Bhatt et al. (2010) discussed about the operational use of remote sensing technology for near real time flood mapping, monitoring of Kosi floods and the satellite based observations made for the Kosi river breach.

Patro et al. (2009) used a coupled 1-D and 2-D hydrodynamic model, MIKE FLOOD to simulate the flood inundation extent and flooding depth in the delta region of Mahanadi River basin in India. They used SRTM-DEM to prepare a bathymetry of the study area and provided as an input

to the 2D model, MIKE 21. Using lateral links in MIKE 11 and MIKE 21 models flood inundated area was obtained. Results were compared with actual inundated area obtained from IRS-1D WiFS image.

Samarasinghe et al. (2010) derived flood extent from the flood extent obtained for the 50-year rainfall using HEC-HMS and HEC-RAS in Kalu-Ganga River, Sri Lanka.

Ahmad et al. (2010) generated flood hazard map for Nullah Lai in Rawalpindi using HEC-RAS and HEC-GeoRAS hydrological models with GIS. They found relationship between inundation depth and specific discharge value.

Shaohong et al. (2010) developed a real-time flood monitoring system that permits integrated handling of hydrological data coming from a wireless monitoring network. They obtained water surface elevation according to hydrological data and spatial position information using spatial analysis technology in GIS software. Then, flood area information was analsized by minus of water surface elevation and digital elevation model.

Roy et al. (2011) discussed the non-structural measures for flood management on the basis of gauge to gauge co-relation among Basua, Baltara& Kursela with two base stations Barahkshetra and Birpur Barrage in the network.

Adnan et al. (2012) carried out for bathymetry mapping based on remotely sensed imagery coupled with ancillary datasets for River Kelantan, Malaysia using a hydraulic model HEC-RAS. Predicted flood inundation extent using HEC-RAS was compared to flood extent predicted from a RADARSAT image. The accuracy assessment was applied to identify spatial variation in the error between three areas (i.e. upstream, midstream and downstream).

CHAPTER-03
STUDY AREA AND DATA COLLECTION

This chapter deals with the description of the study area, which is the Kosi river basin originating in the Himalaya in Nepal and Tibet and flowing through plains of Bihar state in India before joining the river Ganga. In this chapter data collection including topographic information, rainfall, temperature, soil characteristic and land use pattern of the study area are described. The description about various analysis of input data collected for the HEC-HMS, ANN and HEC-RAS model setup are also presented.

3.1 The Study Area

3.1.1 The Kosi River Basin

The Kosi River Basin is a sub-basin of the Ganga basin situated on the left side of the main Ganga River (Figure 1). Upper catchment of the basin lies in Nepal and Tibet at great heights of the Himalayan range. The total drainage area of the Kosi River is 74,030 km^2 out of which 11,410 km^2 lies in India and the rest 62,620 km^2 lies in Tibet and Nepal (http://fmis.bih.nic.in).

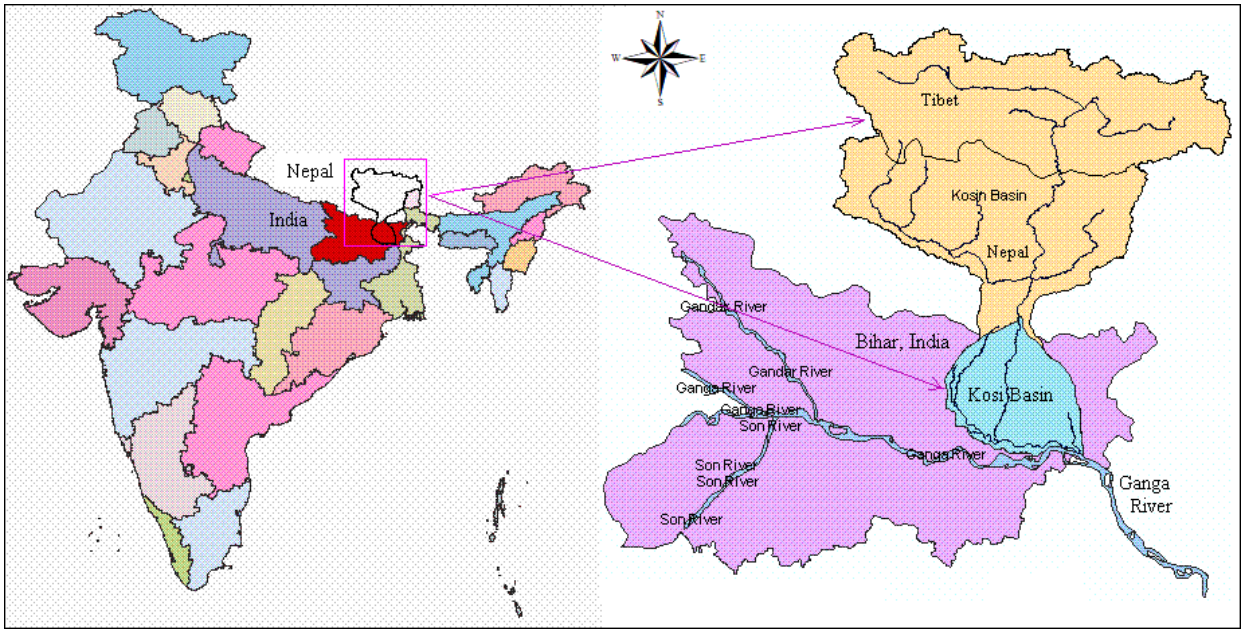

Figure 1: Index Map of Kosi Basin

The location of the basin lies between 85°22'19''- 88°55'44'' East and 25°20'30''- 29°07'48'' North. It is bounded by the ridge on the left side separating it from the Brahmaputra River, while river Ganga forms its southern boundary. The topography of the basin is very steep in upper reaches and mild in lower reaches as shown in Figure 2. According to (Kale, 2008) Digital Elevation Model (DEM) analysis, based on SRTM-DEM data, reveals that approximately 50% of the basin area is above 4000 m above mean sea level (msl) and the area below 120 m above msl is only 16% as shown in Figure 3. The Kosi Basin maps were generated using SRTM-DEM.

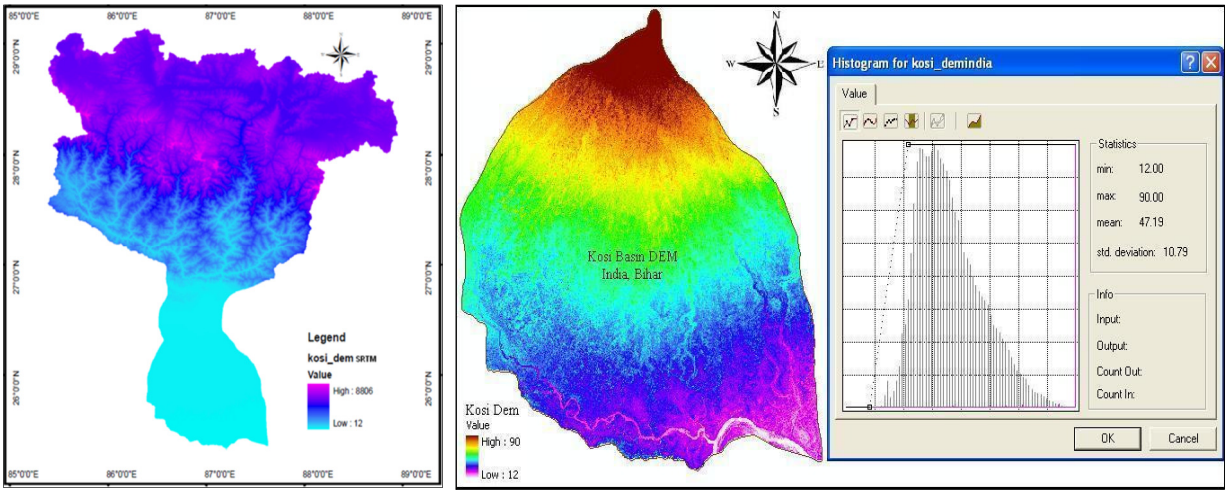

Figure 2: Digital Elevation Model for Kosi River Basin (Source: SRTM)

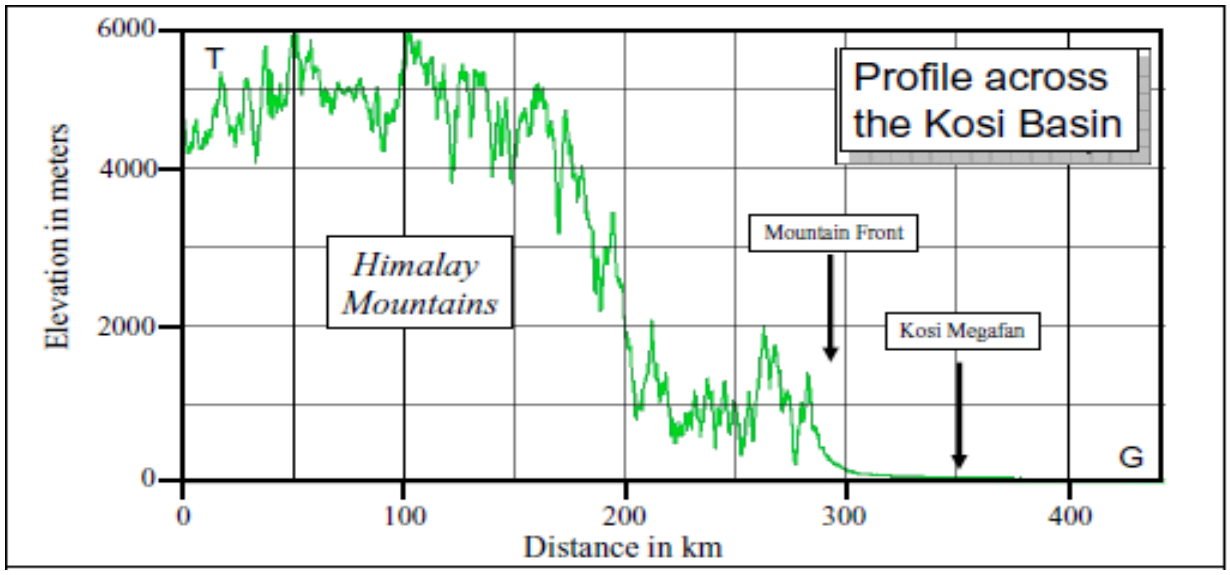

Figure 3: Elevation Profile across the Kosi Basin, T=Tibet=Ganga River (Source: Kale, 2008)

3.1.2 Kosi River and its Tributaries

The Kosi River is one of the major left bank tributaries of the Ganga rising at an altitude of over 7000 m above msl in the Himalayas. The Kosi, known as Kaushiki in Sanskrit books, is one of the most ancient rivers of India. Total length of main river in Bihar is 260 Km. In Nepal, this river is known as "Sapt-Kosi", deriving its name from the seven streams. The seven tributaries are; Arun Kosi, Tamur Kosi, Sun-Kosi, Indravati, Dudh Kosi, Tamba Kosi and Likhukhola (Figure 4). Tributaries of Kosi River are Kamla-Balan, Baghmati, Bhuthi Balan and Trijuga on the right side and Fariani dhar, Dhemama dhar on the left side (http://fmis.bih.nic.in).

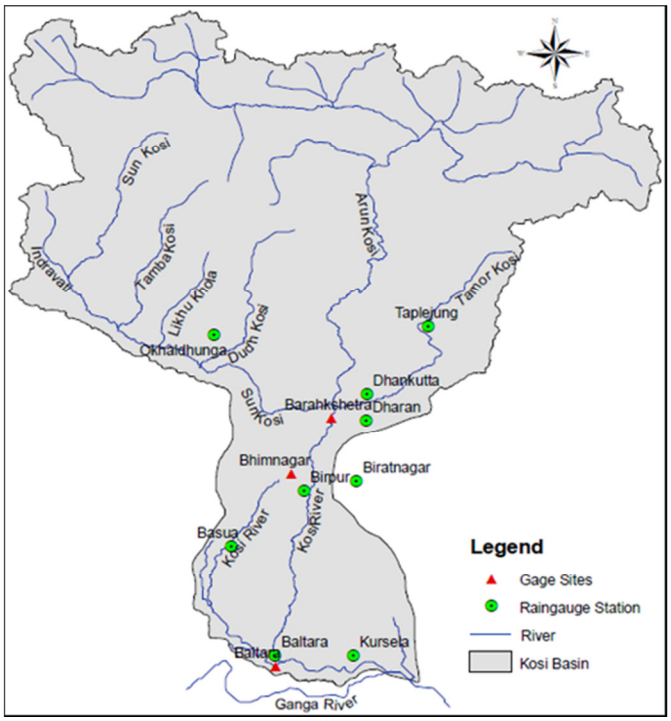

Figure 4: Kosi River System and location map of raingauge-discharge station

3.1.3 Rainfall-Runoff

The mean annual rainfall for the Kosi Basin is about 1456 mm (FMIS). Most of the rainfall (80 to 90%) is received from mid-June to mid-October. The Kosi River has an average discharge of 1560 cumec, which increases 18 to 20 times during peak floods. The highest flood recorded in recent history of the river is reported to be 24,100 cumec on 24thAug. 1954 (Reddy et al. 2008).

3.1.4 Temperature

The temperature in upper Kosi basin below 0^0C and maximum is approximately 10^0C. Kosi Basin has monsoon type tropical climate with high temperature and medium to high rainfall. The temperatures in lower Kosi Basin are lowest during December-January with an average minimum of 08-10^0C and maximum of 24-25^0C. The temperatures in the hottest months of April to June are minimum 23-25^0C and maximum 35-38^0C (FMIS).

3.1.5 Humidity

The humidity in the catchment is the highest during the months of July to September and lowest during March to April.

3.1.6 Land-use/Land-cover

The land use pattern in upper Kosi basin is open scrubland (approximately 60-65%) and remaining portion is bare ground, grass land and crop land (approximately 30-35%). The land-use/land-cover pattern in lower portion of the Kosi basin in Bihar is majority of cropland area (approximately 76%) and associated fallow lands (approximately 19%) and water bodies (approximately 05%) of the rivers Kosi and Ganga.

3.1.7 Soil Characteristics

The upper catchment of the Kosi basin lies totally in mountainous region. The soils encountered in these regions are usually classified as (GFCC, 1983): Mountain Meadow Soil, Sub-Mountain Meadow Soil, and Brown Hill Soil. The entire lower area of the Kosi Basin in the plains can be regarded as a large inland delta formed by the huge sandy deposit of the Kosi River.

3.2 Data Collection and Analysis

The basic data required for the rainfall-runoff modeling and hydrologic model are rainfall information, time series of discharge data, Digital Elevation Model (DEM), Soil types and Land-use/Land-cover data of the study area. For the setting up of HEC-RAS, the primary data required are the river cross sections, discharge, water level, Digital Terrain Model (DTM), and topographical map. These data sets were collected and procured from different sources as shown in Table 1. They were analyzed and transformed for proper use as input to the models.

Table 1: Types of data and the sources of their collection

Sl. No.	Source	Data Types
1.	India Meteorological Department (IMD), Pune	Daily Rainfall Data
2.	Central Water Commission (CWC), Patna, Govt. of India	Daily Water Level and Discharge Data
3.	WRD/DMD-Bihar FMISC (http://fmis.bih.nic.in)	Flood Inundation Images
4.	CGIAR-CSI (http://srtm.csi.cgiar.org)	SRTM-DEM 90m
5.	http://eros.usgs.gov	USGS' 30 arc-second Digital Elevation Model (GTOPO30), HYDRO1k
6.	NBSS & LUP	Soil Map
7.	https://zulu.ssc.nasa.gov (NASA)	Geo-Cover Data-2000
8.	NRSA/ISRO-AWiFS Data	Land-use/Land-cover-from 2005 to 2009
9.	NOAA	Monthly Mean Soil Moisture Data-2005 to 2009
10.	India Water Portal	Meteorological Datasets
11.	TRMM	Daily TRMM Rainfall 3B42 (V7)

Daily rainfall data for five years starting from July-2005 to Oct-2009 have been collected for nine raingauge stations whereas the discharge and water level data for the same period were collected from three discharge measuring stations. Figure 5 illustrates the rainfall and Figure 6 discharge data for the study period. The discharge data has been modified because the discharge data of River Ganga and its tributaries are confidential and may not be made public.

In addition, TRMM rainfall data representing the whole study area were also collected for different period during the year 2005-2009. Figure 7 illustrated the representative TRMM data sets for different year. The land use maps of lower part of Kosi River Basin prone to floods were procured and transformed as input to the models. Figure 8 (a) to (e) shows the land use map of the lower part for the years 2005-2009 and Figure 8(f) shows the landuse map of the entire basin.

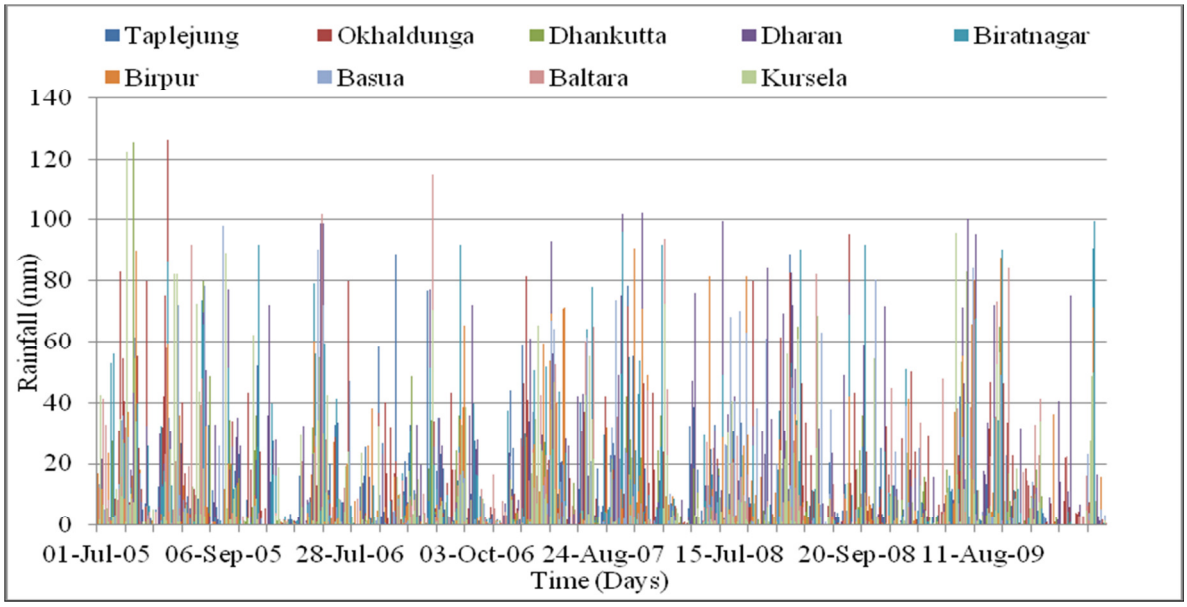

Figure 5: Observed Daily rainfall data of nine stations of Kosi Basin

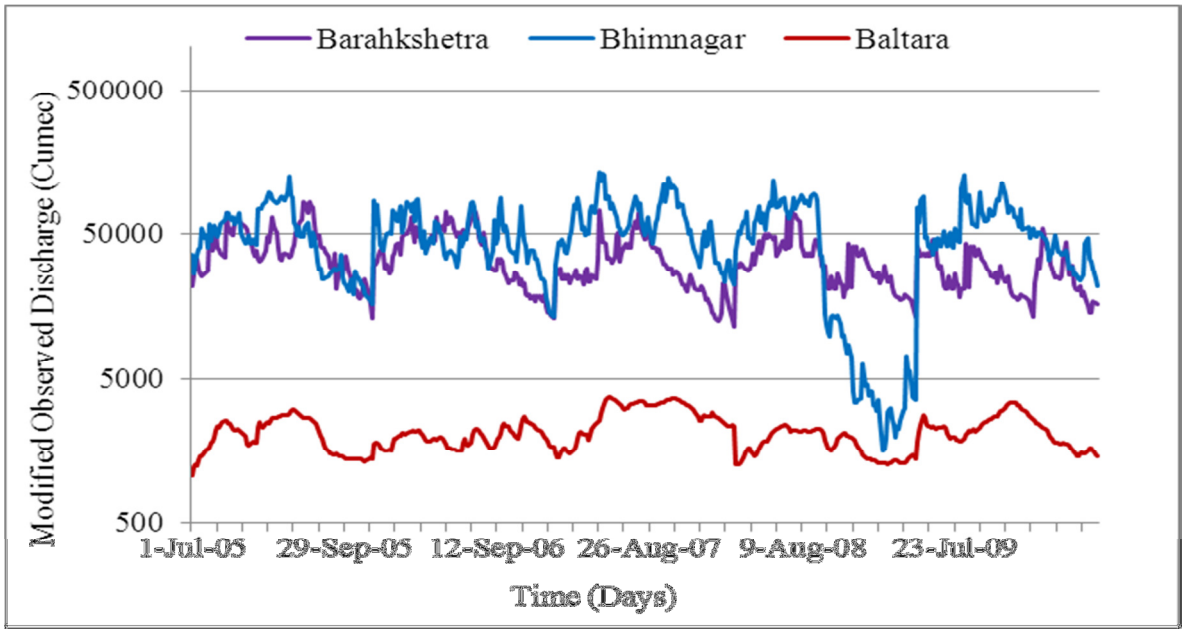

Figure 6: Daily discharge data at three stations of Kosi Basin

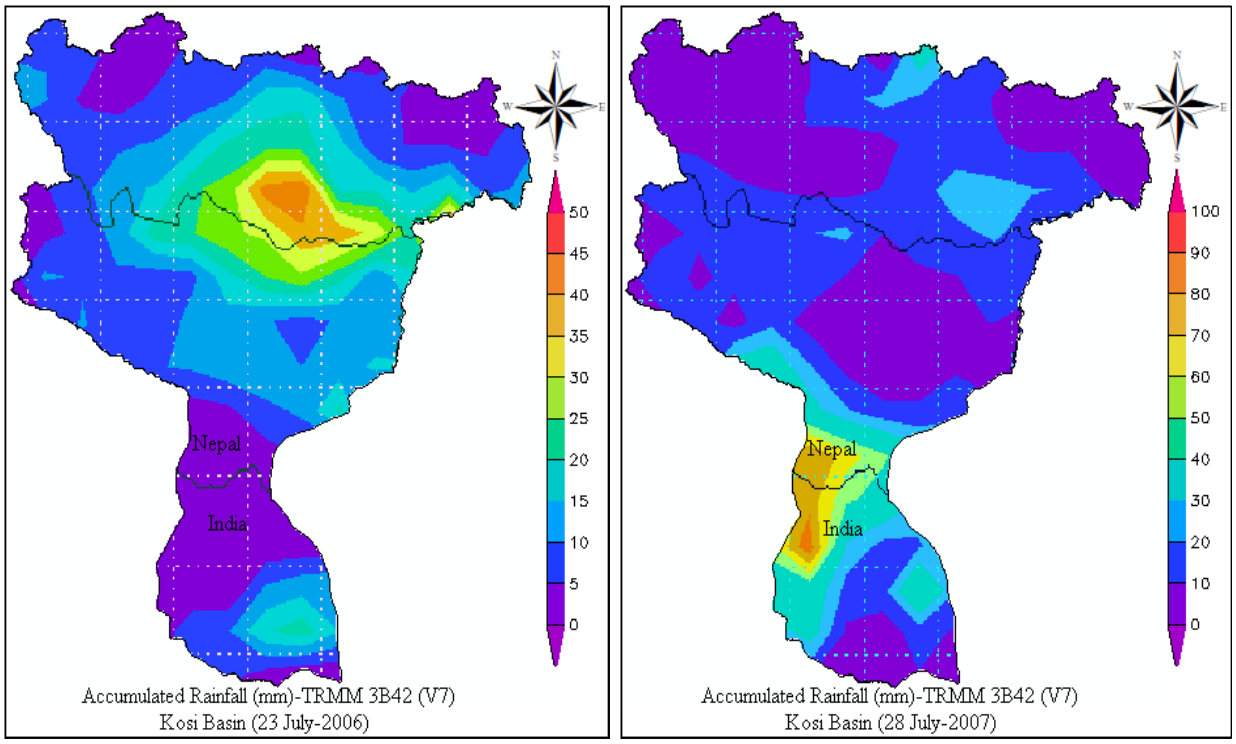

(a) **(b)**

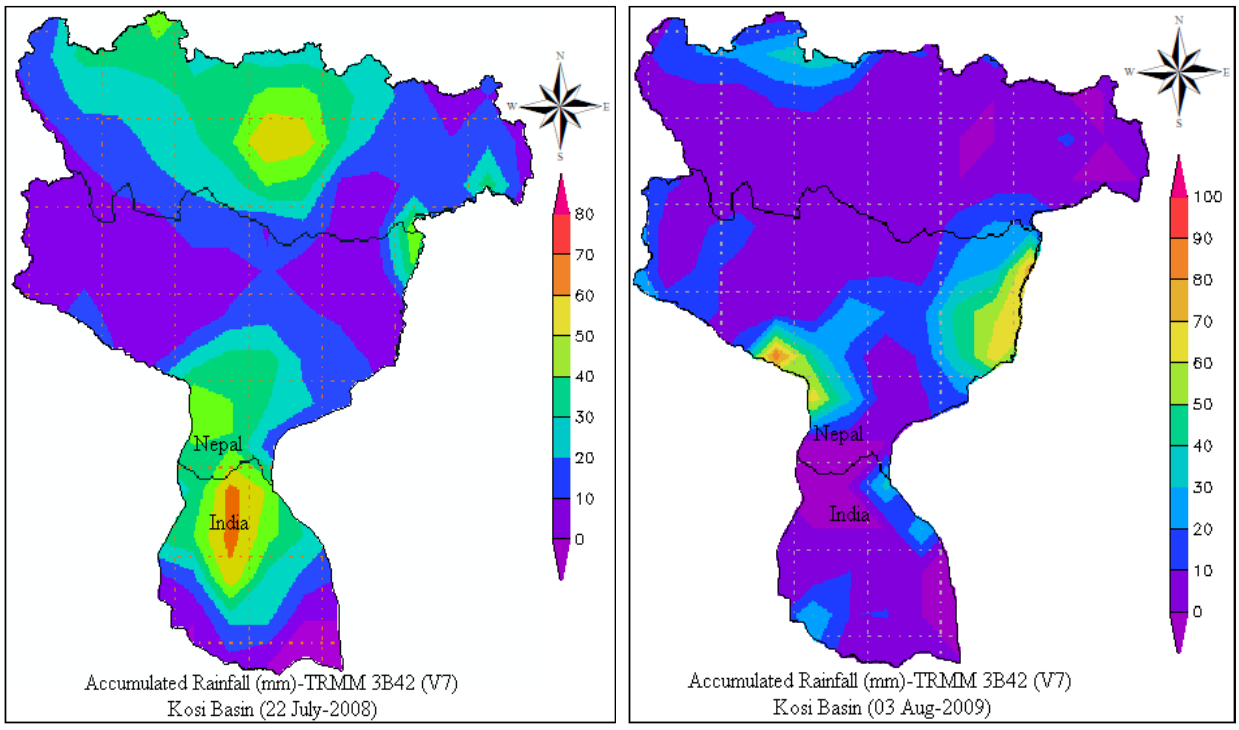

(c) **(d)**

Figure 7: Representative TRMM Daily Rainfall data over Kosi Basin

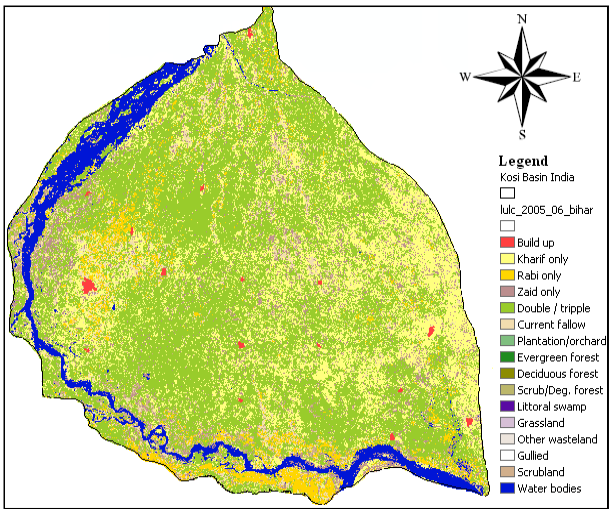

(a) Year-2005

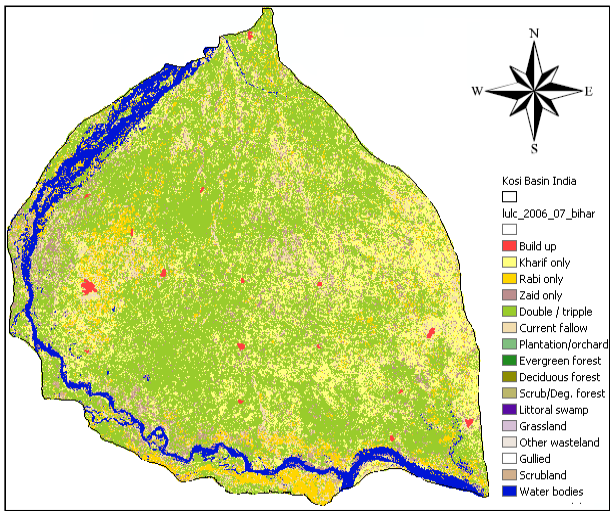

(b) Year-2006

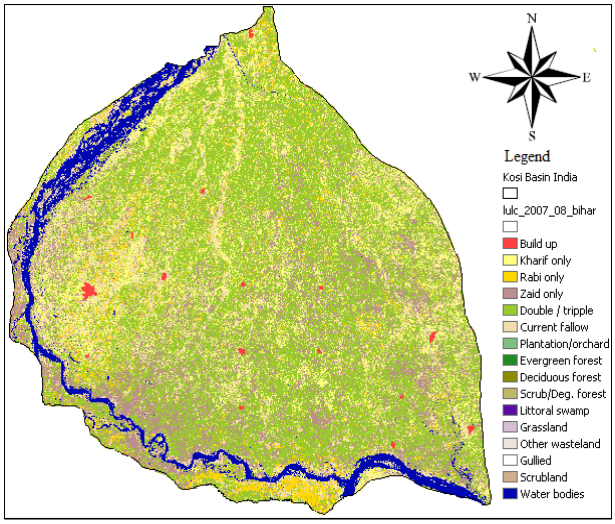

(c) Year-2007

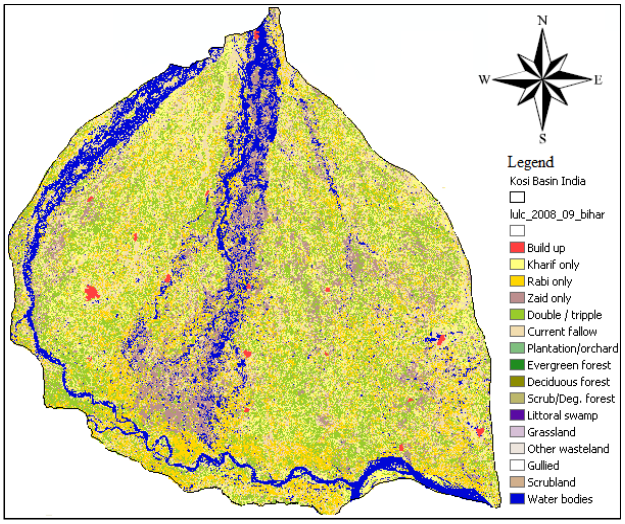

(d) Year-2008

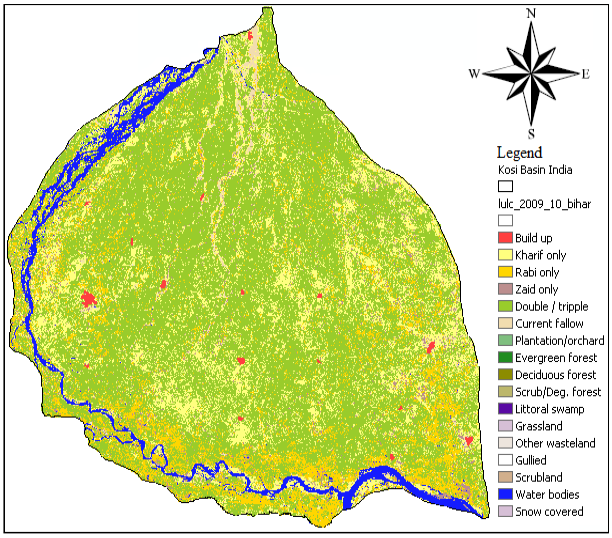

(e) Year-2009

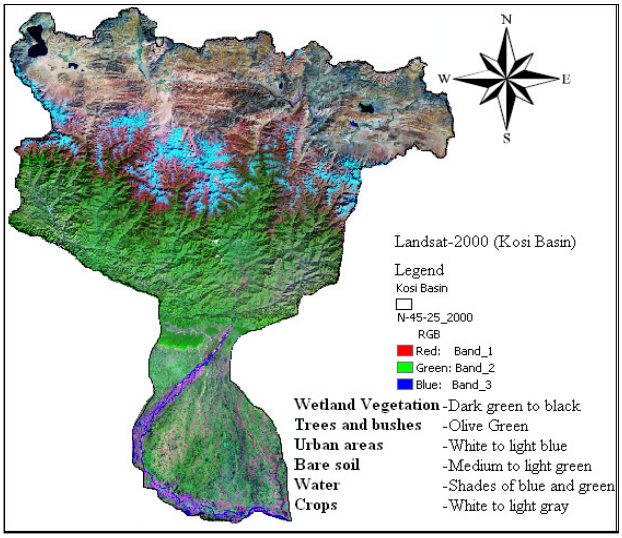

(f) Entire Basin-2000 (https://zulu.ssc.nasa.gov)

Figure 8: Land-use/Land-cover data for Kosi Basin {Source:-figure (a-e) NRSA}

CHAPTER-04
METHODOLOGY

This Chapter includes various methods used in the present work to assess the impact of rainfall on runoff using rainfall-runoff modeling and flood inundation modeling. The time-series data analysis was done prior to any model application. The details are discussed below:

4.1 Time Series Analysis of Rainfall-Runoff

The time series plots of all the daily rainfall data and runoff data were made to look for any possible trend and seasonality in the data set. As the data sets were very small, no trend has been detected. However, seasonal effects are visible. During monsoon the rainfall is found to be very high resulting in flood situation and flood inundation in river Kosi specifically at downstream station (Baltara).

4.1.1 Inter-station correlation of rainfall data

The rainfall data collected for all the stations were correlated with each other using cross-correlation option available in STATISTICA software. This is an essential component to see if any relationship between two raingauge rainfall data exists. This would help in using one raingauge station data in case of missing data of other station having high correlation. In this study cross-correlation among all the nine raingauge stations were carried out.

4.1.2 Basic statistics

Basic statistics such as minimum, maximum, mean, median, mode, standard deviation, variance, skewness, kurtosis, etc. have been computed in STATISTICA to observe the distribution of the

observed data sets. If data sets are not normally distributed, it needs to be transformed using various transformation algorithms prior to analysis.

4.1.3 Estimating spatial distribution of rainfall

Raingauge stations present only point sampling of the areal distribution of a storm. There are suitable methods to convert the point rainfall values at various stations into an average value over a catchment. Important one includes: (a) Arithmetical Average Method, (b) Thiessen Polygon Method and (c) Isohyetal method.

4.1.3.1 Arithmetical Average Method

The governing equations used in Arithmetic mean method can be written as:

$$\bar{P} = \frac{P_1+P_2+\cdots+P_i+\cdots+P_n}{N} = \frac{1}{N}\sum_{i=1}^{N} P_i \quad (1)$$

where $P_1, P_2, \ldots..P_i \ldots..P_n$ are the rainfall values in a given period in N stations within a catchment, $\overline{P}$ = Mean precipitation over the catchment.

4.1.3.2 Thiessen Polygon Method

In this method the rainfall recorded at each station is given a weightage on the basis of areas enclosed by bisectors around each station. The sum of the weights is one.

$$\bar{P} = \frac{P_1A_1+P_2A_2+\cdots+P_iA_i}{A_1+A_2+\cdots+A_i} = \sum_{i=1}^{N} P_i \frac{A_i}{A} \quad (2)$$

where; $P_1, P_2, P_3 \ldots P_i$ are the rainfall magnitudes recorded by the stations 1, 2, 3…i respectively, and $A_1, A_2, A_3 \ldots A_i$ is the respective area of the Thiessen polygons. The ratio $\frac{A_i}{A}$ is called the weightage factor for each station. The Thiessen polygon method is superior to the arithmetic average method as some weightage is given to the various stations on a rational basis.

4.1.3.3 Isohyetal method

An isohyet is a line joining points of equal rainfall magnitude. The equation can be written as:

$$\bar{P} = \frac{a_1\left(\frac{P_1+P_2}{2}\right)+a_2\left(\frac{P_2+P_3}{2}\right)+\cdots+a_{n-1}\left(\frac{P_{n-1}+P_n}{2}\right)}{A} \quad (3)$$

where, P_1, P_2,…….P_n are the values of Isohyets rainfall a_1, a_2,…..…a_{n-1} are inter-isohyets areas, A = catchment area. $\overline{P}$ = mean rainfall

4.1.4 Regression analysis of upstream-downstream flow

Similar to the rainfall inter-station cross-correlation, analysis has been carried out to develop inter-station correlation between upstream and downstream discharge data. The purpose for the relation is to generate the discharge value for the downstream region knowing the upstream discharge data. This would help to know discharge at any location, knowing the discharge of upstream/downstream location as in the Himalayan Kosi Basin it is difficult to measure accurate discharge due to high slope, high velocity of water and huge amount of sedimentation. Regression models linear, Exponential, Gaussian and Power model has been developed to obtain downstream discharge, knowing the upstream discharge. The governing equations are

Linear Model

$$y = a + bx \quad (4)$$

Exponential Model

$$y = ae^{bx} \quad (5)$$

Gaussian Model

$$y = ae^{\frac{-(x-b)^2}{2c^2}} \quad (6)$$

Power Function Model

$$y = ax^b \quad (7)$$

where a, b, and c are constants, x is input (rainfall) in mm and y is output (runoff) in mm.

4.1.5 Relationship between water level and discharge data

The measured value of the discharges when plotted against the corresponding stages gives relationship that represents the integrated effect of a wide range of channel and flow parameters. The stage-discharge relationship is known as the rating curve. A relationship has been obtained using Gaussian equation (equation 6) and power equation (equation 7).

4.1.6 Rainfall-runoff linear and non-linear correlation

Once the rainfall and runoff data were obtained, the following relationships were tried:

(a) Rainfall (each station) Vs discharge (each station);

(b) Rainfall (Arithmetic mean) Vs discharge (each station); and

(b) Rainfall (Thiessen polygon) Vs discharge (each station).

All possible linear and non-linear models given in equations (4) to (7) were tested for their applicability to predict runoff with known rainfall values.

4.2 Rainfall-Runoff Modelling

4.2.1 HEC-HMS and HEC-GeoHMS Model

(USACE, 2010) The Hydrologic Modelling System (HEC-HMS) is designed to simulate the precipitation-runoff processes of dendritic watershed systems. Hydrographs produced by the program are used directly or in conjunction with other software for studies of water availability, urban drainage, flow forecasting, future urbanization impact, reservoir spillway design, flood damage reduction, floodplain regulation, and systems operation. (USACE, 2009) The Geospatial

Hydrologic Modelling Extension (HEC-GeoHMS) has been developed in year 2000 by Hydrologic Engineering Centre (HEC), California, USA, as a geospatial hydrology toolkit for engineers and hydrologists with limited GIS experience. HEC-GeoHMS uses ArcView and the Spatial Analyst extension to visualize spatial information, document watershed characteristics, perform spatial analysis, and delineate sub basins; streams and develop a number of hydrologic modelling inputs for the HEC-HMS. The following steps describe the major steps in starting a project and taking it through the HEC-GeoHMS process.

4.2.1.1 Input Data for HEC-HMS

Data describing the terrain should be in ESRI's ARC Grid Format while vector data, such as stream alignments and stream flow gage locations, should be in the shapefile format. The input data for HEC-HMS model setup includes Digital Elevation Model (DEM), stream-flow gage data, soil types, land-use/land-cover data etc.

In the present work SRTM 90m DEM in ESRI Arc Grid format has been used to develop HEC-HMS basin model. Meteorological parameters like precipitation, discharge, water level are collected mostly from measured datasets. Land-use/land-cover data are obtained from NASA and NRSA/ISRO-AWiFS data.

4.2.1.2 Terrain Preprocessing

Using the terrain data as input, terrain preprocessing is a series of steps to derive the drainage network. The steps consist of computing the fill sinks, flow direction, flow accumulation, stream definition, and watershed delineation.

(a) Depressionless DEM: The Depressionless DEM is created by filling the depressions or pits by increasing the elevation of the pit cells to the level of the surrounding terrain. The pits are often considered as errors in the DEM due to re-sampling and interpolating the grid.

(b) Flow Direction: Flow direction map generated using Hydro DEM as input data, which defines the direction of the steepest descent for each terrain cell. Similar to a compass, the eight-point pour algorithm specifies the following eight possible directions as shown in Figure 9.

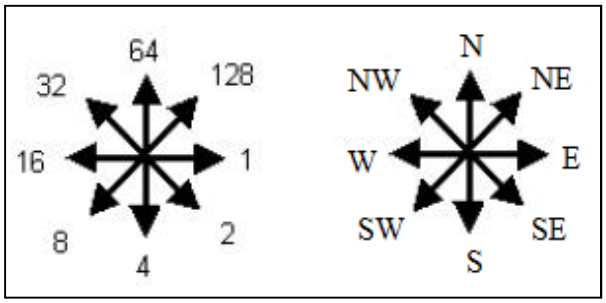

Figure 9: Eight-point pour algorithm for flow direction

(c) Flow Accumulation: Flow accumulation map determines the number of upstream cells draining to a given cell, using flow direction data as input. Upstream drainage area at a given cell can be calculated by multiplying the flow accumulation value by the grid cell area.

(d) Stream Definition: This step classifies all cells with a flow accumulation greater than the user-defined threshold as cells belonging to the stream network. The user specified threshold may be specified as an area in distance units squared. e.g., square kilometres, or as number of cells. The flow accumulation for a particular cell must exceed the user-defined threshold for a stream to be initiated. The default is one percent (1%) of the largest drainage area in the entire DEM.

(e) Stream Segmentation: Flow direction and stream grids are used to divide the stream grid into segments. Streams segments, or links, are the sections of a stream that connect two successive junctions, a junction and an outlet, or a junction and the drainage divide.

(f) Catchment Grid Delineation: The watershed is delineated in subbasins for every stream segment using flow direction and stream link grids.

(g) Catchment Polygon Processing: A vector layer (polygon subbasin layer) of subbasin is created using the catchment grid.

(h) Drainage Line Processing: A vector stream layer is generated using stream link and flow direction grid.

(i) Watershed Aggregation: This step aggregates the upstream subbasin at every stream confluence using drainage line and catchment layer. This is a required step and is performed to improve computational performance for interactively delineating subbasins and to enhance data extraction when defining a HEC-GeoHMS project.

(j) Hydrological Processing: Hydrologic process is generally responsible for hydrological model construction and setup. HEC-HMS project area is generated defining the outlet of the watershed. After defining the downstream outlet new datasets MainViewDEM, RawDEM, HydroDEM, flow direction grid, Flow accumulation grid, stream grid, stream link grid, catchment grid, subbasin, project point and river are created for new project.

4.2.1.3 Basin Processing

After the terrain preprocessing is completed and a new project has been created, basin processing is used to revise the subbasin delineations. Basin processing includes basin merge, basin subdivision, river merge, river profile, extract physical characteristics of streams-subbasins, develop hydrologic parameters and develop HMS inputs.

(a) Basin Merge: Multiple subbasins are merged together into one subbasin. There are following rules for subbasins merge:

i. The subbasin must share a common confluence

ii. The subbasin must be adjacent in an upstream and downstream manner.

iii. More than two subbasins are permitted.

(b) River Profile: The river profile is created by extracting elevation values from the terrain model along the stream line which, provides information on slopes and grade breaks that can be useful for selecting delineation points

(c) Stream and Watershed Characteristics: When the stream and subbasin delineation has been finalized, physical characteristics for a stream line such as length, upstream and downstream elevations, and slope are extracted from the terrain data. Similarly, physical characteristics for a subbasin, such as longest flow length, centroidal flow lengths, and slopes are extracted from the terrain data.

(i) River Length: River length is computed using river layer for selected or all routing reaches in the river layer.

(ii) River Slope: Upstream and downstream elevation and slope of a river is computed using RawDEM and River layer as input data.

(iii) Basin Slope: Average basin slope in the watershed is computed using subbasin and slope grid. Basin slope is used for the computation of the CN Lag time parameter.

(iv) Longest Flow Path: A number of physical characteristics such as the longest flow length, upstream/downstream elevation and slope between endpoints are computed using RawDEM, flow direction grid and subbasin.

(v) Basin Centroid: Basin centroid is identified for each subbasin. There are three algorithm Center of gravity method, longest flow path method and 50% area method.

(vi) Basin Centroid Elevation: Elevation for each centroid point is calculated using RawDEM.

(vii) Centroidal Flow Path: Centroidal flow path is calculated using subbasin, centroid and longest flow path. It is measured from the projected point on the longest flow path to the subbasin outlet.

(d) Hydrologic Parameters

After the physical characterises of streams and subbasins hydrologic parameters are defined such as HMS process (loss method, transform method, base-flow type, and routing method), river auto name, basin auto name, time of concentration, CN Lag method etc.

(e) Develop HEC-HMS Model Files: HEC-GeoHMS produces a number of files that can be used directly by HEC-HMS. These files include background map files, the basin model file, the meteorologic model file and a project file.

(i) Map to HMS Units: Physical characteristics of RawDEM, Subbasin, Longest flow path, centroidal longest flow path, river and centroid are converted to English or International System (SI) units.

(ii) HMS Data Check: Data check is necessary to keep track of the relationship between the stream segments, subbasins, and outlet points.

(iii) HEC-HMS Basin Schematic: The HMS basin schematic is the GIS representation of the HEC-HMS model. It shows the network of basin elements (nodes/links or junctions/edges) and their connectivity.

(iv) HMS Legend: Point and line features in the HMS Node and HMS Link layers are presented.

(v) Add Coordinates: Geographic coordinates are attached to features in the HMS Node and HMS Link layers using RawDEM. The coordinates are added to attribute tables.

(vi) Prepare Data for Model Export: Basin model file is exported with hydrologic elements, their connectivity, and related parameters using subbasin and river layers.

(vii) Background Map File: Background map layers capture the geographic information of the subbasin boundaries and stream reaches in ASCII text file or shape file format.

(viii) Basin File: The basin model captures the hydrologic elements, their connectivity, and related geographic information in ASCII text file that can be loaded into an HEC-HMS project.

4.2.1.4 Hydrologic Modeling System

Basin model created in HEC-GeoHMS imported in HEC-HMS. Gage weights of each raingauge station are defined in meteorological model manager. Control-specification is defined to set start time and end time of process. Time series data of rainfall and runoff are defined for each station. In the present study Soil Conservation Service-Curve Number (SCS-CN) method used to estimate daily runoff using daily rainfall data as input.

(a) SCS-CN Method

The SCS-CN method estimates precipitation excess as a function of cumulative precipitation, soil cover, land use, and antecedent moisture. The SCS-CN method is based on the water balance equation of the rainfall in a known interval of time Δt and two fundamental hypotheses.

$$P = I_a + F + Q \tag{8}$$

The first concept is that the ratio of actual amount of direct runoff (Q) to maximum potential runoff $(= P - I_a)$ is equal to the ratio of actual infiltration (F) to the potential maximum retention (S).

$$\frac{Q}{(P-I_a)} = \frac{F}{S} \tag{9}$$

The second concept is that the amount of initial abstraction (I_a) is some fraction of the potential maximum retention (S).

$$I_a = \lambda S \tag{10}$$

where, P is the total precipitation, I_a is the initial abstraction, F is the cumulative infiltration excluding I_a, Q is the direct runoff, S is the potential maximum retention or infiltration and λ is the regional parameter dependent on geologic and climatic factors ($0.1<\lambda<0.3$). By solving equation (9&10), we get

$$Q = \frac{(P-I_a)}{P-I_a+S} \tag{11}$$

$$Q = \frac{(P-\lambda S)^2}{P+(1-\lambda)S} \qquad \text{for } P > \lambda S,\ Q=0 \text{ for } P \leq \lambda S \tag{12}$$

The relation between I_a and S was developed by analyzing the rainfall and runoff data from experimental small watersheds (SCS, 1985) and is expressed as $I_a=0.2S$ (for $\lambda=0.2$). With this equation (12) becomes

$$Q = \frac{(P-0.2S)^2}{P+0.8S} \tag{13}$$

The potential maximum retention storage S of watershed is related to a CN, which is a function of land use, land treatments, soil type and antecedent moisture condition of watershed. The CN is dimensionless and its value varies from 0 to 100. The S-value in mm can be obtained from CN by using the relationship:

$$S = \frac{25400}{CN} - 254 = 254\left(\frac{100}{CN} - 1\right) \tag{14}$$

4.2.2 ANN Model

In the present work, both the Multilayer Perceptron (MLP) network and the Radial Basis Function (RBF) network have been considered for rainfall-runoff modelling using STATISTICA. The data sets were divided in training, testing and validation components randomly. In the present work, following models, as shown below, are used to investigate the number of antecedent events needed to obtain optimal results for daily runoff forecasting:

(i) Q(t)= {P(t)}

(ii) Q(t)= {Q(t-1}

(iii) Q(t)= {P(t), P(t-1)}

(iv) Q(t)= {Q(t-1), Q(t-2)}

(v) Q(t)= {P(t), P(t-1) P(t-2)}

(vi) Q(t)= {P(t), P(t-1), P(t-2), Q(t-1)}

(vii) Q(t)= {P(t), P(t-1), P(t-2), Q(t-1), Q(t-2)}

(Which can be written as MLP-1, MLP-2……..MLP-7 and RBF-1, RBF-2…….....RBF-7)

4.2.2.1 MLP Network

An ANN model with n input neurons ($x_1 . . . x_n$), h hidden neurons ($w_1, . . . , w_h$) and m output neurons ($Z_1,...,Z_m$) is considered in this study. The function used in the model is

$$Z_k = f\left(\sum_{j=1}^{h} \alpha_{kj} w_j + \in_k\right) \quad (15)$$

$$w_j = g\left(\sum_{i=1}^{n} \beta_{ji} x_i + \tau_j\right) \quad (16)$$

where g and f are activation functions, i, j, and k are representing input, hidden and output layers respectively, j is the bias for neuron w_j and k is the bias for neuron z_k, ij is the weight of the connection from neuron x_i to w_j and jk is the weight of the connection from neuron w_j to z_k.

The hyperbolic tangent sigmoid function is used as activation function for the hidden nodes. The function can be written as

$$g(S_i) = \frac{e^{S_i} - e^{-S_i}}{e^{S_i} + e^{-S_i}} \quad (17)$$

where s_i is the weighted sum of all incoming information and is also referred to as the input signal

$$S_i = \left(\sum_{i=1}^{n} \beta_{ji} x_i + \tau_j\right) \quad (18)$$

The major advantage of the MLP is that it is less complex than other artificial neural networks and has the same nonlinear input–output mapping capability (Coulibaly and Evora, 2007). The training of the MLP involves finding an optimal weight vector for the network. The objective function of the training process is:

$$E = \frac{1}{2} min \sum_{p=1}^{N} \sum_{k=1}^{M} \left(t_{kp} - z_{kp}\right)^2 \quad (19)$$

where N is the number of training data pairs, M is the output node number, t_{kp} is the desired value of the *kth* output node for input pattern p, and z_{kp} is the *kth* element of the actual output associated with input p (Antar et al., 2006).

The training algorithm used was Broyden-Fletcher-Goldfarb-Shanno (BFGS), error function used was sum of squares (SOS) and the hidden activation for different MLPS used were exponential, tank, identity or logistics. No weighting decay was considered in the analysis for hidden units. The training was stopped at 1000 epochs. The learning rate was set from 0.7 to 0.1 and the learning rule is momentum.

4.2.2.2 RBF Network

The second technique of the neural network modeling is the Radial Basis Function (RBF). RBF is supervised and feed forward neural network. The RBF can be considered as a three layer network. The hidden layer of RBF network consists of a number of nodes and a parameter vector called a “center” which can be considered the weight vector. The standard Euclidean distance is used to measure how far an input vector from the center is. In the RBF, the design of neural networks is a curve-fitting problem in a high dimensional space (Govindaraju, 2000). Training the RBF network implies finding the set of basis nodes and weights. Therefore, the learning process is to find the best fit to the training data. The transfer function of a RBF network is

mostly built up of Gaussian rather than sigmoids. The Gaussian functions decrease with distance from the center. The Euclidean length is represented by r_j that measures the radial distance between the datum vector y (y_1, y_2... y_m); and the radial center can be written as

$$R_j = \|y - y^j\| = \left[\sum_{i=1}^{m}(y_i - w_{ij})^2\right]^{1/2} \quad (20)$$

A suitable transfer function is then applied to r_j to give,

$$\Phi(r_j) = \Phi(\|y - y^k\|) \quad (21)$$

Finally the output layer (k=1) receives a weighted linear combination of Φ_{rj},

$$y^k = w_0 + \sum_{j=1}^{n} c_{kj}\Phi(r_j) = w_0 + \sum_{j=1}^{n} c_{kj}\Phi\left(\left(\|y - y^j\|\right)\right) \quad (22)$$

Figure 10 illustrates the designed architecture of the RBF model.

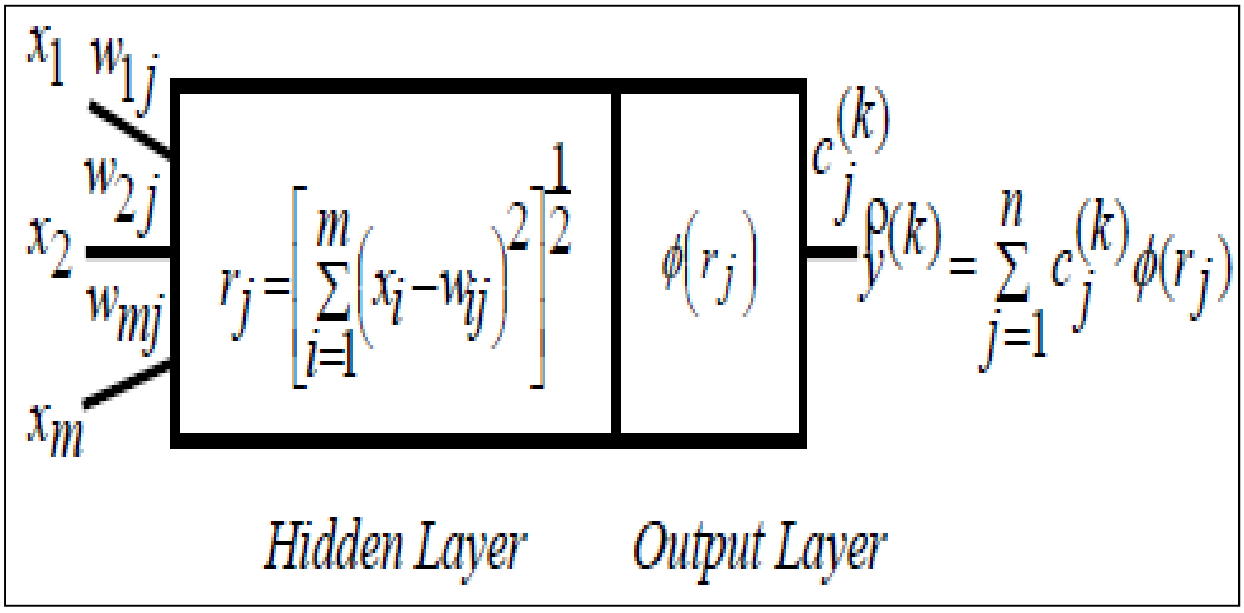

Figure 10: Structure of a RBF model

4.3 Flood Inundation Modelling

4.3.1 HEC-RAS and HEC-GeoRAS Model

The HEC-RAS model allows to performing one-dimensional steady flow, unsteady flow, sediment transport/mobile bed computations, and water temperature modelling. This model is used to obtain flood extent and depth due to high rainfall in the basin. HEC-RAS is a 1-D flow model in which the stream morphology is represented by a series of cross sections indexed by river station.

4.3.1.1 Input Data

HEC-GeoRAS requires a Digital Terrain Model (DTM) of the river system in the form of a TIN or a GRID. Land-use/land-cover data is required in shapefile to generate Manning's n values.

4.3.1.2 Creating RAS Layers

HEC-RAS layers stream centerline, flow path center lines, main channel banks, and cross-section cut Lines are generated using Digital Terrain Model (DTM) of the river in HEC-GeoRAS. RAS layers are used to extract additional geometric data for import in HEC-RAS. These themes include Land Use, Levee Alignment, Ineffective Flow Areas, and Storage Areas.

(a) Creating Stream Centerline: The stream centerline is used to establish the river reach network. The river network must be digitized in the direction of flow. Unique river and reach name is assigned using river reach ID tool. Connectivity, length of each river and reach is calculated from starting station to end station.

(b) Bank Lines: The bank lines layer is used to identify the main channel conveyance area from that of the overbank floodplain areas. Identification of main channel will also provide greater

insight into the terrain, movement of water in the floodplain, and in identifying non-conveyance areas.

(c) Flow Path Centerlines: The flow path lines layer is used to determine the downstream reach lengths between cross section in the channel and overbank areas. A flow path line should be created in the center-of-mass of flow in the main channel, left overbank, and right overbank for the water surface profile of interest. Flow path lines are digitized in the downstream direction, following the movement of water. Label of flow path line is assigned using flow path tool as left line, main channel and right line.

(d) Cross-Section Cut Lines: Cross-section cut lines are used to identify the locations where cross-sectional data are extracted from the Digital Terrain Model (DTM). The intersection of the cut lines with the other RAS Layers will determine bank station locations, downstream reach lengths, Manning's n values, ineffective areas, blocked obstructions and levee positions. Cut lines should always be located perpendicular to the direction of flow and oriented from the left to right bank. Cut lines must cover the entire extent area of the flood plain to be modeled. River/reach name, station to each cross section is assigned based on the intersection with the stream centerline. Bank station locations to each cross section are assigned. Lastly, reach length is assigned based on the flow path lines using downstream reach length menu.

The elevation for each cross-section is extracted from the terrain model. The elevation extraction process will convert the 2-D features to 3-D features. This will result in the generation of a new feature class.

(e) Land Use: The final task before exporting the GIS data to HEC-RAS geometry file is assigning Manning's n value to individual cross-sections. In HEC-GeoRAS, this is accomplished by using a land use feature class with Manning's n stored for different land use types. The land

use layer is polygon data set used to establish roughness coefficients for each cut line. The land use data set must have a field that holds descriptive information about each polygon. Depending on the intersection of cross-sections with landuse polygons, Manning's n are extracted for each cross-section, and reported in the XS Manning Table.

(f) Generating the RAS GIS import file: Prior to writing the results to the RAS GIS import file, we should set the layers which are to be exported from GeoRAS. For layer setup the following layers should be verified: required surface is terrain type, required layers are stream centerline, cross-section cut lines, cross-section cut lines profiles, optional layers bank lines, flow path centerlines, land use and optional tables Manning table, levee positions, node table etc. After verifying the data GeoRAS will export the GIS data to an XML file and then convert the XML file to the SDF format. Two files will be created: "GIS2RAS.xml" and GIS2RAS.RASImport.sdf".

4.3.1.3 HEC-RAS Hydraulic Analysis

HEC-RAS allows us to perform one-dimensional steady flow and unsteady-flow analysis of river systems. RAS GIS import file is used in HEC-RAS which contains geometric data of the river.

(a) Geometric Data

After importing the geometric data, quality check on the data is required. Make sure there are no obviously erroneous or missing data. Next, we should verify the each plot of cross-section, Manning's n value, bank stations are placed correctly. In this section geometric data can be edited using graphical cross section edit tool.

(b) Flow Data and Boundary Conditions: Flows are typically defined at the most upstream location of each river/tributary, and at junctions. Each flow that needs to be simulated is called a

profile in HEC-RAS. To define downstream boundary, normal depth slope is defined using reach boundary condition button.

(c) Run Steady/Unsteady Flow analysis

Now water surface profiles are computed for the flow data. After successful simulation HEC-RAS results are exported to ArcGIS to view the inundation extent.

(d) Exporting HEC-RAS Output: HEC-RAS Data are exported to ArcGIS using Export GIS Data button. Profile of flow is exported using export data button, which create a SDF file.

(e) Flood Inundation Mapping

In ArcMap SDF file is converted into an XML file using Import RAS SDF file button. RAS Mapping is done using Layers: file name, RAS GIS export file, terrain type, output directory etc. Using RAS Mapping (Read RAS GIS Export File) bounding polygon is created, which basically defines the analysis extent for the inundation mapping, by connecting the endpoints of cross-section cut lines. After the analysis extent is defined water surface profile is generated using profile with highest flow. This creates a surface with water surface elevation for the selected profile. The TIN that is created in this step will define a zone that will connect the outer points of the bounding polygon, which means the TIN will include area outside the possible inundation.

(f) Water surface Profiles: Water surface profiles are computed from one cross section to the next by solving the energy equation with an iterative procedure called the standard step method as shown in Figure 11 (HEC-RAS, 2010).

$$Z_2 + Y_2 + \frac{a_2 {V_2}^2}{2g} = Z_1 + Y_1 + \frac{a_1 {V_1}^2}{2g} + h_e \quad (23)$$

where, Z_1, Z_2 = Elevation of the main channel inverts, Y_1, Y_2 = Depth of water at cross sections, V_1, V_2 = Average velocities (total discharge/total flow area), a_1, a_2 = Velocity weighting coefficients, g = Gravitational acceleration, h_e = Energy head loss

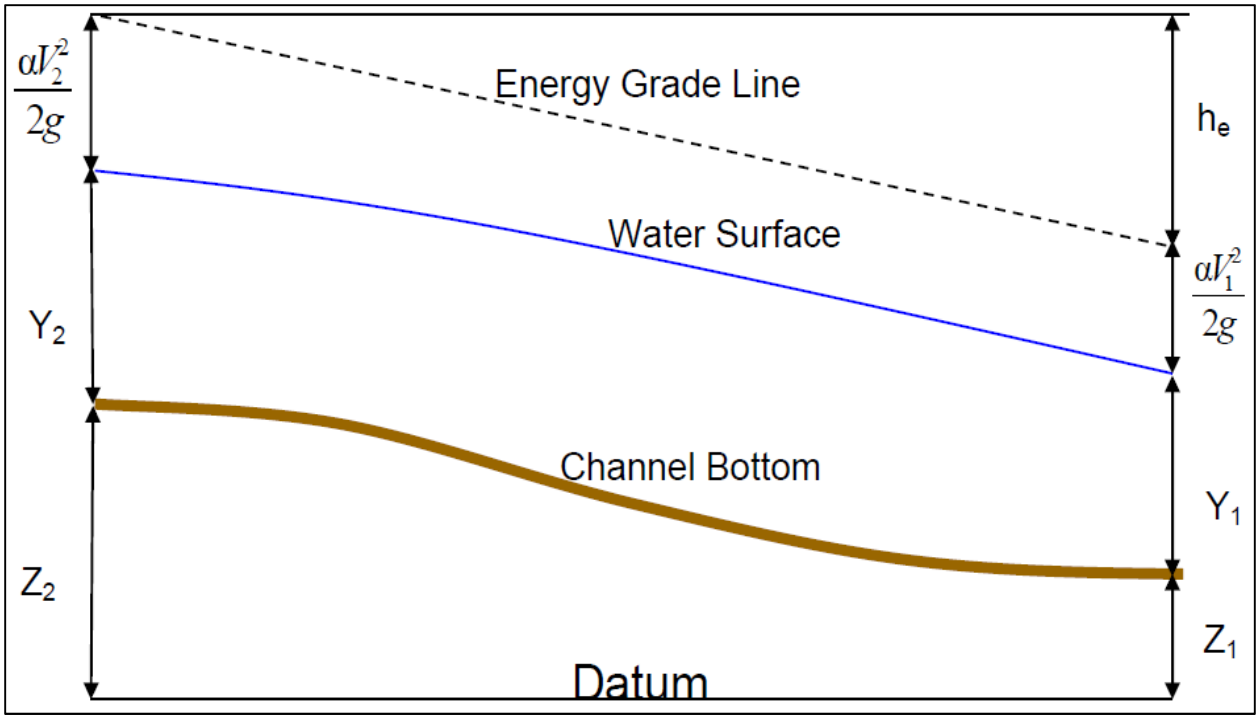

Figure 11: Representation of terms in the Energy equation (Source: - HEC-RAS User Manual, 2010)

The energy head loss (h_e) between two cross sections is comprised friction losses and contractions or expansion losses. The equation for the energy head loss is as follow:

$$h_e = L\bar{S}_f + C\left|\frac{a_2{V_2}^2}{2g} - \frac{a_1{V_1}^2}{2g}\right| \quad (24)$$

Where, L = Discharge weighted reach length, $\bar{S}_f$ = Representative friction slope between two sections, C = expansion or contraction loss coefficient, the distance weighted length L is calculated as:

$$L = \frac{L_{lob}\bar{Q}_{lob}+L_{ch}\bar{Q}_{ch}+L_{rob}\bar{Q}_{rob}}{\bar{Q}_{lob}+\bar{Q}_{ch}+\bar{Q}_{rob}} \quad (25)$$

where: L_{lob}, L_{ch}, L_{rob} = Cross section reach lengths specified for flow in the left over bank, main channel, and right over bank, respectively, $\bar{Q}_{lob} + \bar{Q}_{ch} + \bar{Q}_{rob}$= Arithmetic average of the flows between sections for the left overbank, main channel, and right overbank, respectively.

Using Inundation Mapping (Floodplain Delineation) button water surface TIN is first converted to a GRID, and then DTM grid is subtracted from the water surface grid. The area with positive results (meaning water surface is higher than the terrain) is flood area, and the area with negative results is dry. All the cells in water surface grid that result in positive values after subtraction are converted to a polygon, which is the final flood inundation polygon.

4.3.2 Linear and non-linear modelling

Due to limitation of one dimensional model, it is found essential to develop a linear/non-linear relationship between various parameters with the observed flood inundated areas. Various parameters such as, rainfall, rainfall distribution over an area, discharge, water level, soil moisture, were related with the flood inundated area using best possible combination of linear and non-linear models. The results were tested for their validity using various error statistics.

Rational Model

$$y = \frac{a+bx}{1+cx+dx^2} \tag{26}$$

Full Cubic Model

$$y = a + bx_1 + cx_2 + d{x_1}^2 + c{x_2}^2 + f{x_1}^3 + g{x_2}^3 + hx_1x_2 + i{x_1}^2x_2 + jx_1{x_2}^2 \tag{27}$$

4.4 Performance Evaluation

The performance of all the models has been evaluated using the Root Mean Square Error (RMSE) and correlation coefficient. The global statistics Root Mean Squared Error and Correlation Coefficients (Legates and McCabe, 1999; Harmel and Smith, 2007) are usually used for model calibration or comparison of different models. The Root Mean Square Error (RMSE) (also called the Root Mean Square Deviation, RMSD) is a frequently used measure of the

difference between the values predicted by a model and the values actually observed from the environment that is being modelled. These individual differences are also called residuals, and the RMSE serves to aggregate them into a single measure of predictive power. The RMSE of a model prediction with respect to the estimated variable X_{model} is defined as the square root of the mean squared error. The RMSE can be estimated by

$$RMSE = \sqrt{\frac{\sum_{i=1}^{n}(X_{obs,i} - X_{model,i})^2}{n}} \quad (28)$$

where X_{obs} is observed values and X_{model} is modelled values at time/place i.

Correlation-often measured as a correlation coefficient – indicates the strength and direction of a linear relationship between two variables (for example model output and observed values). A number of different coefficients are used for different situations. The best known is the Pearson product-moment correlation coefficient (also called Pearson correlation coefficient or the sample correlation coefficient), which is obtained by dividing the covariance of the two variables by the product of their standard deviations. If we have a series n observations and n model values, then the Pearson product-moment correlation coefficient can be used to estimate the correlation between model and observations.

$$r = \frac{\sum_{i=1}^{n}(x_i - \bar{x}).(y_i - \bar{y})}{\sqrt{\sum_{i=1}^{n}(x_i - \bar{x})^2 . \sum_{i=1}^{n}(y_i - \bar{y})^2}} \quad (29)$$

The correlation is +1 in the case of a perfect increasing linear relationship, and -1 in case of a decreasing linear relationship, and the values in between indicates the degree of linear relationship between for example model and observations. A correlation coefficient of 0 means the there is no linear relationship between the variables.

CHAPTER~5
RSULTS AND DISCUSSION

This chapter describes the results obtained using time series analysis of rainfall-runoff data, rainfall-runoff modeling using HEC-HMS (SCS-CN) and ANN technique, and flood inundation modeling using HEC-GeoRAS and other linear/nonlinear models.

5.1 Time Series Analysis of Rainfall-Runoff

5.1.1 Inter-station correlation of rainfall data

As discussed earlier, time series analysis was done prior to rainfall-runoff and flood inundation modeling. The rainfall data cross-correlation obtained in STATISTICA software is shown in Table 2. It has been observed that no good correlation among any two raingauge stations exists due to different terrain, topography, and land use. The best correlation (0.56) has been observed between Baltara and Kursela rainfall data, followed by Dharan and Biratnagar having correlation (0.54). Keeping this in view, satellite based TRMM data are used sometimes to substantiate the point rainfall and to estimate the rainfall of different locations.

Similarly, correlation matrix between discharge sites was observed and is shown in Table 3. Highest correlation (0.59) has been found between Bhimnagar and Baltara as shown in Table 3. Barahkshetra and Bhimnagar shows poor correlation (0.36) as Barahkshetra lies in the mountain region and Bhimnagar lies in relatively plain area.

Table 2: Correlation Matrix between the Raingauge Stations

Stations	Taplejung	Okhaldunga	Dhankutta	Dharan	Biratnagar	Birpur	Basua	Baltara	Kursela
Taplejung	1.00	0.50	0.40	0.34	0.37	0.24	0.14	0.01	0.05
Okhaldunga	0.50	1.00	0.31	0.33	0.41	0.19	0.18	0.11	0.03
Dhankutta	0.40	0.31	1.00	0.47	0.50	0.34	0.25	0.09	0.15
Dharan	0.34	0.33	0.47	1.00	0.54	0.25	0.14	0.09	0.04
Biratnagar	0.37	0.41	0.50	0.54	1.00	0.28	0.14	0.13	0.11
Birpur	0.24	0.19	0.34	0.25	0.28	1.00	0.38	0.20	0.23
Basua	0.14	0.18	0.25	0.14	0.14	0.38	1.00	0.40	0.44
Baltara	0.01	0.11	0.09	0.09	0.13	0.20	0.40	1.00	0.56
Kursela	0.05	0.03	0.15	0.04	0.11	0.23	0.44	0.56	1.00

Table 3: Correlation Matrix between the Discharge Stations

Station	Barahkshetra	Bhimnagar	Baltara
Barahkshetra	1.00	0.36	0.15
Bhimnagar	0.36	1.00	0.59
Baltara	0.15	0.59	1.00

5.1.2 Basic statistics

Daily rainfall data from the meteorological station in Kosi Basin are analyzed for the years from 2005 to 2009. Basic statistical analyses were conducted on the seasonal rainfall data including the mean, median, mode, minimum, maximum variance, standard deviation, coefficient of variance, skewness and kurtosis. Table 4 summarizes the basic descriptive statistical measures of seasonal rainfall data.

Highest mean rainfall 12.38 mm is found at Dharan raingauge station. The values of mode and minimum for all stations are zero. For a symmetrical distribution the mean and the median should be similar. Here distribution is skewed to the right, as median < mean. Maximum rainfall 126.2 mm observed at Okhaldunga station. The values of standard deviation are found greater

than mean values. A large value of standard deviation indicates that the observed values are spread over a larger range. The skewness for a normal distribution is zero, and any symmetric data should have skewness near zero. All stations have positive values of skewness which indicate that data are skewed to the right. The standard normal distribution has a kurtosis of zero. Here positive kurtosis indicates a peaked distribution.

Table 4: Basic statistics of rainfall data

	Taplejung	Okhaldunga	Dhankutta	Dharan	Biratnagar	Birpur	Basua	Baltara	Kursela
Mean	9.18	9.82	5.92	12.38	9.27	7.26	7.77	7.21	7.23
Median	4.50	1.70	0.60	2.30	1.00	0.50	0.00	0.00	0.50
Mode	0.00	0.00	0.00	0.00	0.00	0.00	0.00	0.00	0.00
Minimum	0.00	0.00	0.00	0.00	0.00	0.00	0.00	0.00	0.00
Maximum	95.40	126.20	125.80	102.40	99.60	90.60	98.20	115.00	122.40
Variance	194.93	288.08	167.09	428.57	332.63	234.72	282.47	248.07	250.89
Std. Deviation	13.96	16.97	12.93	20.70	18.24	15.32	16.81	15.75	15.84
Coef. of Variance	152.12	172.84	218.33	167.28	196.71	210.97	216.38	218.45	219.23
Skewness	2.87	2.80	3.75	2.30	2.81	3.14	3.11	3.42	3.37
Kurtosis	10.28	9.74	19.68	5.23	8.21	10.52	10.30	13.71	13.23

Table 5 summarizes the basic descriptive statistical measures of seasonal runoff data. For discharge data, highest values of mean, median, mode, maximum, variance, standard deviation and coefficient of variance are found at Bhimnagar at station. Bhimnagar stations getting water from Barahkshetra station and some other streams. Baltara station shows minimum values for all parameters except skewness. The flow is regulated at Baltara, so indicating low flow rate. The detailed graphs and data of basic statistics are shown in Appendix I.

Table 5: Basic statistics of discharge data

	Barahkshetra	Bhimnagar	Baltara
Mean	33960.71	50570.32	2170.94
Median	31000.00	48436.00	2105.00
Mode	20540.00	43067.00	2195.00
Minimum	11425.00	1577.50	1055.00
Maximum	82190.00	134793.00	3732.50
Variance	203150445.69	716555188.12	388127.41
Std. Deviation	14253.09	26768.55	623.00
Coef. of Variance	41.97	52.93	28.70
Skewness	0.85	0.28	0.62
Kurtosis	0.30	-0.11	-0.42

5.1.3 Estimating spatial distribution of rainfall

For estimating impact of rainfall over the entire basin, point rainfall data were transformed to the aerial rainfall using Arithmetical average method and Thiessen polygon method (equation 1 and 2). The Isohyet method especially used when the stations are large in number. Thiessen polygon method is used widely to calculate average precipitation over a catchment area as some weightage is given to the various stations on a rational basis. The basin area lying in each raingauge is shown in Figure 12. Thiessen Polygon map was generated using ArcGIS Desktop 9.3 software. The mean rainfall over the Kosi Basin has been estimated knowing the Thiessen weights of each station and using (equation 2). Thiessen mean rainfall over Kosi Basin is shown in Figure 13.

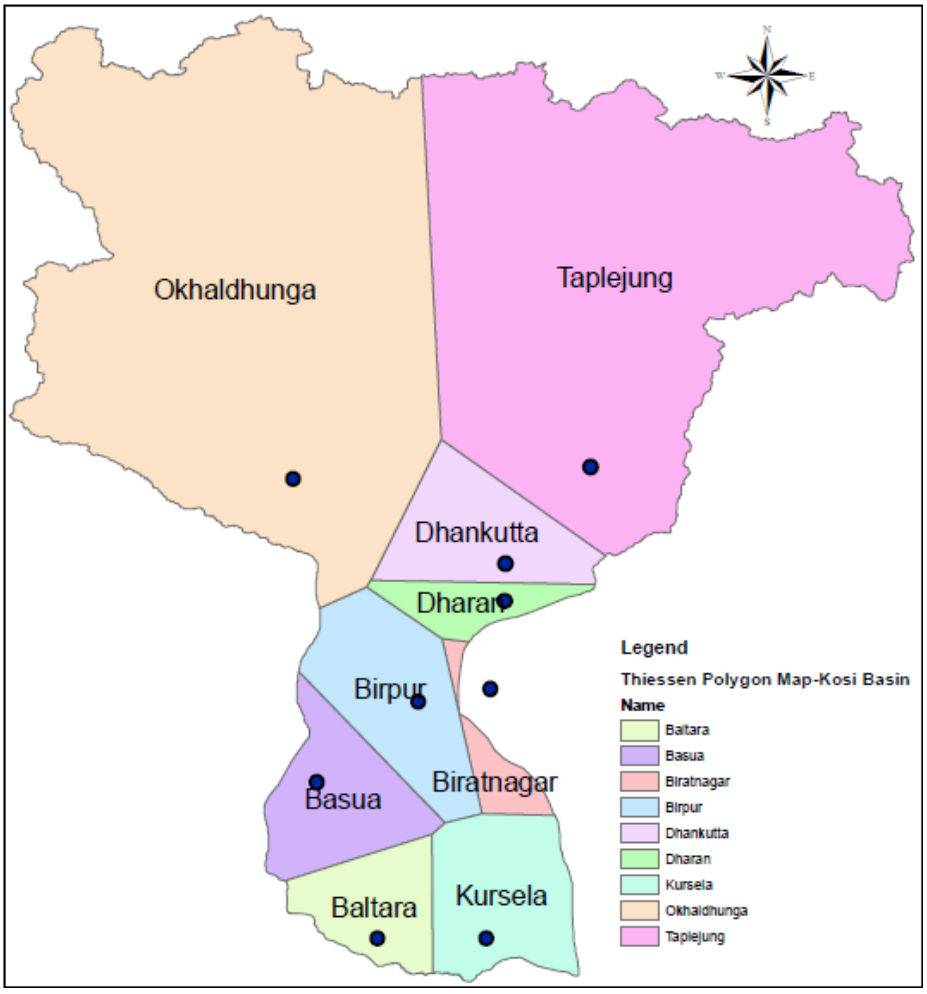

Figure 12: Thiessen Polygon Map Kosi Basin

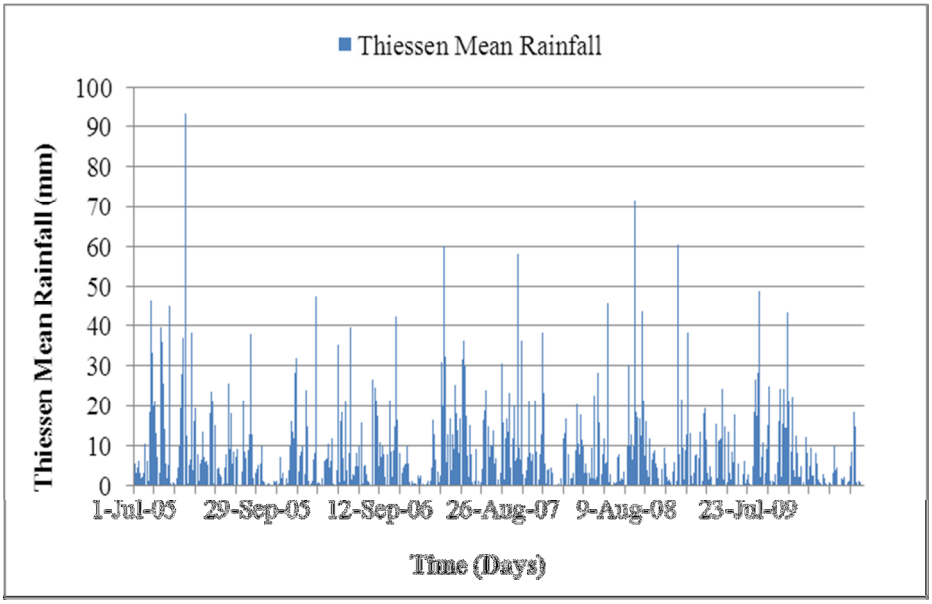

Figure 13: Thiessen Mean Rainfall over Kosi Basin

5.1.4 Upstream-downstream discharge regression analysis

Regression models have been developed to obtain downstream discharge, knowing the upstream discharge for all the three discharge measuring sites using equations 4 to 7. Modified discharge data were used for analysis. It has been observed that no model is showing good result and no relationship exists between discharge of upstream and downstream stations as shown in Figure 14(a-c).

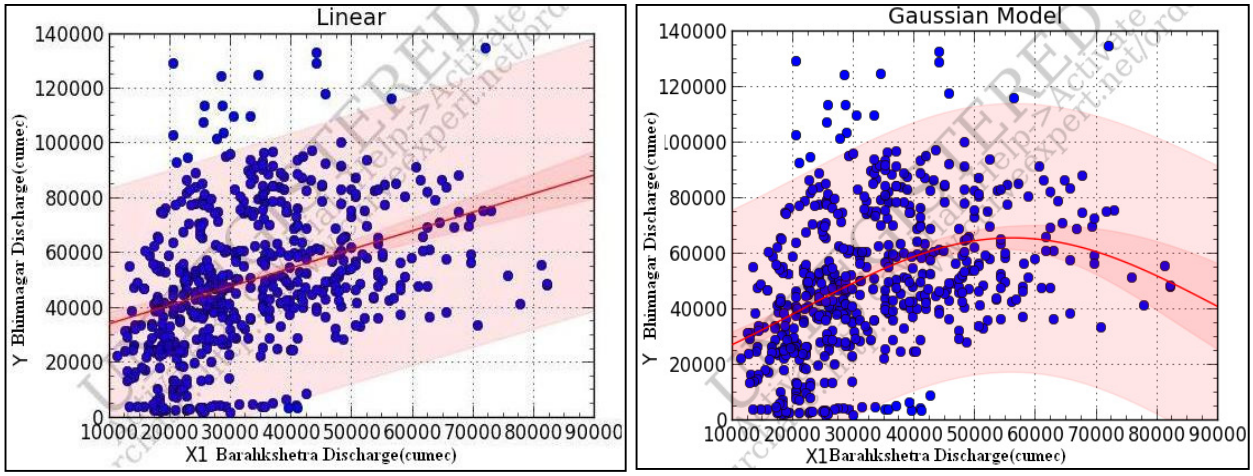

$y = 2.7501 + 6.7927x$, (r^2=0.1308) $y = 6.5836e^{\frac{-(x-5.6112)^2}{2*3.4857^2}}$, ($r^2$=0.1615)

(a) Barahkshetra-Bhimnagar

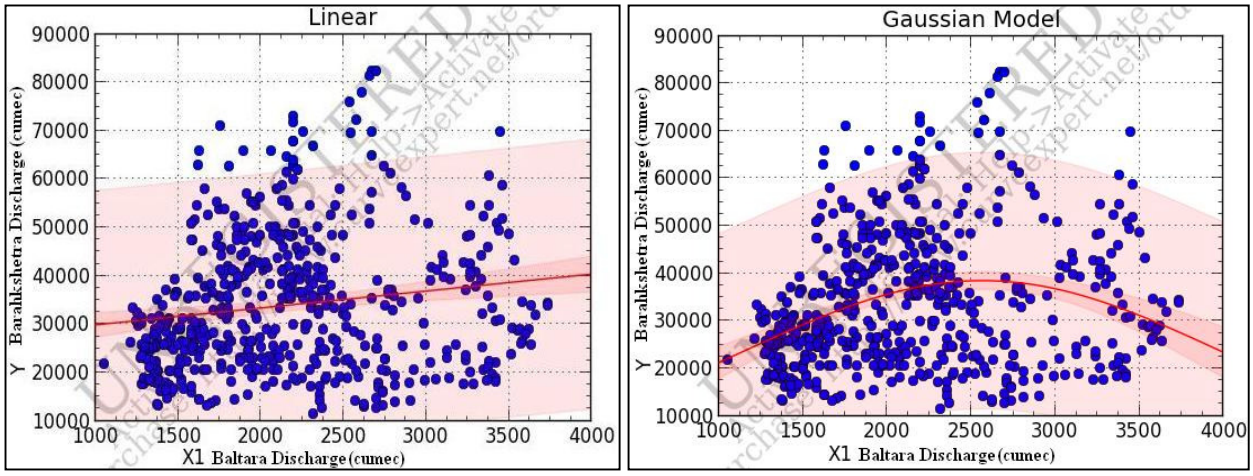

$y = 2.6357 + 3.5021x$, (r^2=0.0234) $y = 3.8485e^{\frac{-(x-2.5658)^2}{2*1.4361^2}}$, ($r^2$=0.0778)

(b) Barahkshetra-Baltara

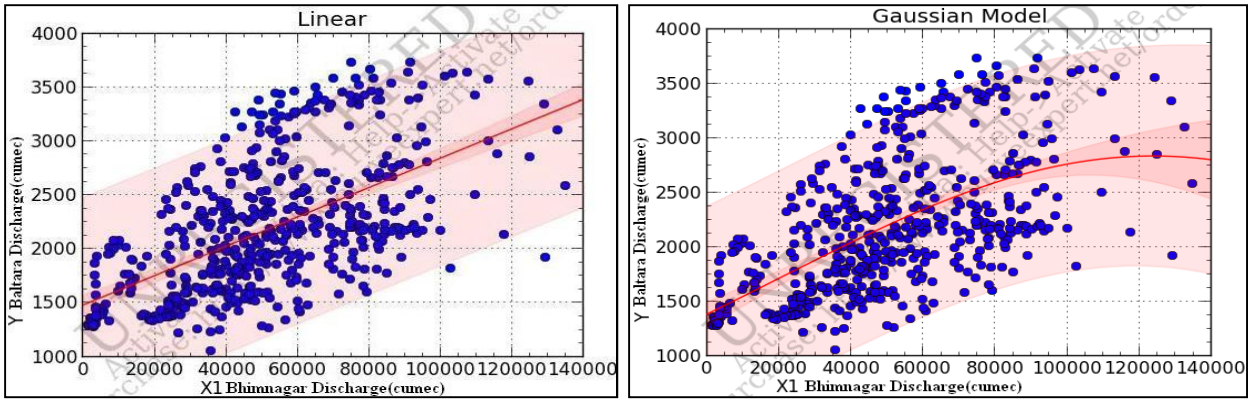

$y = 1.4816 + 1.3630x$, (r^2=0.3429)

$y = 2.8398e^{\frac{-(x-1.2378)^2}{2*1.1034^2}}$, (r^2=0.3532)

(c) Bhimnagar-Baltara

Figure 14: Relationship between upstream-downstream discharge data

5.1.5 Relationship between water level and discharge data

To obtain rating curve, a relationship between the water level and modified discharge at three locations were developed. The relationship between discharge and water level at Barahkshetra gage site is found to be very poor (with r^2=0.2361) due to various reasons. Bhimnagar gage site shows reasonably better results for discharge and water level relationship (r^2=0.5120). It has been observed that both Gaussian model and Power function model are showing good results for Baltara discharge measuring site with r^2=0.9974 and r^2=0.9970 respectively. Rating curves are shown in the Figure 15(a-d) for Barahkshetra, Bhimnagar and Baltara gage sites.

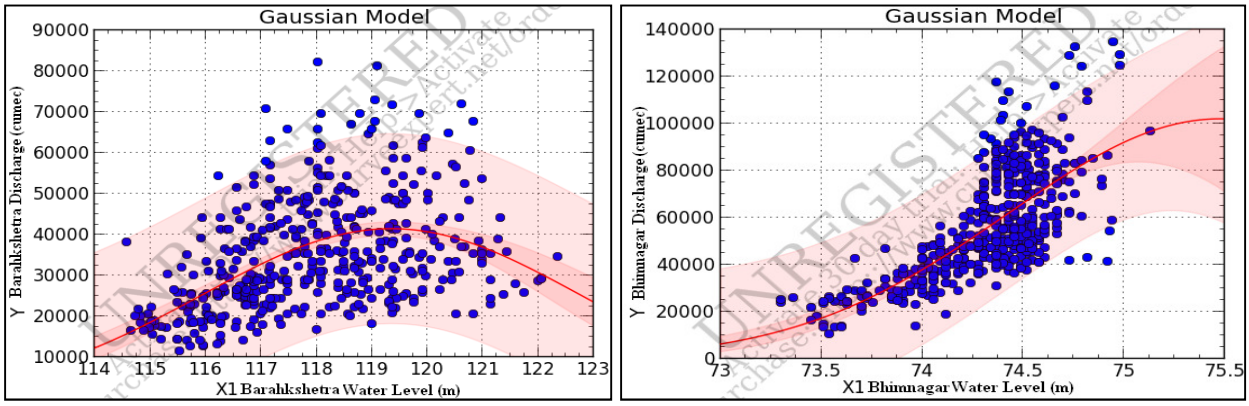

$y = 4.1493e^{\frac{-(x-1.1934)^2}{2*3.4271^2}}$, (r^2=0.2361)

$y = 1.0217e^{\frac{-(x-7.5475)^2}{2*1.0488^2}}$, (r^2=0.5120)

(a) Barahkshetra **(b) Bhimnagar**

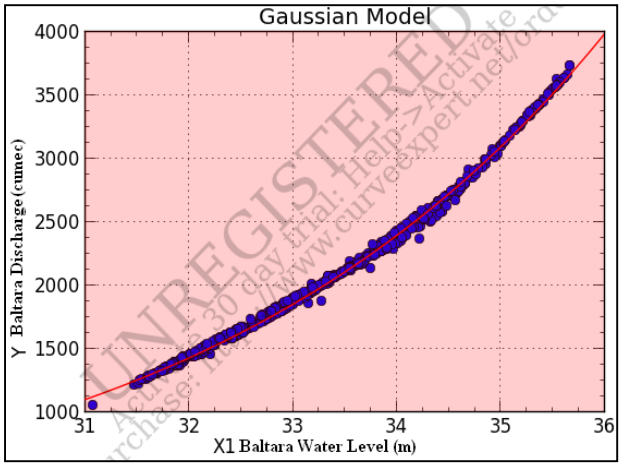

$y = 1.1762e^{\frac{-(x-1.7201)^2}{2*2.3191^2}}$, ($r^2$=0.9974)

(c) Baltara (Gaussian model)

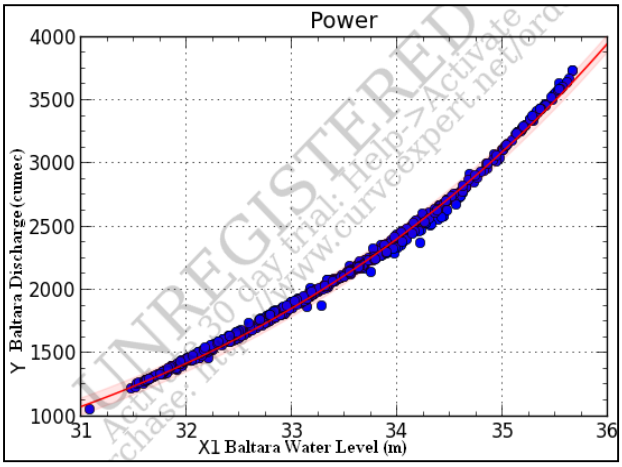

$y = 1.1912x^{8.6879}$, (r^2=0.9970)

(d) Baltara (Power function model)

Figure 15: Relationship between water level and discharge

5.1.6 Rainfall-runoff linear and non-linear correlation

Prior to the use of rainfall-runoff models, simple regression model has been attempted to obtain discharge, knowing the mean rainfall over the entire basin using equations 4 to 7. All possible linear and non-linear models were tested for their applicability to predict runoff with known rainfall values. It can be seen from the Figure 16 that in all the cases rainfall-runoff relationship are very poorly correlated for Thiessen mean rainfall data over the entire basin. Relationships obtained using individual stations and arithmetic mean methods are shown in Appendix II. Therefore, rainfall-runoff models with different input variables were attempted and are discussed later.

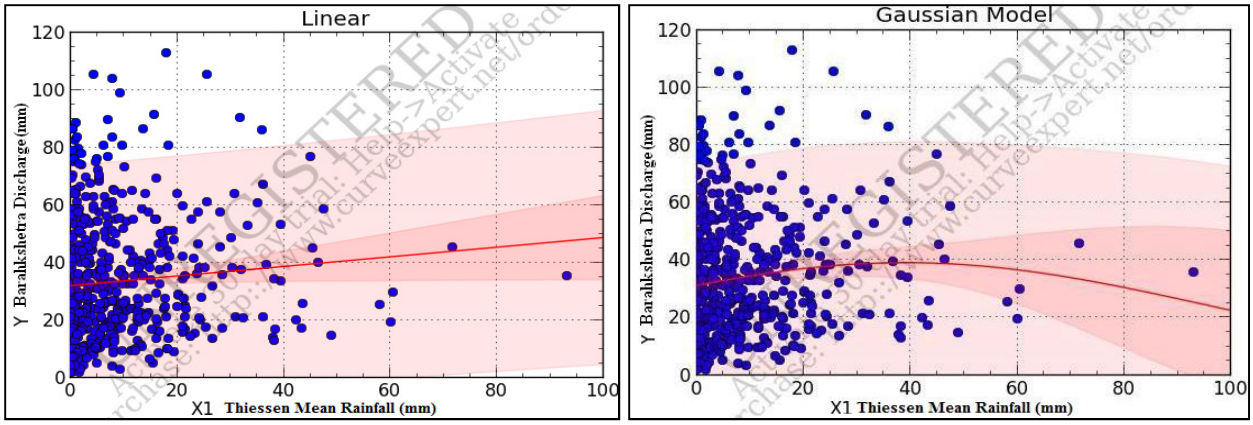

$y = 3.2126 + 1.6730x$, (r^2=0.00787) $y = 3.9084e^{\frac{-(x-3.8987)^2}{2*5.7993^2}}$, ($r^2$=0.01185)

(a) Barahkshetra

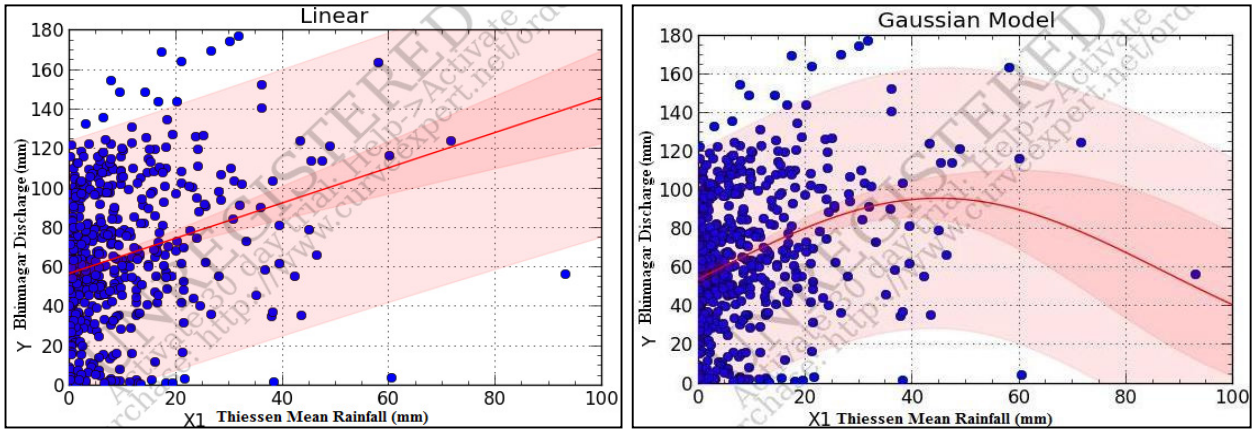

$y = 5.7059 + 8.9336x$, (r^2=0.08065) $y = 9.5906e^{\frac{-(x-4.4889)^2}{2*4.2043^2}}$, ($r^2$=0.10136)

(b) Bhimnagar

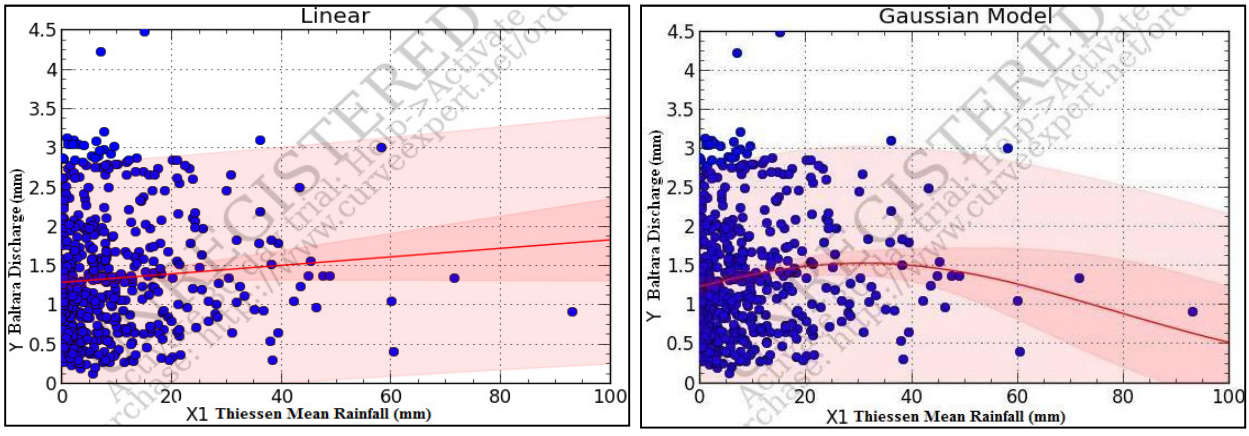

$y = 1.2948 + 5.4144x$, (r^2=0.00645) $y = 1.5371e^{\frac{-(x-3.0876)^2}{2*4.6937^2}}$, ($r^2$=0.01659)

(c) Baltara

Figure 16: Thiessen mean Rainfall Vs Runoff

5.2 Rainfall-Runoff Modelling

5.2.1 HEC-HMS and HEC-GeoHMS Model

The input data required for modeling were downloaded, analysed and delineated using ERDAS-Imagine and Arc-GIS. SRTM 90m Digital Elevation Model (DEM) of the Kosi Basin has been used as input data to generate HEC-HMS model input files (Figure 17a). Fill sinks, Flow direction, flow accumulation, stream definition and catchment grid delineation, catchment polygon, watershed aggregation, project setup, stream and sub-basin characteristics, HEC-HMS schematic maps are shown in Figure 17 (a-l). The detail procedures of HEC-GeoHMS and HEC-HMS process have been discussed earlier in Chapter 4.

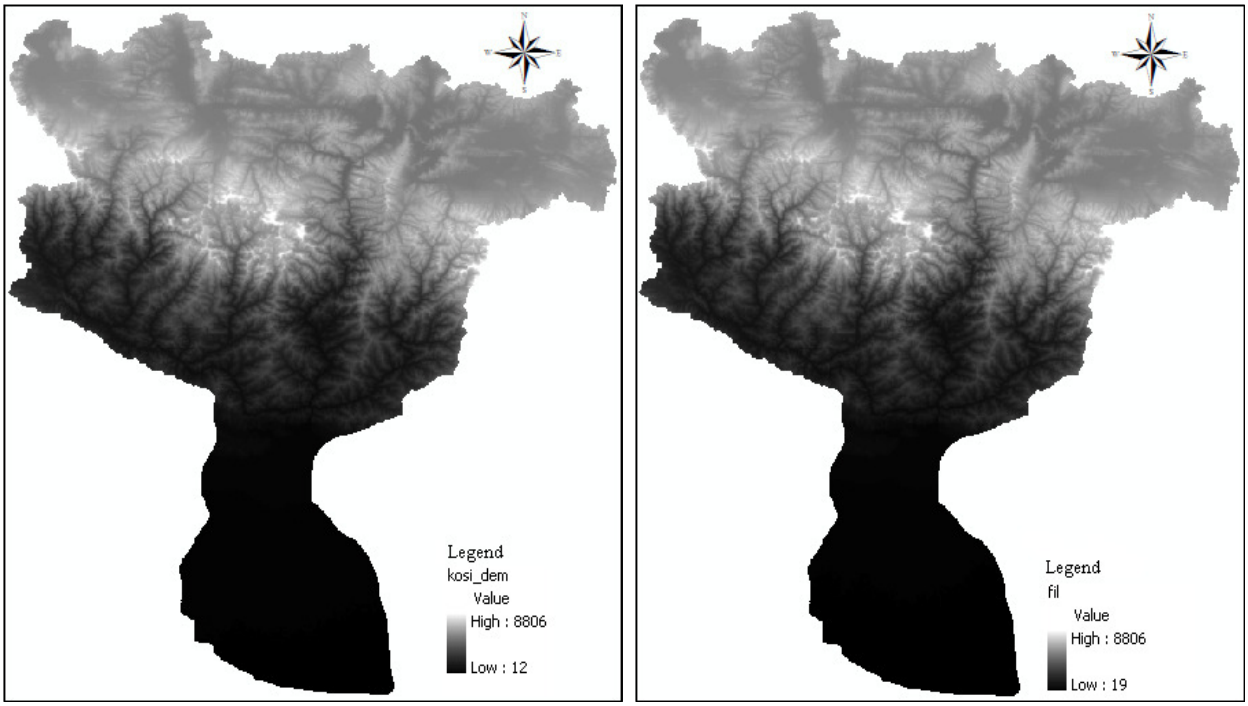

(a) Kosi Basin SRTM 90m DEM **(b) Fill DEM**

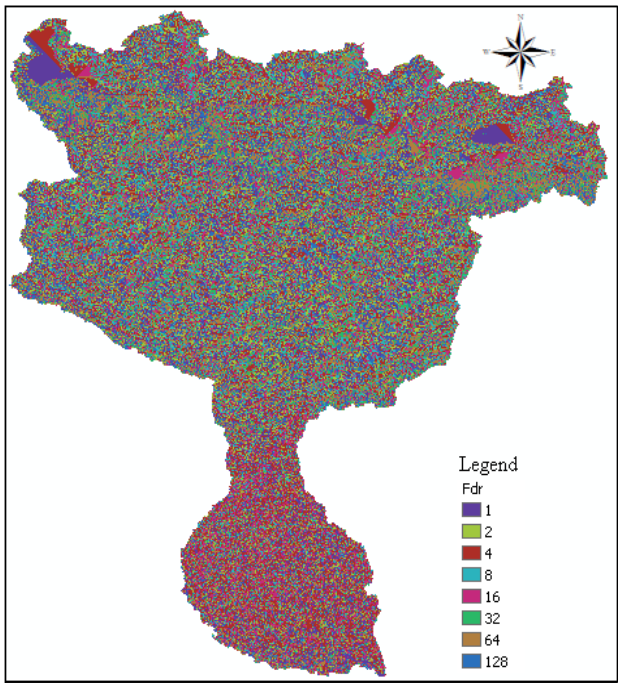

(c) Flow Direction Map

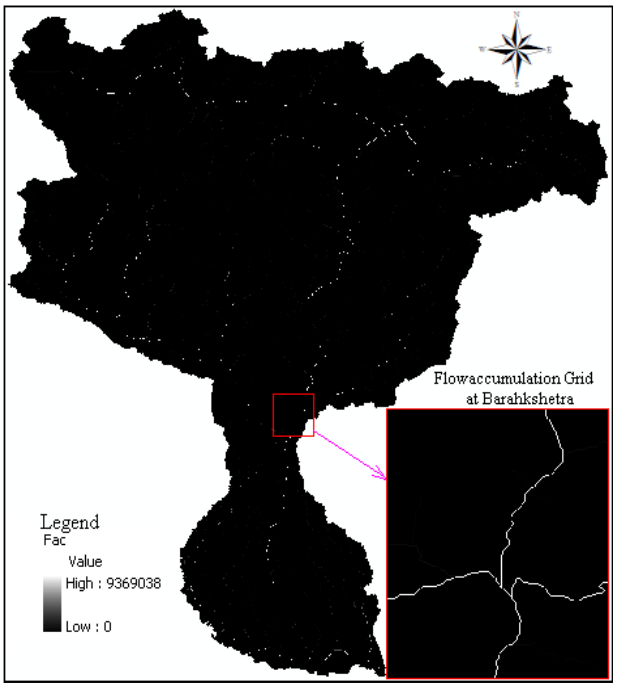

(d) Flow Accumulation Map

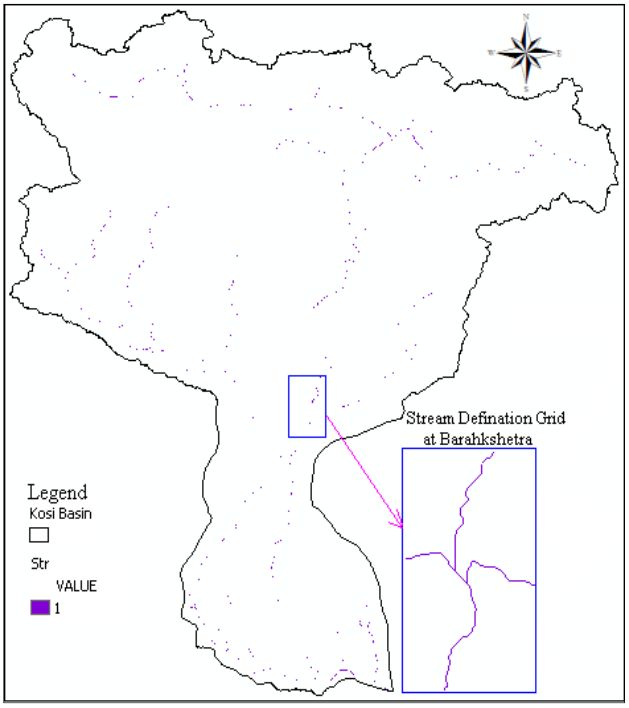

(e) Stream Definition

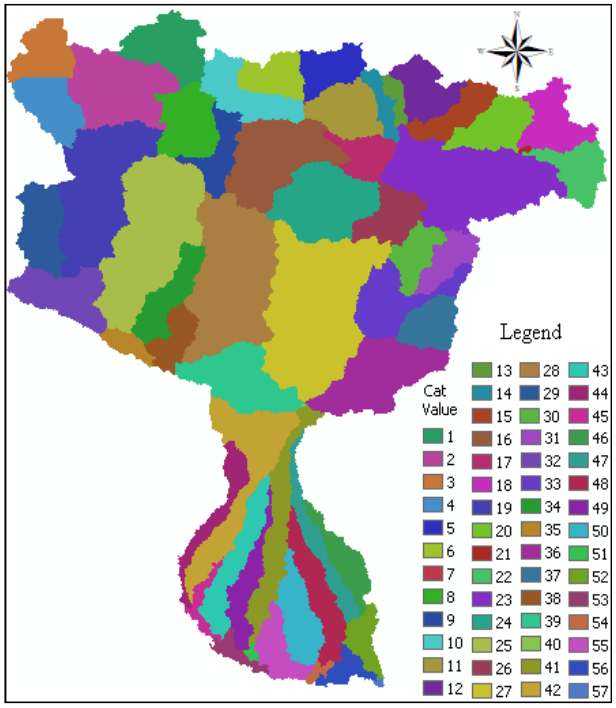

(f) Basin Catchment

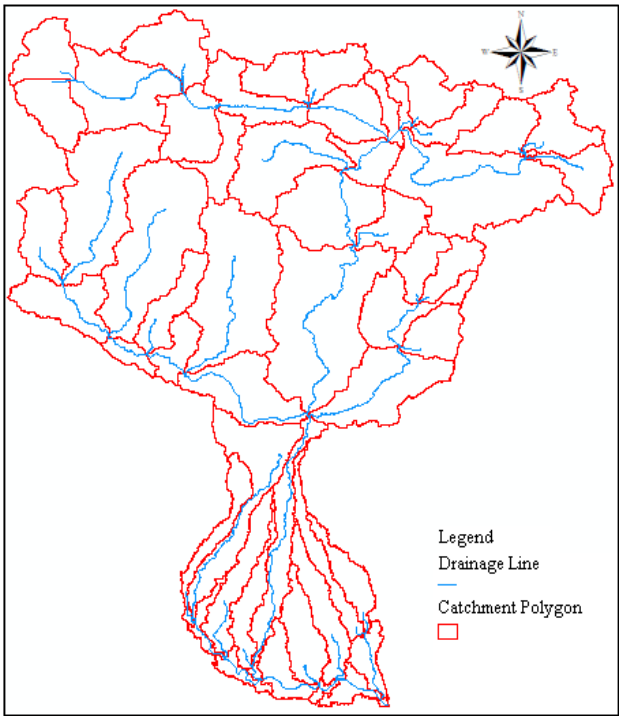

(g) Catchment Polygon & Drainage Line

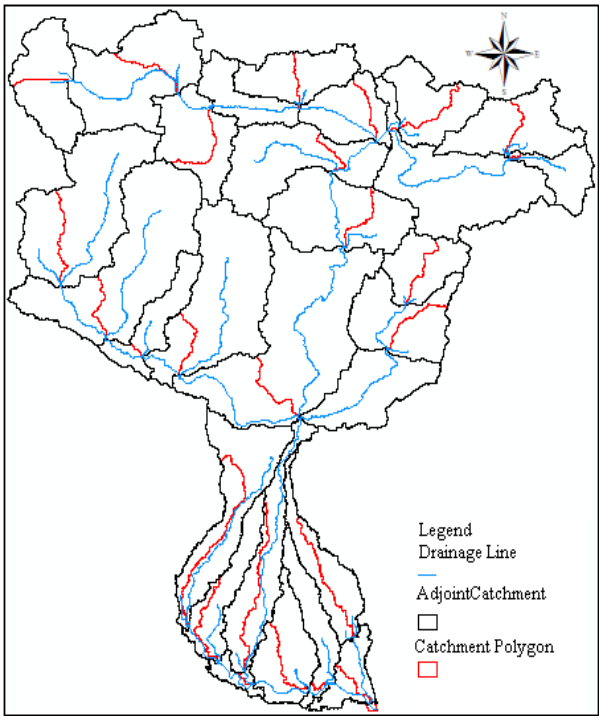

(h) Adjoint Catchment

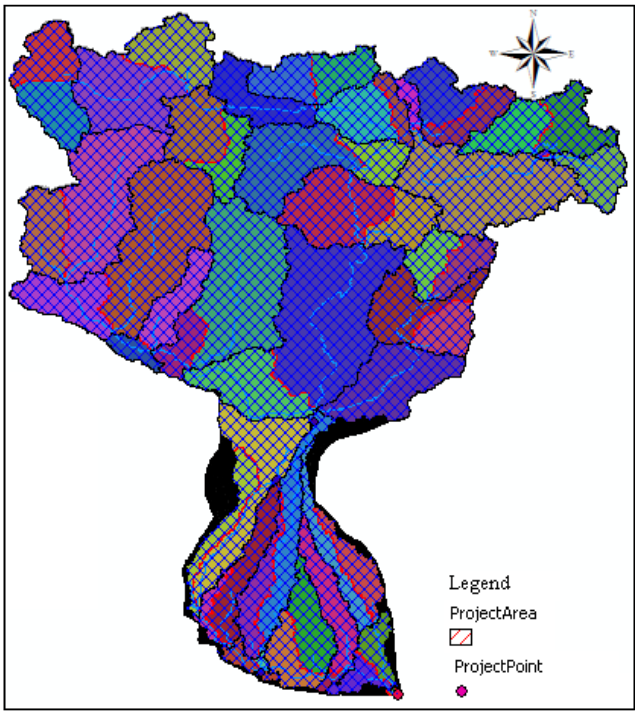

(i) Project Area

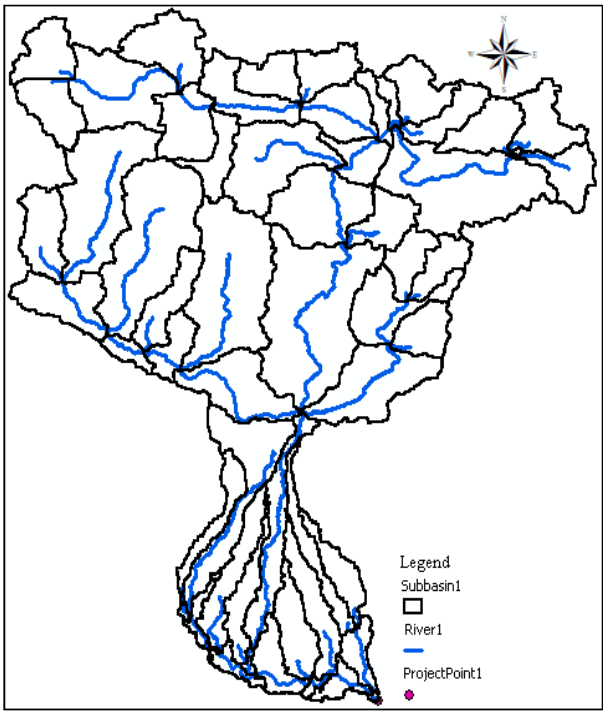

(j) Subbasins

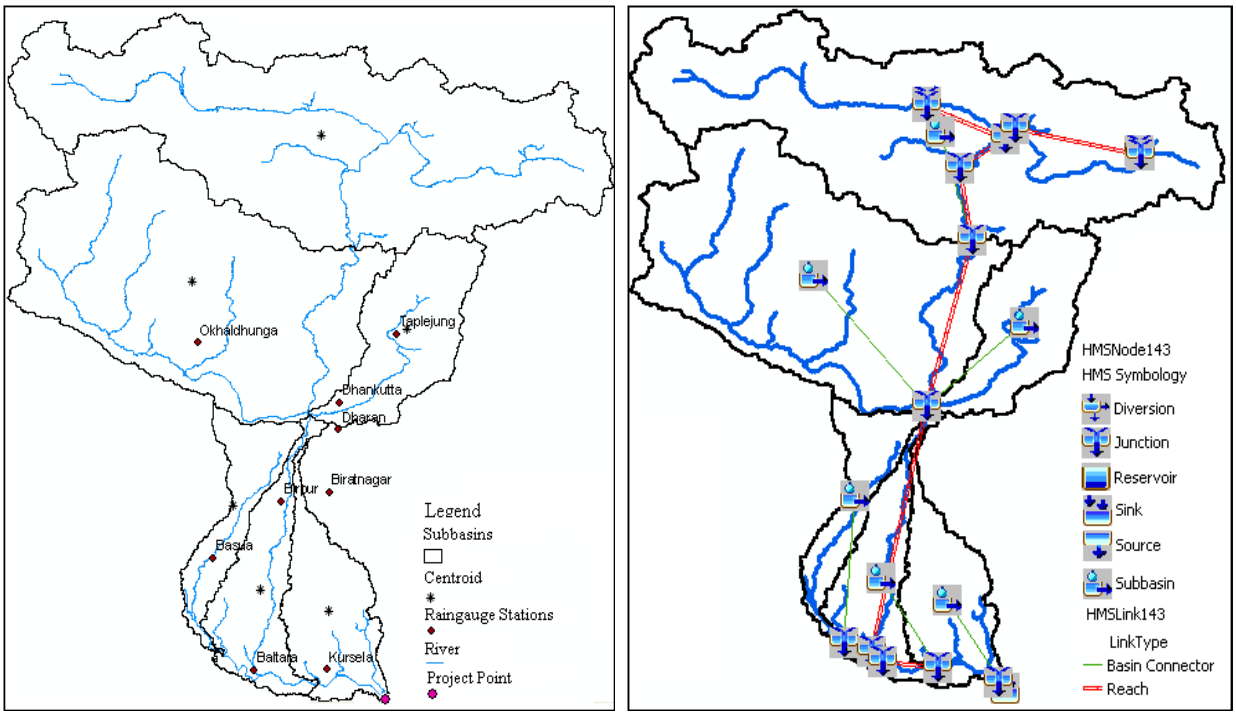

(k) Subbasins merge, Centroid & Raingauge Stations **(l) HMS Schematics**

Figure 17: HEC-GeoHMS Process Maps

The HEC-HMS model was run with SCS-CN method to estimate daily runoff from daily rainfall data (provided station wise) by selecting proper model parameters. After detailed study, the parameters used are (a) Antecedent Moisture Conditions-I, II, III (AMC), (b) Hydrologic Soil Group (HSG B & C), (c) Curve Number, (d) DEM, and (e) land use. The curve numbers obtained using above parameters for different AMCs are shown in Table 6. The results obtained using SCS-CN methods are shown in Figures 18, 19 and 20.

Table 6: Hydrologic Soil Group (HSG) and Curve Number (CN)

AMC Type	AMC-I (CN_I)		AMC-II (CN_{II})		AMC-III (CN_{III})	
Discharge Measuring Stations	Hydrological Soil Group		Hydrological Soil Group		Hydrological Soil Group	
	B	C	B	C	B	C
Barahkshetra	22.62	37.71	40	58	60.96	76.38
Bhimnagar	22.62	37.71	40	58	60.96	76.38
Baltara	49.39	58.13	69	76	83.90	88.12

It has been observed from the figure 18(a-e) that the results are very promising for simulating runoff using rainfall data and other information as input in each location. High values of correlation coefficients are obtained for observed and predicted runoff values.

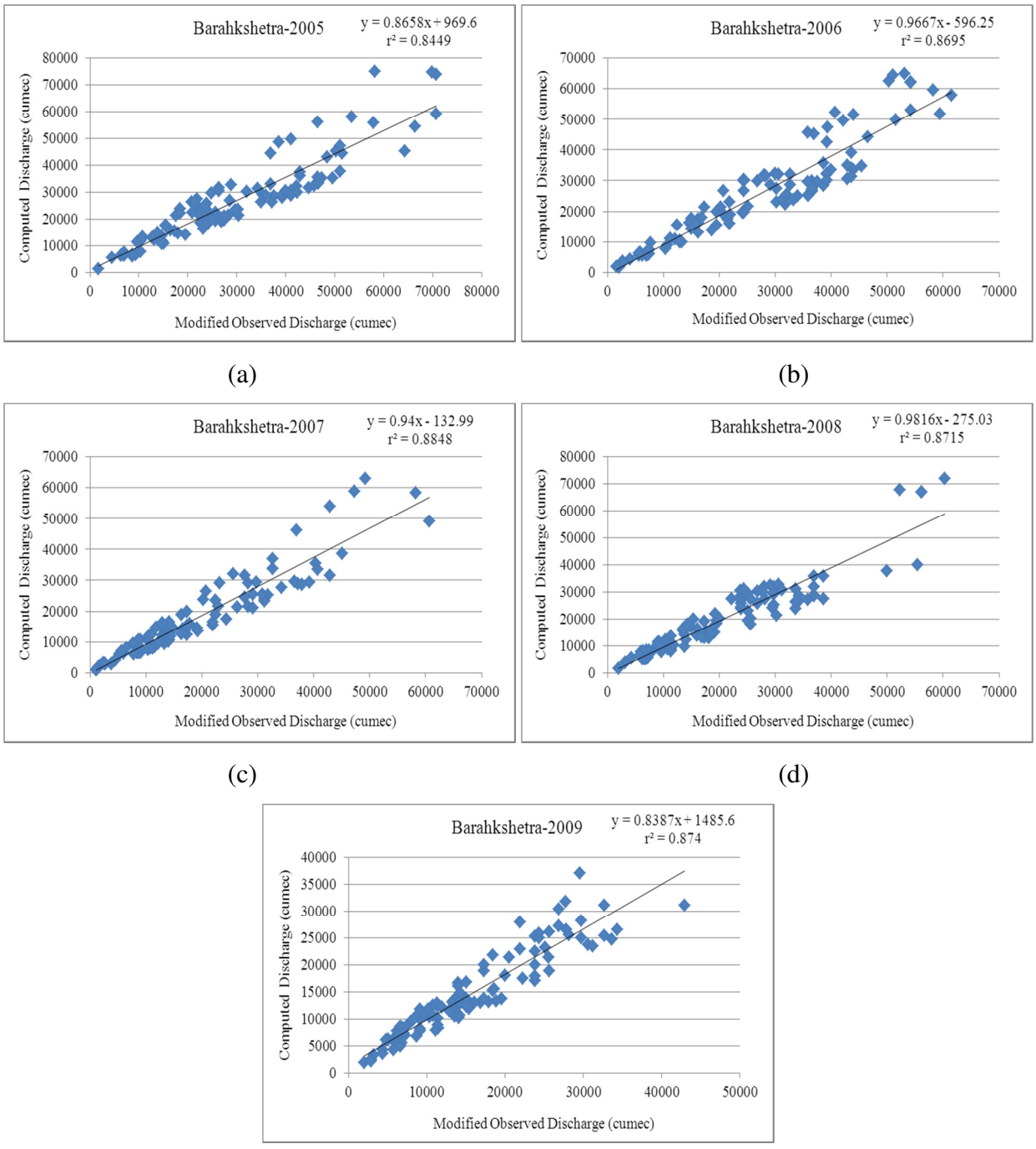

Figure 18: Relationship between observed Vs computed discharge at Barahkshetra (2005-2009)

For Bhimnagar stations the r^2 values are greater than 0.75 which means that results are satisfactory. The results obtained using all the data sets combined together are shown in Appendix III.

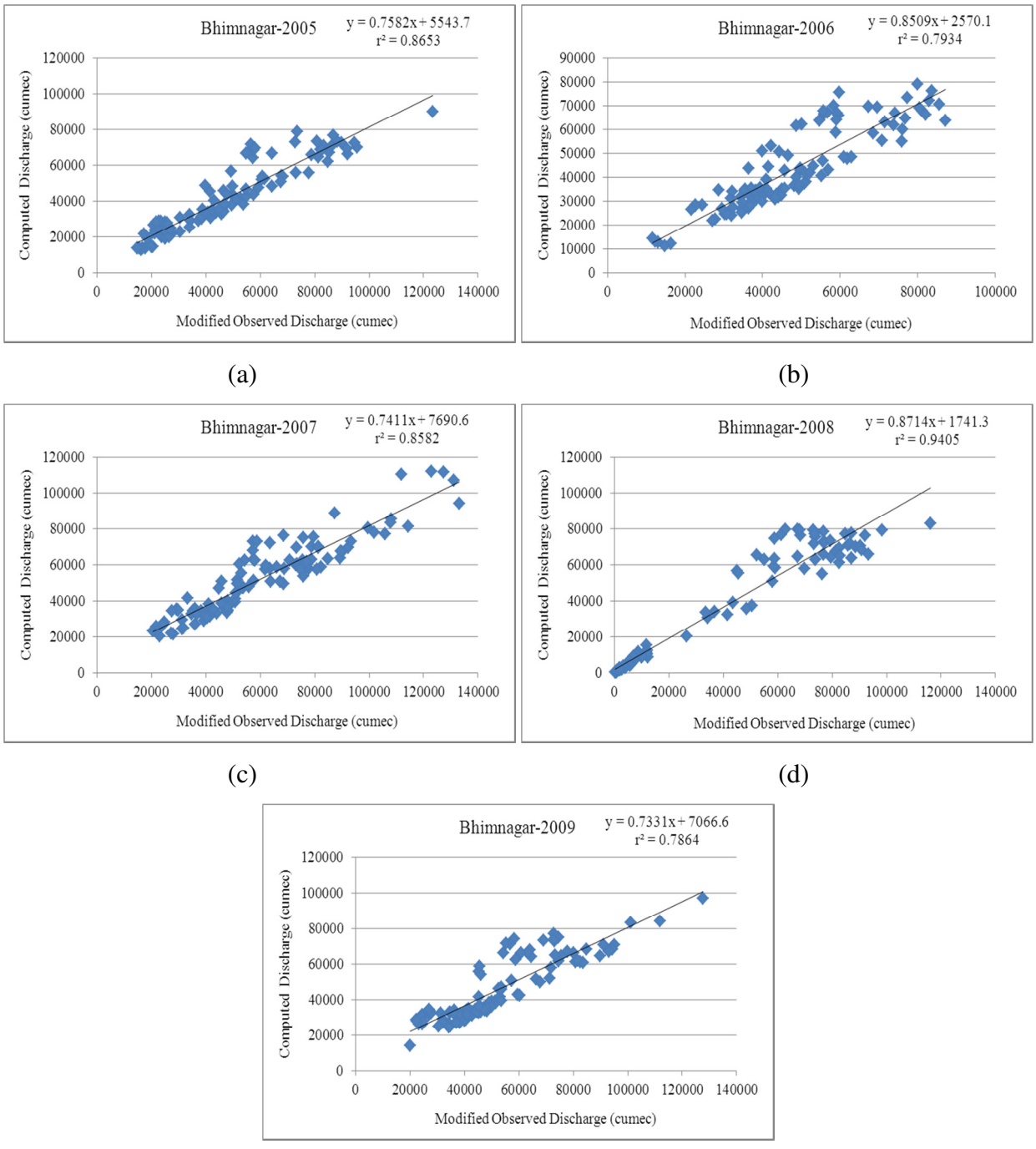

Figure 19: Relationship between observed Vs computed discharge at Bhimnagar (2005-2009)

As seen from the Figure 22(a) r^2 value is highest for the year-2005 (r^2=0.09209) which means the error is least in that year so the accuracy of prediction of runoff is high for the year 2005 and for other years is greater than 0.7 so it gives satisfactory results.

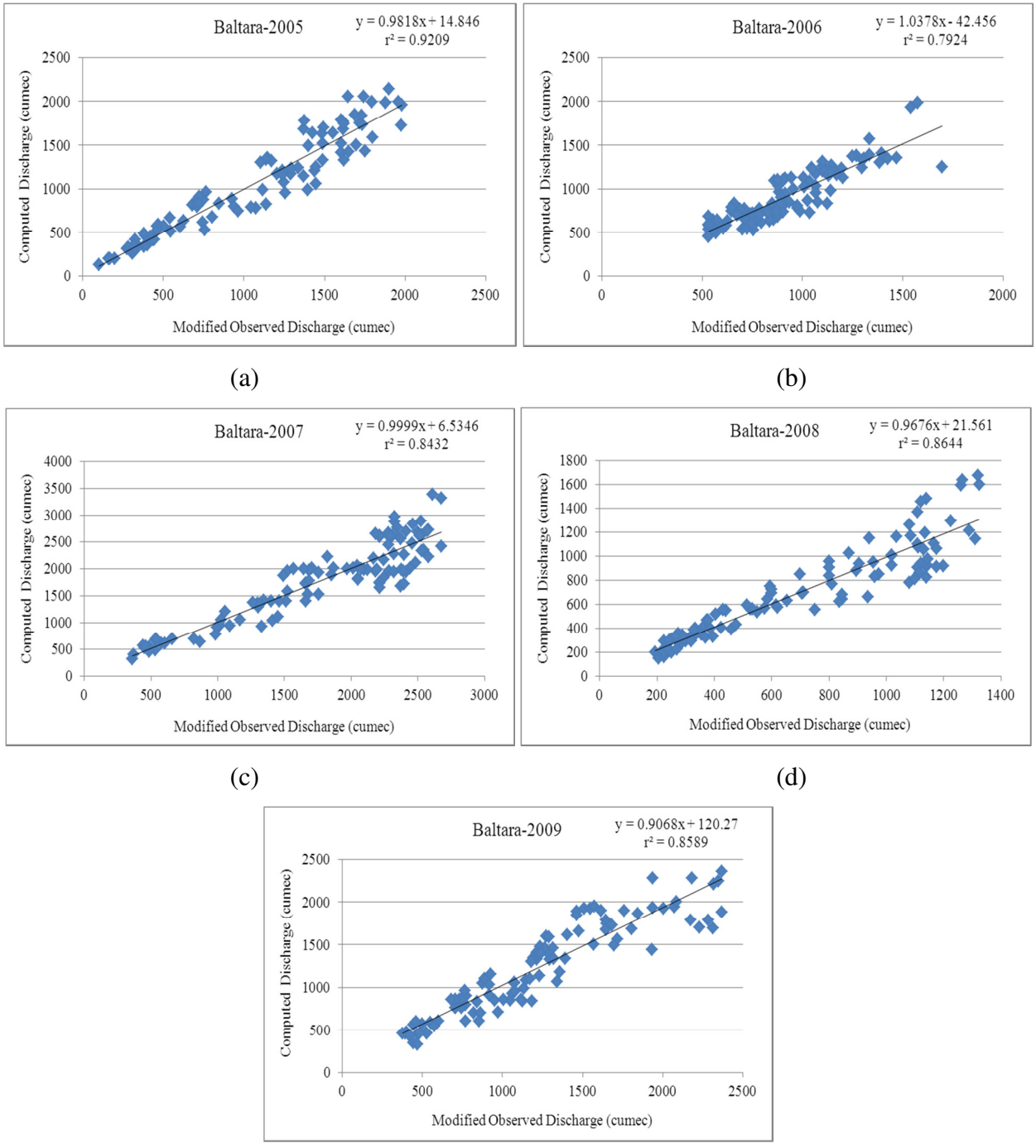

Figure 20: Relationship between observed Vs computed discharge at Baltara (2005-2009)

5.2.2 ANN Model

SCS-CN method used in HEC-HMS requires a large number of input datasets. To overcome that situation, an attempt has been made to use ANN model available in STATISTICA to simulate rainfall-runoff process and predict runoff using rainfall as input for different data combinations as discussed in Chapter 4. MLP and RBF models were used for the analysis and the results are shown in Figures 21 and 22. It has been observed that the results obtained using MLP with BFGS Training Algorithm, SOS Error Function, and Exponential hidden activation shows best simulation. RBF network was used with RBFT Training Algorithm, SOS Error Function, Gaussian Hidden Activation and identity output activation. The r^2 and RMSE values obtained for different MLP network is shown in Table 7. It is clearly visible from Table 7 that for MLP-4 network shows best results for all discharge measuring stations. MLP-6 also shows good results with 3-day lag rainfall and 1-day lag runoff data as input variables. MLP-2 and MLP-7 also shows reasonably good result.

Table 7: The r^2 and RMSE Values for MLP network

Input Variables	Suitable Network	Barahkshetra		Bhimnagar		Baltara	
		(r^2)	RMSE	(r^2)	RMSE	(r^2)	RMSE
Q(t) = {Q(t-1}}	MLP-2	0.7874	9.089	0.9067	10.974	0.9839	0.104
Q(t) = {Q(t-1), Q(t-2)}	MLP-4	0.7995	8.890	0.9080	11.049	0.9919	0.071
Q(t) = {P(t), P(t-1), P(t-2), Q(t-1)}	MLP-6	0.7967	8.873	0.9207	10.035	0.9894	0.082
Q(t) = {P(t), P(t-1), P(t-2), Q(t-1), Q(t-2)}	MLP-7	0.7959	8.997	0.9206	10.049	0.9914	0.075

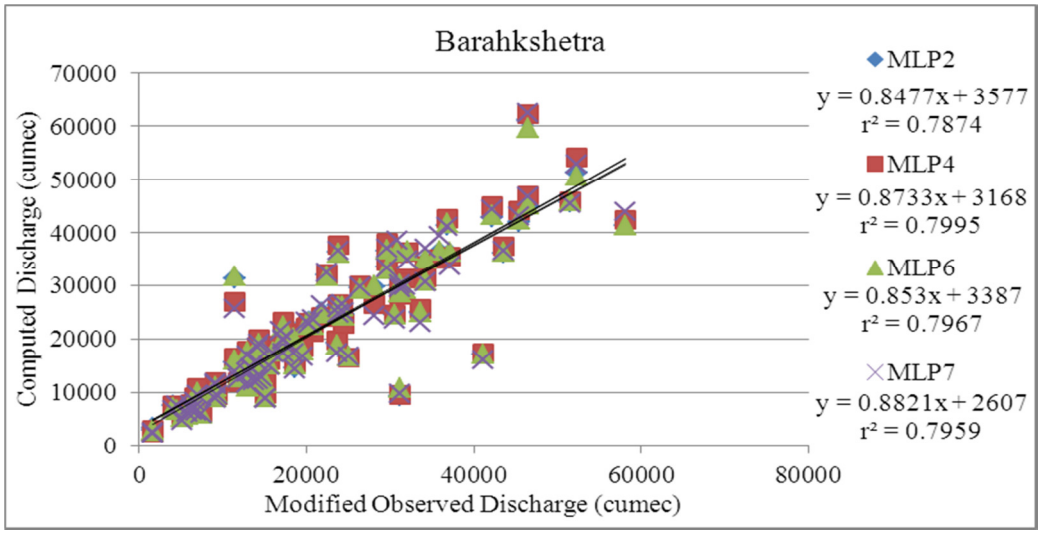

(a)

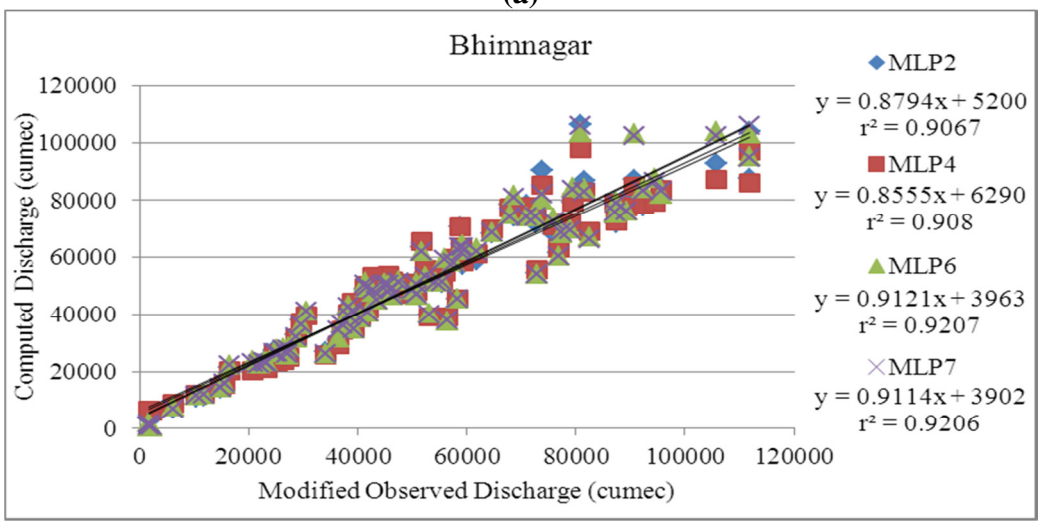

(b)

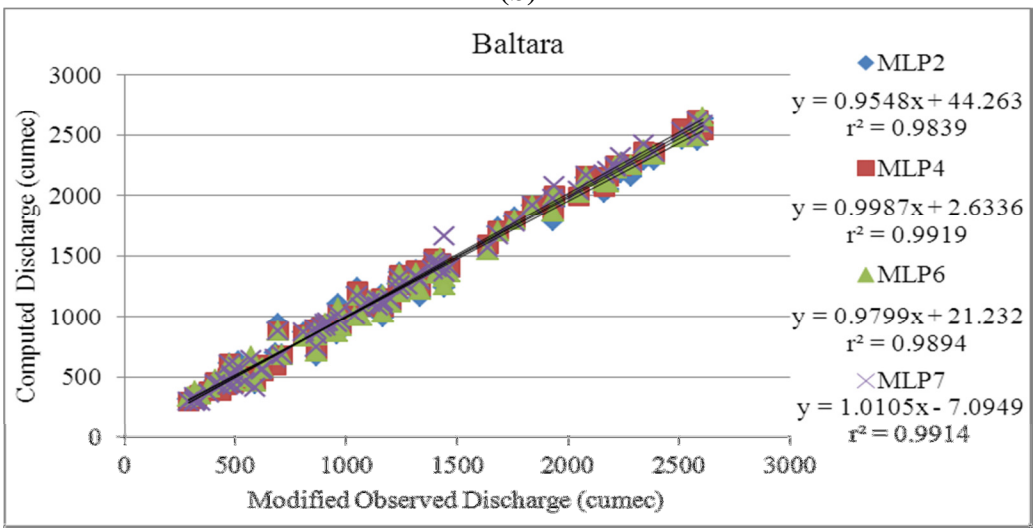

(c)

Figure 21: Relationship between observed and computed discharge (MLP Network)

The r^2 and RMSE values obtained for different RBF network is shown in Table 8. RBF-2, RBF-4, RBF6 and RBF-7 are showing comparable results. However, different RBF networks are suitable at different stations. For Barahkshetra stations RBF-4 shows the best result. RBF-7 shows best results for Bhimnagar station. RBF-2 also shows satisfactory results. Baltara station showing best result for RBF-6 network.

Table 8: The r^2 and RMSE Values for RBF network

Input Variables	Suitable Network	Barahkshetra		Bhimnagar		Baltara	
		(r^2)	RMSE	(r^2)	RMSE	(r^2)	RMSE
Q(t) = {Q(t-1}}	RBF-2	0.7905	8.992	0.8992	11.351	0.9741	0.127
Q(t) = {Q(t-1), Q(t-2)}	RBF-4	0.8117	8.470	0.9055	11.569	0.9190	0.227
Q(t) = {P(t), P(t-1), P(t-2), Q(t-1)}	RBF-6	0.7822	9.180	0.9109	10.632	0.9352	0.222
Q(t) = {P(t), P(t-1), P(t-2), Q(t-1), Q(t-2)}	RBF-7	0.7594	9.715	0.9224	9.915	0.9283	0.214

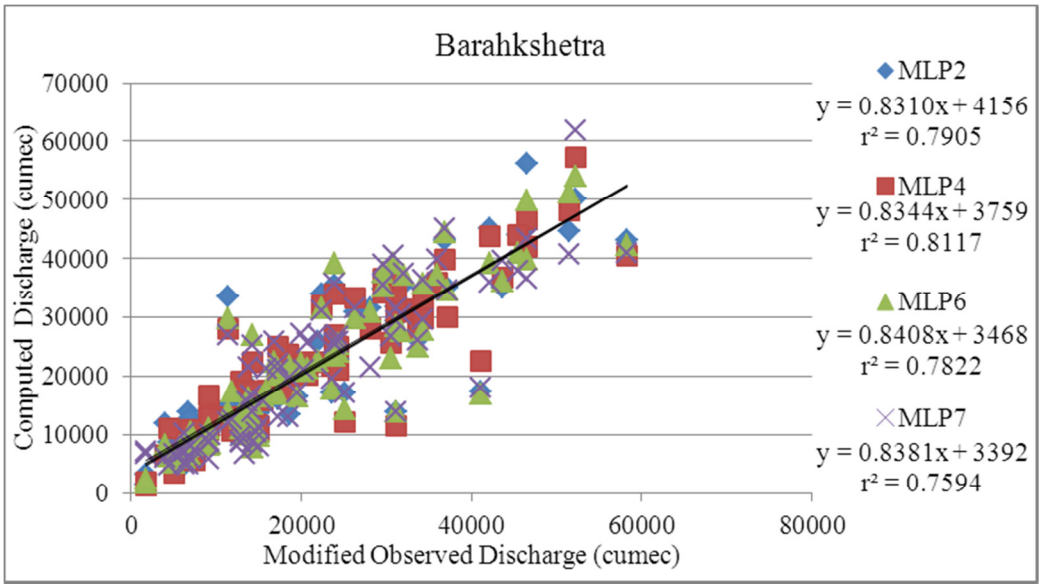

(a)

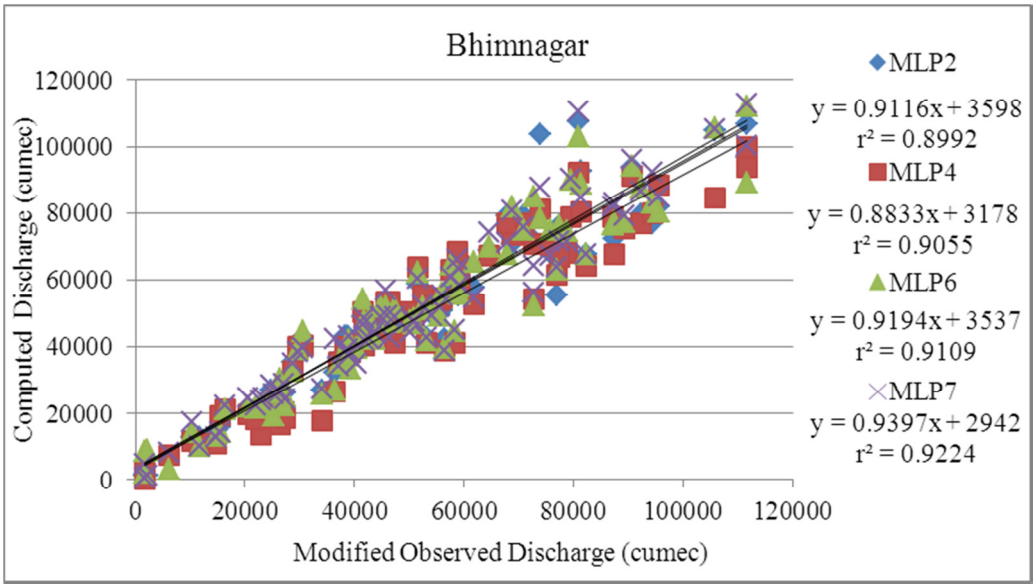

(b)

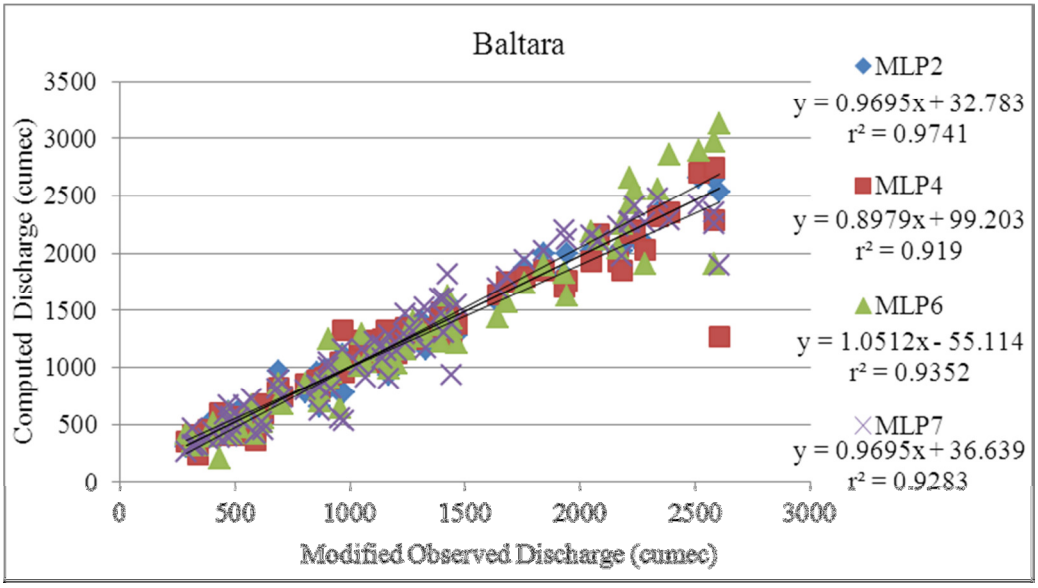

(c)

Figure 22: Relationship between observed and computed discharge (RBF Network)

The results obtained using ANN algorithms are showing comparable results with traditional SCS-CN method used in HEC-HMS with very few input variables. Thus, ANN model may be used in case of non-availability of input data used in SCS-CN method.

5.3 Flood Inundation Modelling

5.3.1 HEC-RAS and HEC-GeoRAS Model

The HEC-RAS model parameters (discharge and water level data using Manning' n value) were calibrated and used to estimate the flood inundation in the channel reach. USGS 30 arc-second Digital Elevation Model (GTOPO30) was downloaded. Digital Elevation Model (DEM) of the Kosi Basin converted into Triangulated Irregular Network (TIN) format using 3-D Analyst tool in ArcGIS 9.3 as shown in Figure 23 for further analysis.

Using the RAS Geometry function stream centreline, river bank, flow path lines, cross-sections have been created as shapes files for preprocessing of the data (Figure 24). The land-use/land-cover map was used to generate the Manning's n values for river and basin. After creating and digitizing all the required layers, GIS data are exported (GIS2RAS) to HEC-RAS. Figure 25 shows geometric data of Kosi River. Discharge data was used as the upstream boundary condition. Normal depth was used as the downstream boundary condition. This boundary condition requires the input of the Energy Grade Line (EGL) slope at the downstream boundary. Daily discharge and water level data were used for analysis. River cross sections were used at 20 km distance each. Rating curve is shown in Figure 26.

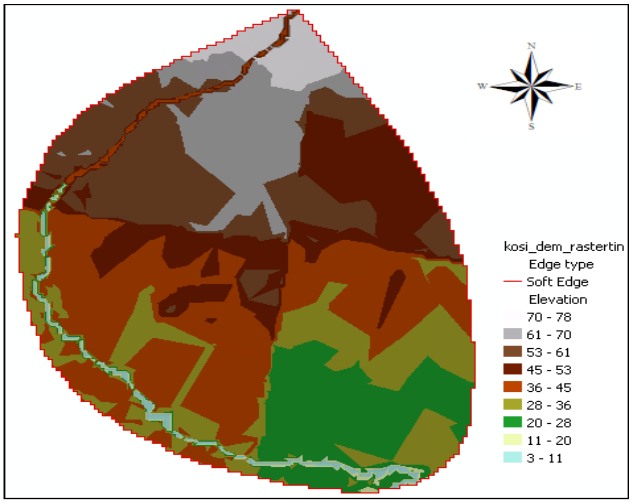

Figure 23: Digital Terrain Model of Kosi Basin

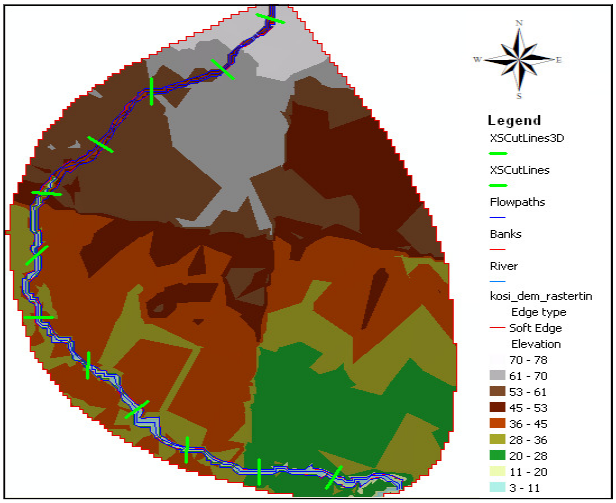

Figure 24: RAS layers created in HEC-GeoRAS

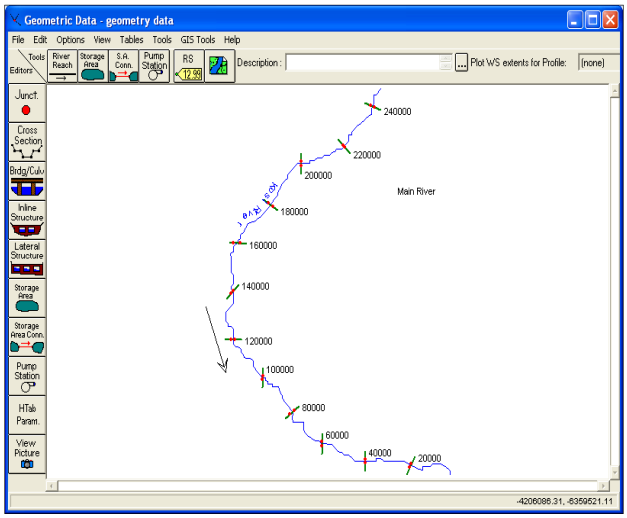

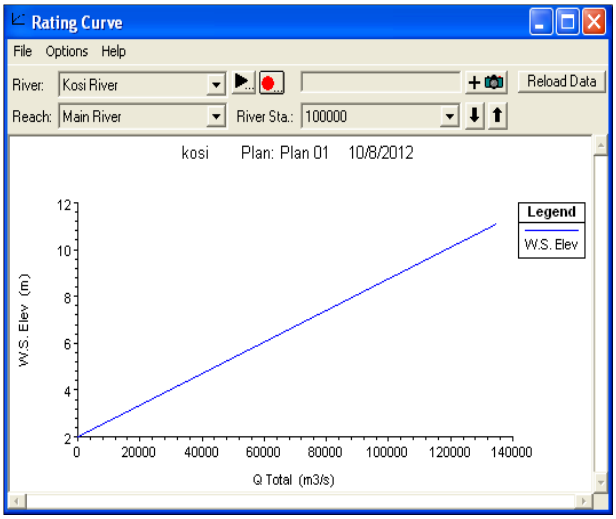

Figure 25: Geometric Data of Kosi River **Figure 26: Rating Curve**

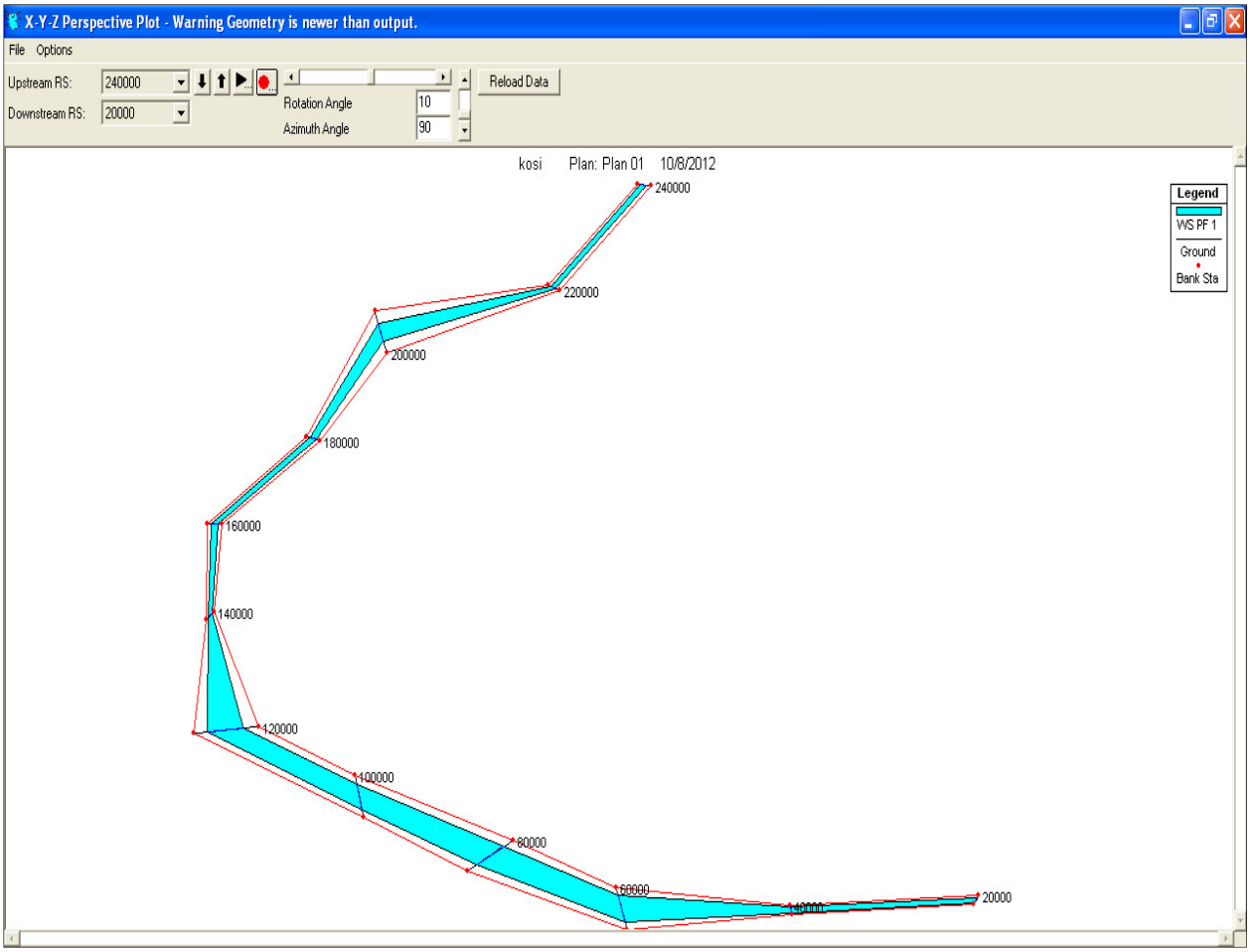

Figure 27: Water Surface Profile of Kosi River in HEC-RAS

Results obtained from the analysis of HEC-RAS were used in HEC-GeoRAS to generate the water surface profile. The water surface profiles were obtained for the river reach showing of 10

km (5 km on each side of the river). Therefore the results obtained are indicating the flood inundation at low lying areas within the river reach of 10 km. Water Surface profile in Kosi River is shown in Figure 27. The results obtained were compared with the flood inundated areas of Kosi river basin (for different periods) as shown in Figure 28. The results showed r^2 values ranging from 0.80 to 0.95 for the inundated areas within the reach. As can be seen from the Figure 28(a-c), the inundated area is more on outside the reach due to various reasons including excess rainfall, seepage, waterlogging, soil moisture, topography, land use etc.

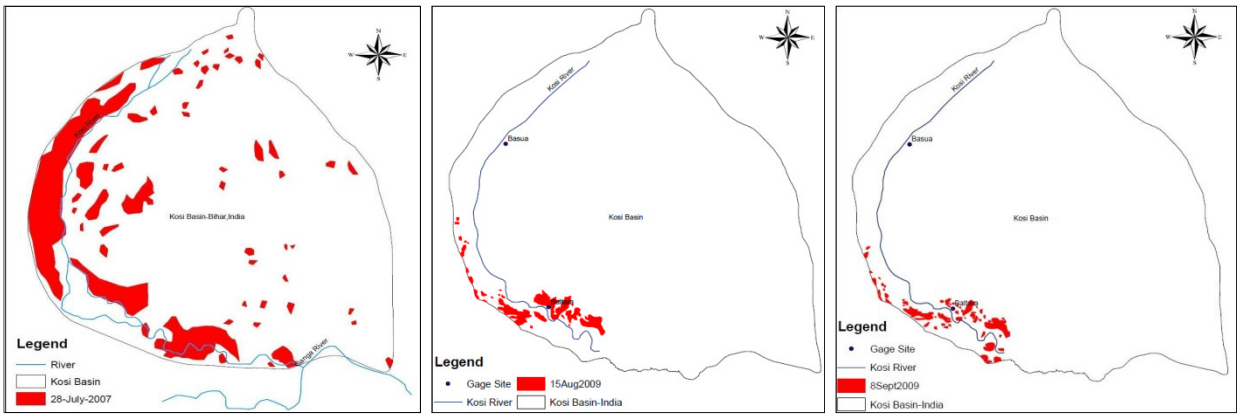

(a) 28-July-2007 **(b) 15-August-2009** **(c) 8-Sept-2009**

Figure 28: Inundation Map Kosi Basin for different periods

5.3.2 Linear and non-linear modeling

It is found essential to develop a linear/non-linear models along with HEC-RAS model to estimate flood inundated areas. Again, various parameters such as, rainfall, discharge, water level, soil moisture, TRMM rainfall and other variables were used as input to develop models for flood inundation mapping. Rainfall and soil moisture data were used for 0.5^0 grids. Different algorithms used in equations (4) to (7), equations (26) and (27), were applied to obtain flood inundated area in Kosi Basin. Linear and non-linear relationship has been developed for the year 2006, 2007 and 2009. There was Kosi breach during the year-2008, so this year has not been considered for analysis. Figure 29 shows the inundation in Kosi Basin for different years.

Rational model and Full cubic model shows best result for all possible combination of water level, discharge, rainfall, soil moisture and inundated area (Figure 30). Table 9 shows the r^2 values for linear and nonlinear modeling of inundation. Discharge of Baltara and soil moisture shows best result (r^2=0.98). Water level and soil moisture also shows similar result (r^2=0.98). The inundated area is directly related to the water level and discharge of Baltara which shows satisfactory results. Discharge and water level of Barahkshetra and Bhimnagar shows very poor relationship with inundated area. Other combination of water level, discharge, rainfall, soil moisture also indicates poor results for Barahkshetra and Bhimnagar stations. Rainfall data shows poor relationship with inundated area. TRMM rainfall data shows the results (r^2= 0.17) and (r^2=0.29) for linear and nonlinear model respectively. Linear modeling for Baltara water level, discharge, soil moisture and rainfall shows good results with inundated area (r^2=0.92). Appendix IV shows the equations for other combinations.

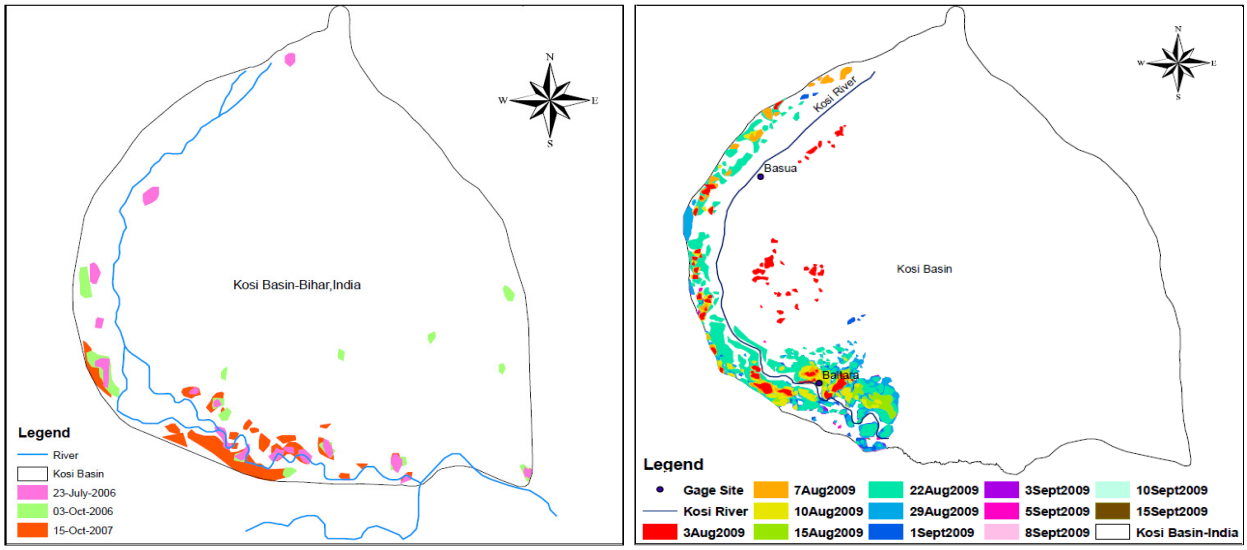

(a) (b)

Figure 29: Inundated Area in the year-2006, 2007 and 2009 (Source:-FMIS)

Once the models were obtained, the map showing flood inundated areas for different period were prepared using DEM map of the lower region prone to floods and are shown in Figure 30. This provides the efficacy of the combination of HEC-GeoRAS and non-linear models.

Table 9: The r^2 values for linear and non-linear modelling

Sl. No.	Relationship between	Linear (r^2)	Non-Linear (r^2)
1.	BK-WL-IA	0.08	0.23
2.	BM-WL-IA	0.02	0.11
3.	BL-WL-IA	0.83	0.92
4.	BK-Q-IA	0.00	0.01
5.	BM-Q-IA	0.02	0.31
6.	BL-Q-IA	0.88	0.93
7.	Arithmetic P-IA	0.08	0.23
8.	Thiessen P-IA	0.01	0.23
9.	TRMM P-IA	0.17	0.29
10.	BK-WL-P-IA	0.09	0.82
11.	BM-WL-P-IA	0.02	0.65
12.	BL-WL-P-IA	0.83	0.93
13.	BK-WL-Q-IA	0.13	0.71
14.	BM-WL-Q-IA	0.02	0.59
15.	BL-WL-Q-IA	0.92	0.99
16.	BK-WL-SM-IA	0.16	0.42
17.	BM-WL-SM-IA	0.02	0.30
18.	BL-WL-SM-IA	0.83	0.99
19.	BK-Q-P-IA	0.01	0.47
20.	BM-Q-P-IA	0.02	0.59
21.	BL-Q-P-IA	0.88	0.93
22.	BK-Q-SM-IA	0.00	0.51
23.	BM-Q-SM-IA	0.03	0.52
24.	BL-Q-SM-IA	0.89	0.99
25.	BK-WL-Q-P-IA	0.20	Not done
26.	BM-WL-Q-P-IA	0.03	Not done
27.	BL-WL-Q-P-IA	0.92	Not done
28.	BK-WL-Q-SM-IA	0.20	Not done
29.	BM-WL-Q-SM-IA	0.03	Not done
30.	BL-WL-Q-SM-IA	0.92	Not done
31.	BK-WL-Q-SM-P-IA	0.26	Not done
32.	BM-WL-Q-SM-P-IA	0.03	Not done
33.	BL-WL-Q-SM-P-IA	0.92	Not done

{where, BK=Barahkshetra, BM=Bhimnagar, BL=Baltara, WL=Water Level, IA=Inundated Area, Q=Discharge, P= Thiessen Mean Rainfall, SM=Soil Moisture}

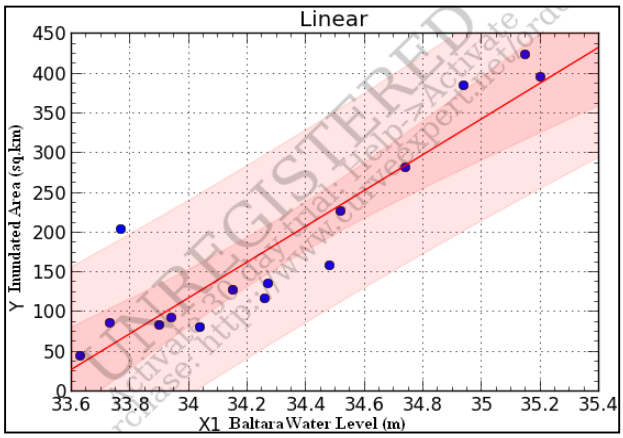

(a) $y = -7.5382 + 2.2519x$, (r^2=0.83)

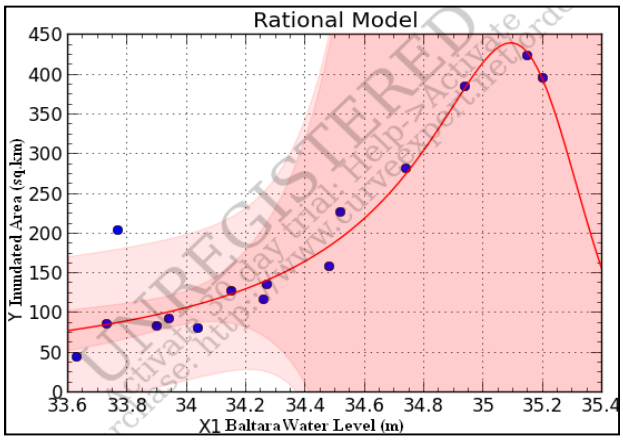

(b) $y = \frac{3.0060+(-8.4404)x}{1+(-5.6796)x+8.0652x^2}$, ($r^2$=0.92)

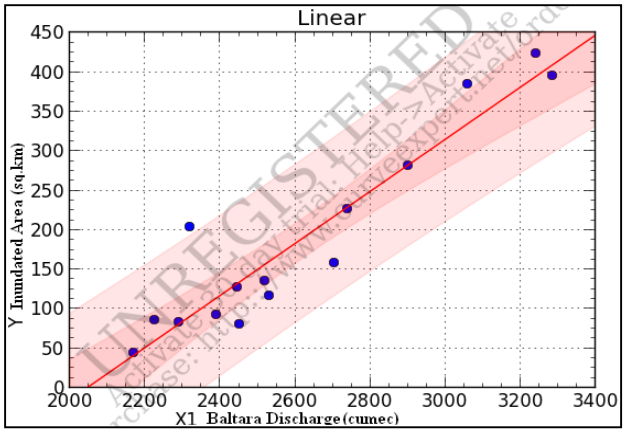

(c) $y = -6.7544 + 3.3032x$, (r^2=0.88)

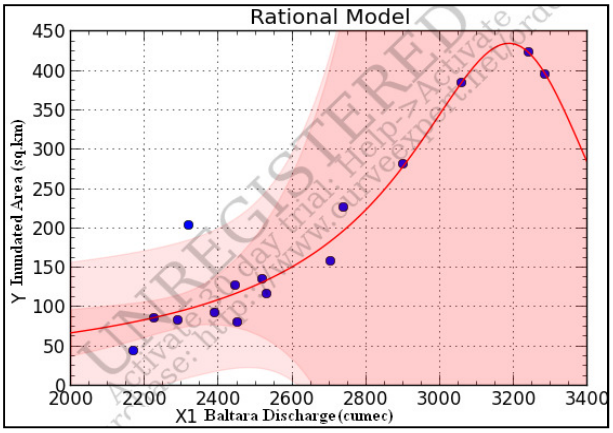

(d) $y = \frac{2.0650+(-5.0590)x}{1+(-6.0958)x+9.3842x^2}$, ($r^2$=0.93)

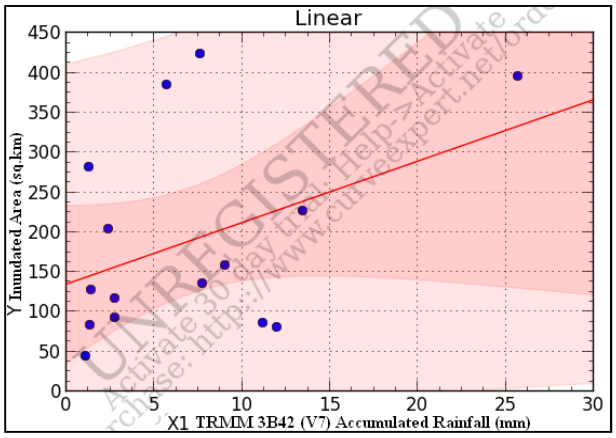

(e) $y = 1.3512 + 7.7139x$, (r^2=0.17)

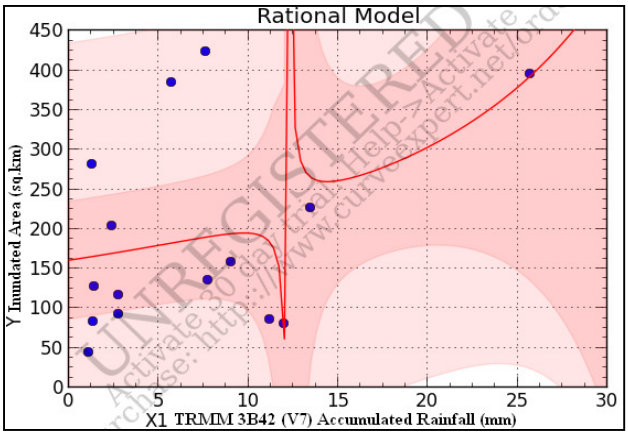

(f) $y = \frac{1.6071+(-1.3323)x}{1+(-1.0436)x+1.8465x^2}$, ($r^2$=0.29)

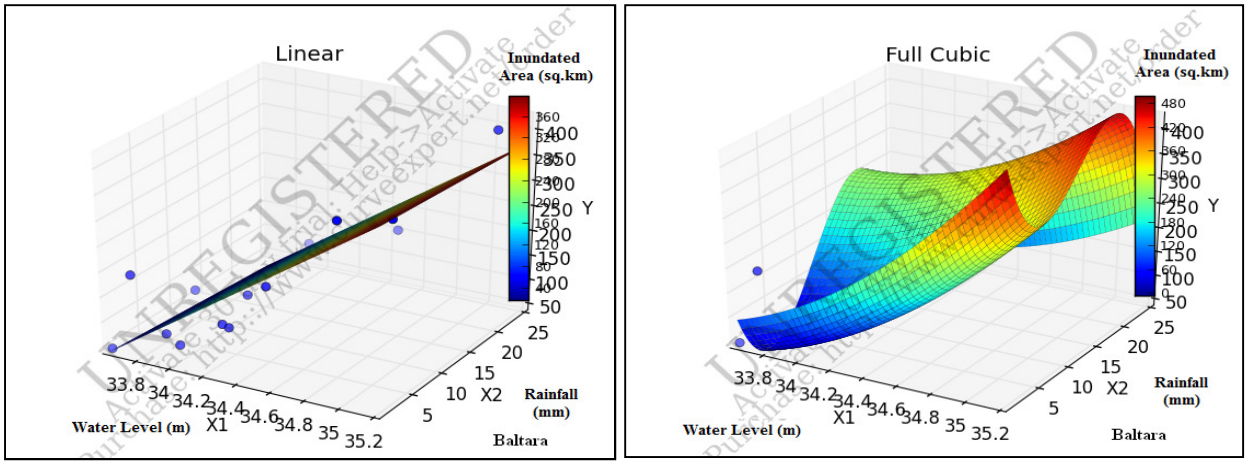

(g) (h)

(g) Linear Equation $y = (-7.6271) + 2.2799x_1 + (-9.6360)x_2$, (r^2=0.83)

(h) Equation for Full Cubic Model

$$y = 2.8585 + (-2.2268)x_1 + (-5.4537)x_2 + 5.6307{x_1}^2 + 8.0898{x_2}^2 + (-4.5669){x_1}^3 + (-1.7721){x_2}^3 + 3.4179x_1x_2 + (-5.7651){x_1}^2x_2 + (-5.1994)x_1{x_2}^2,$$ (r^2=0.93)

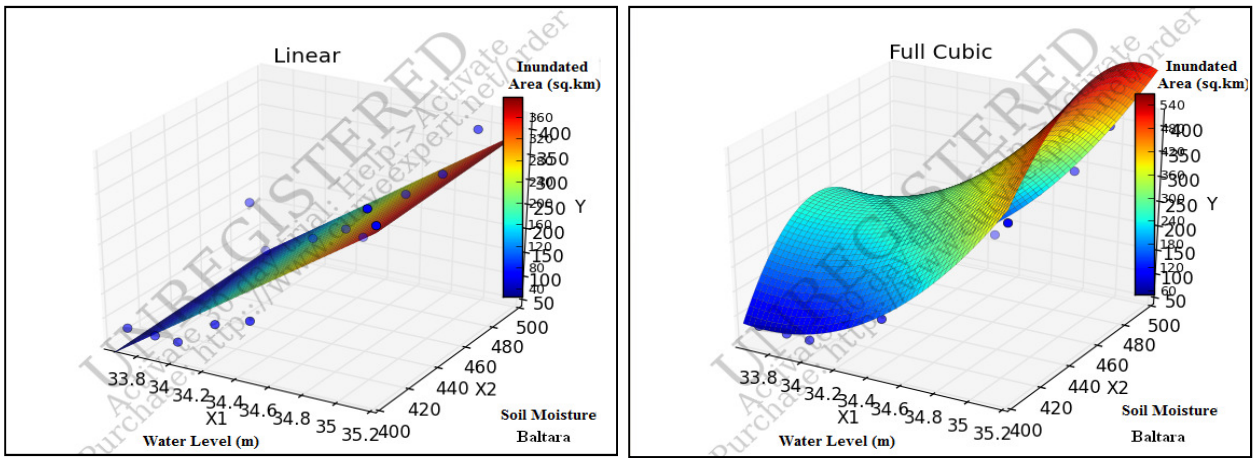

(i) (j)

(i) Linear Equation $y = (-7.6744) + 2.2707x_1 + 1.5898x_2$, (r^2=0.83)

(j) Equation for Full Cubic Model

$$y = 3.6677 + (-6.4507)x_1 + 6.4665x_2 + 1.2344{x_1}^2 + (-8.3938){x_2}^2 + 7.3201{x_1}^3 + (-2.6113){x_2}^3 + (-1.4860)x_1x_2 + (-8.2865){x_1}^2x_2 + 2.3721x_1{x_2}^2,$$ (r^2=0.98)

Figure 30: Linear and nonlinear modeling for inundated area Kosi Basin

CHAPTER~6
CONCLUSION

The following conclusions are drawn from the present work:

1. There is no good cross-correlation obtained between two raingauge stations, which may be due to their topographical location, land use changes and monsoon pattern in the study area.
2. Correlation between discharge data of Barahkshetra-Bhimnagar was found very poor. However, Bhimnagar-Baltara discharge data relationships are better. Relationship between water level and discharge data for Baltara was found very well with r^2=0.99. The relationship for Bhimnagar was also found satisfactory, but for Barahkshetra it was very poor. This may be due to high velocity, huge amount of sediment and high slope as Barahkshetra station is located in mountain.
3. The rainfall-runoff linear-nonlinear relationships are found to be very poor in all the cases and demanded for the use of sophisticated models.
4. No trend was found as rainfall-runoff data were available for only monsoon season (1st July-15th October) for the year 2005 to 2009. However seasonality was observed in observed data.
5. HEC-HMS model using SCS-CN approach showed very good results for all discharge sites. The minimum r^2 value was 0.7864 for the Bhimnagar during the year-2009. This model required extensive input data such as land use/land cover, soil type, curve number, antecedent soil moisture, base flow type, basin area, river network, location of raingauge and discharge sites, rainfall-runoff data etc., which were not made available from one source.
6. To reduce the data requirement for rainfall-runoff modeling, Artificial Neural Network Technique (ANN) algorithms MLP and RBF were used. The ANN models helped in

reducing the parameters and providing better results. MLP network showed better results than RBF network.

7. Both the methods HEC-HMS and ANN may be used for rainfall-runoff simulation depending on the data availability. Both the methods are being widely used in water resources for rainfall-runoff simulation as well.
8. Assessment of flood inundated area using HEC-RAS was successful for the Kosi channel reach. Due to break of continuity equation beyond the river reach, it was difficult to obtain flood inundated area beyond river reach using HEC-GeoRAS model.
9. Integrated model using linear and non-linear relationships in association with HEC-GeoRAS were used and tested for their applicability. Non-linear models developed for flood inundation modelling using rational model and full cubic model showed very promising results.
10. Different input combinations were tried to estimated flood inundated areas and it has been observed that the water level of Baltara alone can be used to represent the flood inundated area of the region. Other combinations of water level, Thiessen mean rainfall, TRMM rainfall, runoff, soil moisture also show fairly good results.
11. The inundated area obtained using integrated approach can be graphically represented in DEM map of the study region and flood risk analysis can be done.

CHAPTER~7
REFERENCES

1. Adeloye A.J. and Montaseri M. Preliminary streamflow data analyses prior to water resources planning study, Hydrological Sciences J., 47(5) (2002): pp. 679-692
2. Adnan N.A., Atkinson P.M. Remote Sensing of River Bathymetry for Use in Hydraulic Model Prediction of Flood Inundation, IEEE 8th International Colloquium on Signal Processing and its Applications, (2012): pp. 159-163
3. Ahlawat R. Space-Time Variation in Rainfall and Runoff: Upper Betwa Catchment, World Academy of Science, Engineering and Technology, 71 (2010): pp. 675-681
4. Ahmad B., Kaleem M.S., Butt M.J., and Dahri Z.H. Hydrological modelling and flood hazard mapping of Nullah lai, Proc. Pakistan Acad. Sci., 47(4) (2010): pp. 215-226
5. Ahmad S., Simonovic S.P. An artificial neural network model for generating hydrograph from hydro-meteorological parameters, J Hydrol (Amst)., 315(1–4) (2005): pp. 236–251
6. Akbari A., Samah A.A., and Othman F. Integration of SRTM and TRMM date into the GIS-based hydrological model for the purpose of flood modelling, Hydrol. Earth Syst. Sci. Discuss., 9 (2012): pp. 4747-4775
7. Andersen M.L., Chen Z.Q., Kavvas M.L., Feldman A. Coupling HEC-HMS with atmospheric models for prediction of watershed runoff, Journal of Hydrologic Engineering, 4 (2002): pp. 312-318
8. Anderson D.J. GIS-based hydrologic and hydraulic modeling for flood delineation at highway river crossings, “Master’s Thesis”, Univ. of Texas at Austin, Austin, Texas, (2000)

9. Antar M.A., Elassiouti I., and Allam M.N. Rainfall-runoff modeling using artificial neural networks technique: a Blue Nile catchment case study, Hydrological Process, 20 (2006): pp. 1201-1216
10. Bates P.D., Horrit M.S., Smith C.N. and Dason D. Integrating remote sensing observations of flood hydrology and hydraulic modeling, Hydrological process, 11 (1997): pp. 1777-1795
11. Becker A., and Grunewald U. Flood risk in Central Europe, Science, 300 (2003): pp. 1099
12. Bessaih N., Mah Y.S., Muhammad S.M., Kuok K.K., and Rosmina A.B. Artificial Neural Networks for Daily Runoff Simulation, Faculty of Engineering, University Malaysia Sarawak, (2003)
13. Bhadra A., Bandyopadhyay A., Singh R., Raghuwanshi N.S. Rainfall-runoff modeling: comparison of two approaches with different data requirements, Water Resources Management, 24 (2010): pp. 37-62
14. Bhatt C.M., Rao G.S., Manjushree P., and Bhanumurthy V. Space Based Disaster Management of 2008 Kosi Floods, North Bihar, India. J. Indian Soc. Remote Sens., 38 (2010): pp. 99-108
15. Blanchard B.J. Investigation of use of space data in watershed hydrology, Final Report, National Aeronautics and Space Administration (NASA), Govt. of USA:113, (1975)
16. Bondelid T.R., McCuen R.H., and Jackson T.J. Sensitivity of SCS models to curve number variation, Water Resources Bull, 18(1) (1982): pp. 111-116
17. Burn D.H. and Hag Elnur M.A.H. Detection of Hydrologic Trends and Variability. Journal of Hydrology, 255 (2002): pp.107-122

18. Chaatterjee C., Kumar R., Kumar S., Jain S.K., Lohani A.K., and Singh R.D. Inter-compression of responses of HEC-1 package and Nash model, Journal of Hydrology, 3 (2001): pp. 13-24

19. Chang T.J., Hsu M.K., and Huang C.J. A GIS distributed watershed model for simulating flooding and inundation, Journal of the American Water Resources Association, 36 (2000): pp. 975-988

20. Chen X., Zhongbo Yu Z., and Cui G. Hydrologic simulation with a distributed hydrologic model. Fourth International Conference on Natural Computation, IEEE, (2008): pp. 539-543

21. Coulibaly P., Anctil F., Bobee B. Daily reservoir inflow forecasting using artificial neural networks with stopped training approach, J Hydrol (Amst)., 230 (2000): pp. 244-257

22. Coulibaly P. and Evora N.D. Comparison of neural network methods for infilling missing daily weather records, Journal of. Hydrology, 341 (2007): pp. 27-41

23. Crawford N.H., and Lindsey R.K. Digital Simulation in Hydrology, Stanford Watershed Model IV, Technical Report 39, Civil Engineering Department, Stanford University, California., (1966)

24. Daniel T.M. Neural networks applications in hydrology and water resources engineering, Proc. Int. Hydrol Water Resources Symp., 3 (1991): pp. 797-802

25. Das S.N., Narula N.K., and Laurin R. Runoff potential indices of watersheds in Tilaiya catchment (Bihar) through use of remote sensing and geographic information system, J. Indian Soc. Remote Sens., 20(4) (1992): pp. 207-221

26. Dastorani M.T., and Wright N.G. Artificial Neural Network Based Real-time River Flow Prediction, School of Civil Engineering, University of Nottingham, Nottingham NG7 2RD, UK., (2001)

27. Dawson C.W., and Wilby R.L. An artificial neural network approach to rainfall-runoff modeling, Hydrol Sci., J 43(1) (1998): pp. 47–66

28. Dawson C.W., Abrahart R.J., Shamseldin A.Y., Wilby R.L. Flood estimation at ungauged sites using artificial neural networks, Journal of Hydrology 319(2006): pp. 391-409

29. De Vos. N.J., Rientjes T.H.M. Constraints of artificial neural networks for rainfall-runoff modeling: trade-offs in hydrological state representation and model evaluation, Hydrol Earth Syst. Sci., 9(1) (2005): pp. 111-126

30. Demuth H., and Beale M. Neural Network Toolbox-For Use With MATLAB, The Math Works, Inc. (2001)

31. Elshorbagy A., Simonovic S.P., and Panu U.S. Performance Evaluation of Artificial Neural Networks for Runoff Prediction, Journal of Hydrologic Engineering, 5(4) (2000): pp. 424-427

32. Flood Management Information System (FMIS), Water Resources Department Government of Bihar, Flood Report (2011)

33. Gajbhiye S., Mishra S.K. Application of NRSC-SCS Curve Number Model in Runoff Estimation Using RS & GIS, IEEE-International conference on advances in engineering, science and management (ICAESM -2012), (2012): pp. 346-352

34. Galkate R., B Sc., and Thomas T. Statistical Analysis of Rainfall in Sagar Division, National Institute of Hydrology Report, CS9 (AR) 5/98-99, (1998-1999)

35. Ganga Flood Control Commission (GFCC), Government of India. Report on Comprehensive Plan of Flood Control for the Kosi Sub-Basin, (1983)

36. Garcia-Bartual R. Short Term River Flood Forecasting with Neural Networks, Universidad Politecnica de Valencia, Spain, (2002): pp. 160-165

37. Gautam M.R., Watanabe K., and Saegusa H. Runoff Analysis in Humid Forest Catchment with Artificial Neural Networks, Journal of Hydrology, 235 (2000): pp.117-136

38. Gee D.M., Anderson M.G., Baird L. 1990. Two-dimensional floodplain modelling, In Hydraulic Engineering, Proceedings of the 1990 National Conference, Hydraulic Division, ASCE: Boston, MA; (1990): pp.773-778

39. Govindaraju R.S. Artificial Neural Networks in Hydrology, Part I: Preliminary Concepts. J. of Hydr. Engrg., 5(2) (2000): pp. 115-123

40. Govindaraju R.S. Artificial Neural Networks in Hydrology, Part II: Hydrologic Applications. J. of Hydr. Engg., 5(2) (2000): pp. 124-135

41. Guero P. Rainfall Analysis and Flood Hydrograph Determination in the Munster Blackwater Catchment, Master Thesis, University College Cork, (2006)

42. Han K.Y., Lee J.T., and Park J.K. Flood inundation analysis resulting from levee break, Journal of Hydraulic Research, 36 (1998): pp. 747-759

43. Harun S., Kassim A.H., and Van T.N. Inflow Estimation with Neural Networks, 10th Congress of The Asia and Pacific Division of the International Association for Hydraulic Research, (1996): pp. 150-155

44. Harun S., Nor N.I., and Kassim A.H.M. Artificial Neural Network Model for Rainfall-Runoff Relationship, Jurnal Teknologi B., 37 (2002): pp. 1-12

45. Hill J.M., Singh V.P., and Aminian H. A computerized data base for flood prediction modeling, Water Resources Bull, 23(1) (1987): pp. 21–27

46. Harmel R.D. and Smith P.K. Consideration of measurement uncertainty in the evaluation of goodness-of-fit in hydrologic and water quality, modeling, J. Hydrol., 337 (2007): pp. 326-336

47. Idris A. MATLAB for Engineering Students, Prentice Hall, Pearson Education Malaysia Sdn. Bhd. (2000)

48. Imrie C.E., Durucan S., and Korre A. River Flow Prediction Using Artificial Neural Networks: Generalization Beyond the Calibration Range, Journal of Hydrology, 233 (2000): pp. 138-153

49. Iwasa Y, Inoue K. Mathematical simulations of channel and overland flood flows in view of flood disaster engineering, Natural Disaster Science 4 (1982): pp. 1-30

50. Jackson T.J., Ragan R.M., and Fitch W.N. Test of Landsat-based urban hydrologic modeling, J. Water Resources Plann. Manag., 103(1) (1977): pp. 141-158

51. Jain A. and Srinivasulu S. Development of effective and efficient rainfall-runoff models using integration of deterministic, real-coded genetic algorithms and artificial neural network techniques, Water Res., 40(4) (2004): W04302. doi:10.1029/2003WR002355

52. Jain M.K, Mishra S.K., Babu P.S., Venugopal K., and Singh V.P. Enhanced runoff curve numbermodel incorporating storm duration and a nonlinear Ia-S relation, J Hydrol Eng., 11(6) (2006): pp. 631–635

53. Jain M.K. and Ramshastri K.S. Application of HEC-1 to Hemavati river (upto Sakleshpur) basin, NIH Report No. CS-55 (1990)

54. Jha R. Flood boundary delineation of Punpun catchment, Bihar using Landsat data, Nat. Symp. on Remote Sensing Application for Resource Management with Special Emphasis on N.E. Region, (1993): pp. 50-57

55. Jha R., Sharma K.D. and Neupane B. Technique for Supporting the Identification and Remediation of Water Scarcity Issues and Global Change Impact on Water Resources in India. International Journal of Hydrologic Environment (IHES), Korea, (5)1 (2009): pp 1-11

56. Jha R. and Smakhtin V.U. A review of methods of hydrological estimation at ungauged sites in India. Working Paper 130, IWMI, (2008): 24p

57. Kale, V.S. Himalayan Catastrophe that Engulfed North Bihar, Journal Geological Society of India, 7 (2008): pp. 713-719.

58. Knebl M.R., Yang Z.L., Hutchison K., and Maidment D.R. Regional scale flood modeling using NEXRAD rainfall, GIS, and HEC-HMS/RAS: A case study for the San Antonio River Basin summer 2002 storm event, J. Environ.Manage.,75(4) (2005): pp. 325-336

59. Kottegoda N.T., Natale L., and Raiteri E. Statistical modeling of daily streamflows using rainfall input and curve number technique, J Hydrol (Amst)., 234(3–4) (2000): pp. 170-186

60. Kumar A.R.S., Sudheer K.P., Jain S.K., and Agarwal P.K. Rainfall-runoff modelling using artificial neural networks: comparison of network types, Hydrological Process, 19 (2005): pp. 1277-1291

61. Kumar D.N., Raju K.S., and Sathish T. River flow forecasting using recurrent neural networks. Water Res. Manag., 18 (2004): pp. 143-161

62. Leahy P., Kiely G., and Corcoran G. Minimal input artificial neural networks for flood forecasting, Water Management Journal, in review, (2006)

63. Legates D.R. and McCabe Jr., G.J. Evaluating the use of "goodness-of-fit" measures in hydrologic and hydroclimatic model validation, Water Res. 35(1) (1999): pp. 233–241

64. Mishra S., Singh V. Behaviour of SCS method in Ia C- Ia-λ spectrum, (1999): pp.112

65. Mishra S.K., Pandey R.P., Jain M.K., and Singh V.P. A rain duration and modified AMC dependent SCS-CN procedure for long duration rainfall-runoff events, Water Resources Management, Springer Science, 22 (2007): 861–876

66. Muzik I. Applications of GIS to SCS procedure for design flood hydrographs, In: Proc., mod. agric., forest and rangeland hydrol., Am. Soc. Agric. Engrs. (ASAE), St. Joseph, Mich., USA, (1988): pp. 494–500

67. Nash, J.E. The Form of the Instantaneous Unit Hydrograph, IAHS Publ. No. 45 (1958): pp. 114-121

68. O'Connor K.M. Applied Hydrology Deterministic. Unpublished Lecture Notes, Department of Engineering Hydrology, National University of Ireland, Galway, (1997)

69. Patil J.P., Sarangi A., Singh A., Ahmad A.K. Evaluation of modified CN methods for watershed runoff estimation using a GIS-based interface, Published by Elsevier Ltd., (2008): pp. 137-146

70. Patro S., Chatterjee C., Mohanty S., Singh R., Raghuwanshi N.S. Flood Inundation Modeling using MIKE FLOOD and Remote Sensing Data, J. Indian Soc. Remote Sens., 37 (2009): pp. 107-118

71. Priessmann A. Use of mathematical models, Unsteady flow in open channels, BHRA., (1976): pp. E3.23-E3.28

72. Ragan R.M., and Jackson T.J. Runoff synthesis using Landsat and SCS model, J. Hydraul Div., 106(HY5) (1980): pp. 667–678

73. Rajurkar M.P., Kothyari U.C., and Chaube U.C. Artificial neural networks for daily rainfall-runoff modelling, Hydrological Sciences-Journal-des Sciences Hydrologiques, 47(6) (2002): pp. 865-877

74. Rajurkar M.P., Kothyari U.C., and Chaube U.C. Modeling of the daily rainfall-runoff relationship with artificial neural network, J Hydrol (Amst)., 285 (2004): pp. 96-113

75. Ramamurthy K.V., Sonam M.K. and Muley S.S. Long term variation in the rainfall over upper Narmada Catchment, Mausam., 38 No. 3 (1987): pp. 313-318

76. Ramasastri K.S. and Nirupama P. Statistical analysis of rainfall in Belgaum District, Karnatka, NIH, Technical Reprot, TR-4, (1987)

77. Ranaee E., Mahmoodian M., and Quchani S.R. The Combination of HEC-Geo-HMS, HEC-HMS and MIKE11 Software Utilize in a Two Branches River Flood Routing Modeling, Second International Conference on Environmental and Computer Science, IEEE. (2009): pp. 317-321

78. Reddy D.V., Kumar D., Saha D. and Mandal M.K. The 18 August 2008 Kosi river breach: an evaluation, Current Science., VOL. 95, NO. 12 (2008): pp. 1668-1669

79. Robayo O., Whiteaker T., and Maidment D. Converting a NEXRAD map to a floodplain map, Proc., AWRA GIS and Water Resources III Conf., Nashville, Tenn., (2004)

80. Roy L.B., Kumar S., Kumar J.P. Flood forecasting system in Kosi Basin, Proceeding Recent Advances in Civil Engineering, ITBHU. ISBN 978-81-921121-0-7, (2011): pp. 164-169

81. Sahoo G.B., Ray C., DeCarlo E.H. Use of neural network to predict flash flood and attendant water qualities of a mountainous stream Oahu, Hawaii, Journal of Hydrology, 327 (2006): pp. 525-538

82. Samarasinghe S.M.J.S., Nandalal H.K., Weliwitiya D.P., Fowzed J.S.M., Hazarikad M.K., and Samarakoond L. Application of Remote Sensing and GIS for flood risk analysis: a case study at Kalu- Ganga River, Sri Lanka, International Archives of the Photogrammetry, Remote Sensing and Spatial Information Science, Kyoto Japan, 38(8) (2010): pp. 110-115

83. Samules P.G. Modeling of river and floodplain flow using the finite element method. Hydraulic Research, Technical Report No. SR61: Wallingford, U.K., (1985)

84. Sanaga S. and Jain A.A Comparative Analysis of Training Methods for Artificial Neural Network Rainfall-Runoff Models. Applied Soft Computing, 6(3) (2006): pp. 295-306

85. SCS (1972) National engineering handbook, sec. 4: hydrology, soil conservation service (SCS), USDA, Washington, D.C.

86. SCS (1985) National engineering handbook, sec. 4: hydrology, soil conservation service (SCS), USDA, Washington, D.C.

87. Shahin M., van Oorschot H.J.L., and de Lange S.J., Statistical Analysis in Water Resources Engineering, Balkema Publishers, Rotterdam, Netherlands, (1993)

88. Shaohong S., Chen Pengxiao C. A real-time flood monitoring system based on GIS and hydrological model, 2nd Conference on Environmental Science and Information Application Technology, IEEE (2010): pp. 605-608

89. Sherman L.K., Stream flow from rainfall by the unit-graph method, Engineering News, Rec., 108 (1932): pp. 501-505

90. Singh V.P. and Birsoy Y.K. A Statistical analysis of rainfall-runoff relationship, Partial Technical Completion report, Project No. 3109-206, WRRI Report No. 81 (1976): pp. 1-47

91. Slack R.B., Welch R. SCS runoff curve number estimates from Landsat data, Water Resources Bull, 16(5) (1980): pp. 887-893

92. Smith J. and Eli R.N. Neural Network models of rainfall-runoff process, Journal of Water Resources Planning Management, ASCE, 121(6) (1995): pp. 499-508

93. Solaimani K. Rainfall-runoff Prediction Based on Artificial Neural Network (A Case Study: Jarahi Watershed), American-Eurasian J. Agric. & Environ. Sci., 5 (6) (2009): pp. 856-865

94. Stuebe M.M., Johnston D.M. Runoff volume estimation using GIS technique, Water Resources Bull, 26(4) (1990): pp. 611-620

95. Subramanya K. Engineering Hydrology, New Delhi, Tata McGraw-Hill Publishing Company Ltd., (2008)

96. Tayfur G., Singh V.P. ANN and fuzzy logic models for simulating event-based rainfall-runoff, J. Hydrol Eng., 132(12) (2006): pp. 1321-1330

97. Tiwari K.N., Kannan N., Singh R., Ghosh S.K. Watershed parameter extraction using GIS and remote sensing for hydrologic modeling, Asian Pac Remote Sens. GIS J., 10(1) (1997): pp. 43-52

98. Tiwari K.N., Kumar P., Sebastian M., Pal D.K. Hydrologic modeling for runoff determination: remote sensing techniques, International Journal of Water Resources Dev, 7(3) (1991): pp.178-184

99. Todini E. Rainfall Runoff Modeling-Past, Present and Future. Journal of Hydrology, 100 (1988): pp. 341-352

100. Tokar S.A., Johnson P.A. Rainfall-runoff modeling using artificial neural networks, J. Hydrol. Eng., 4 (1999): pp. 232-239

101. Tokar A.S. and Markus M. Precipitation-runoff using artificial neural networks and conceptual models, J. Hydrol. Eng., 5 (2000): pp. 156-161

102. U.S. Army Corps of Engineers (USACE). HEC-HMS, User's Manual Version 3.5, 2010. Hydrologic Engineering Centre, Davis, CA, USA.

103. U.S. Army Corps of Engineers (USACE), HEC-GeoHMS, User's manual Version 4.2, 2009. Hydrologic Engineering Centre, Davis, CA, USA.

104. U.S. Army Corps of Engineers (USACE). HEC-RAS, User's Manual Version 4.1, 2010. Hydrologic Engineering Centre, Davis, CA, USA.

105. U.S. Army Corps of Engineers (USACE), HEC-GeoRAS, User's manual Version 4.3.93, 2011. Hydrologic Engineering Centre, Davis, CA, USA.

106. White D. Grid-based application of runoff curve number, J. Water Resources Plann. Manag., 114(6) (1988): pp. 601-612

107. Wright N.G., Villanueva I., Bates P.D., Mason D.C., Wilson M.D., Pender G., and Neelz S. Case study of the use of remotely sensed data for modelling flood inundation on the river Severn, U.K., Journal of Hydraulic Engineering ASCE, (2008): pp. 533-540

108. Zhan X., Huang M. ArcCN-Runoff: An ArcGIS tool for generating curve number and runoff maps, Environ Model Softw 19(10) (2004): pp. 875-879. doi:10.1016/j.envsoft.2004.03.001

109. Zheng N., Tachikawa Y., Takara K. A distributed flood inundation model integrating with rainfall-runoff processes using GIS and Remote Sensing data. The International Archives of the Photogrammetry, Remote Sensing and Spatial Information Sciences. Beijing Vol. XXXVII. Part B4. (2008): pp. 1513-1518

110. Zhu M., Fujita M., Hashimoto N. Application of neural networks to runoff prediction, In: Hipel KW (ed) Stochastic and statistical method in hydrology and environmental engineering, Kluwer, New York, vol. 3 (1994): pp. 205-216

111. Zhang B., and Govindaraju R.S. Geomorphology-based artificial neural networks for estimation of direct runoff over watersheds, J. Hydrol., 273 (2003): pp. 18-34

Web links

- http://www.cwc.nic.in
- http://fmis.bih.nic.in
- http://www.nrsc.gov.in/
- http://wrd.bih.nic.in/
- http://www.imd.gov.in
- http://srtm.csi.cgiar.org/
- https://earth.esa.int
- http://zulu.ssc.nasa.gov/
- http://hydrology.gov.np/
- http://trmm.gsfc.nasa.gov/

Accepted Publications

1. Meena R.S., Jha R., and Khatua K.K. Precipitation-runoff simulation for a Himalayan river basin, India using artificial neural network algorithms. (Accepted for International Journal of Sciences in Cold and Arid Regions (SCAR), 2013)
2. Meena R.S., Jha R., and Khatua K.K. Predication of un-gauged basins (PUB). International Association of Hydrological Sciences (IAHS), (Accepted for International Symposium, Delft University of Technology (TU Delft), The Netherlands, 23-25 October 2012)
3. Meena R.S., Jha R., and Khatua K.K. Rainfall-runoff modelling in Himalayan Kosi Basin, India. (Published in HYDRO-2012, IIT Bombay)
4. Meena R.S., Jha R., and Khatua K.K. Flood inundated area assessment in Kosi Basin using linear/non-linear regression models. (Accepted for International Workshop WATGLOBS, Beijing, China, EU-FP7 CEOP-AEGIS Project, European Commission, April 2013)

APPENDIX-I

Basic Statics Summary of Rainfall-Runoff Data

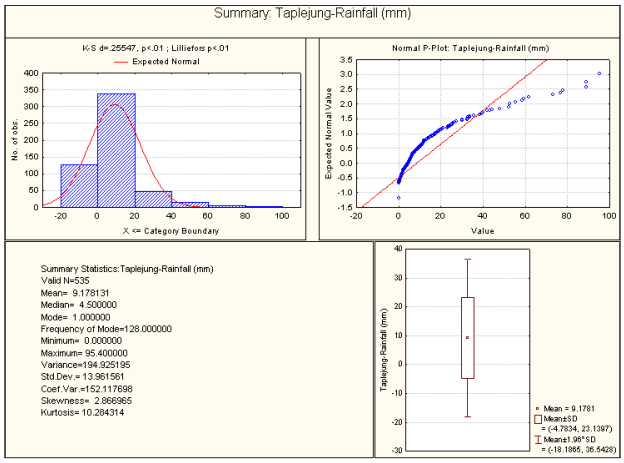

(a) Taplejung Rainfall

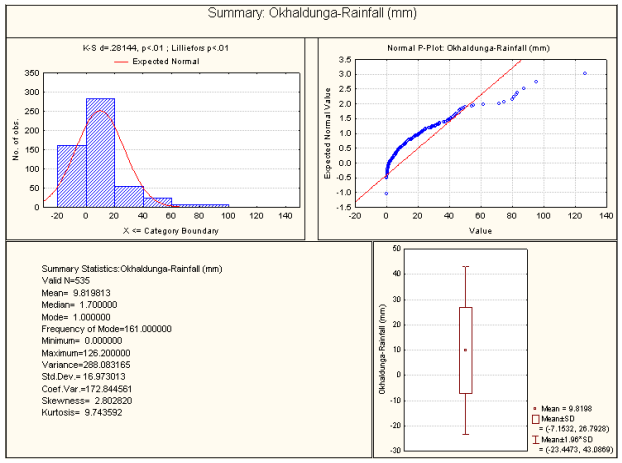

(b) Okhaldunga Rainfall

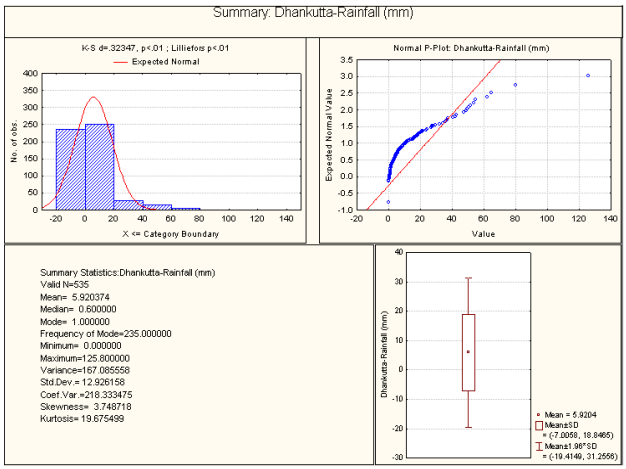

(c) Dhankutta Rainfall

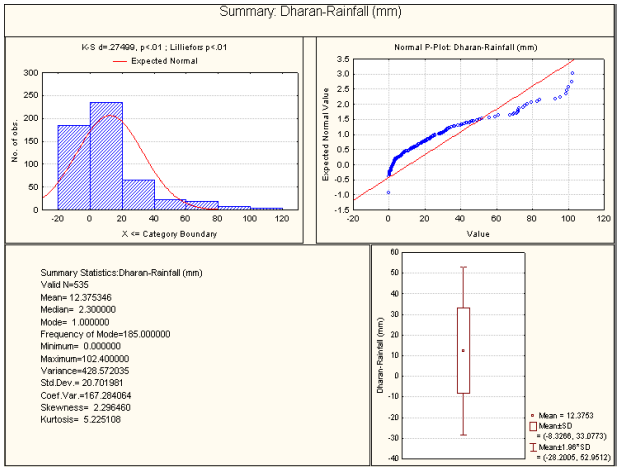

(d) Dharan Rainfall

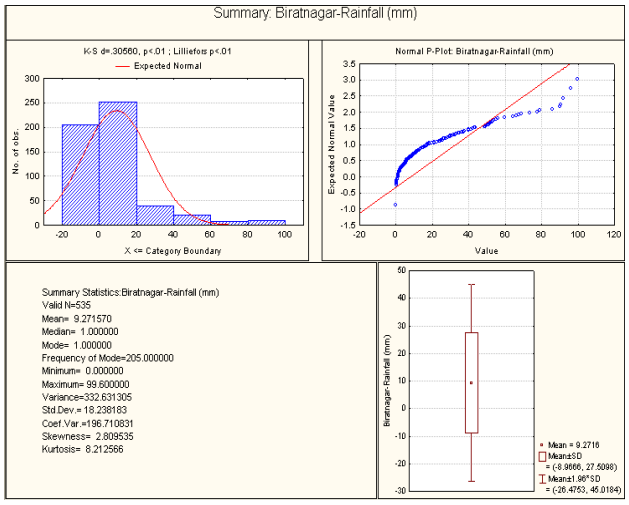

(e) Biratnagar Rainfall

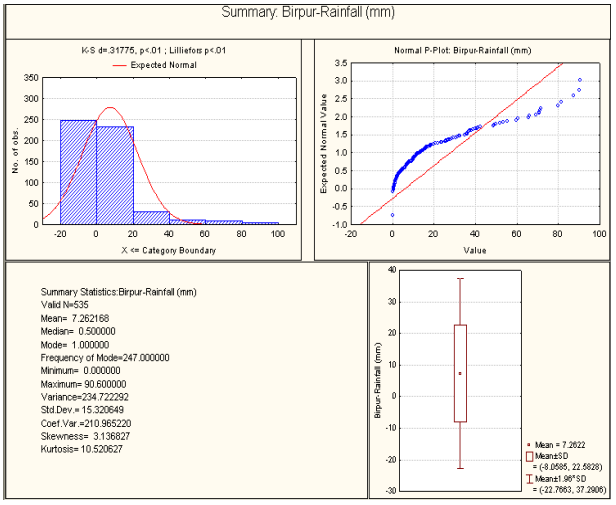

(f) Birpur Rainfall

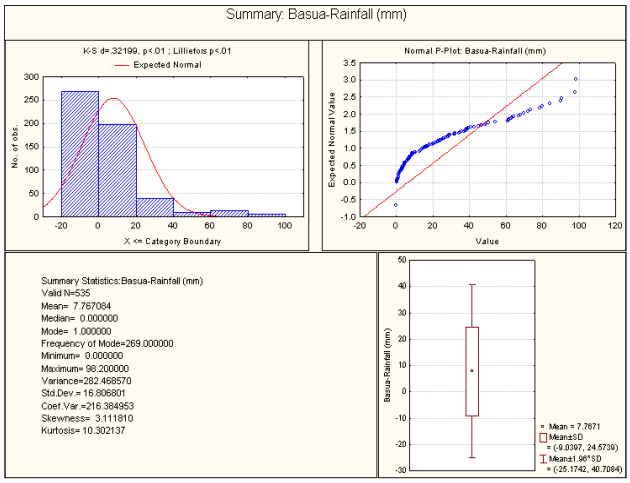

(g) Basua Rainfall

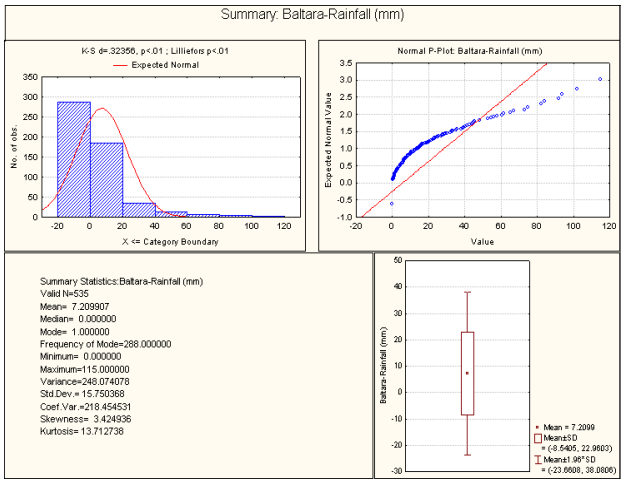

(h) Baltara Rainfall

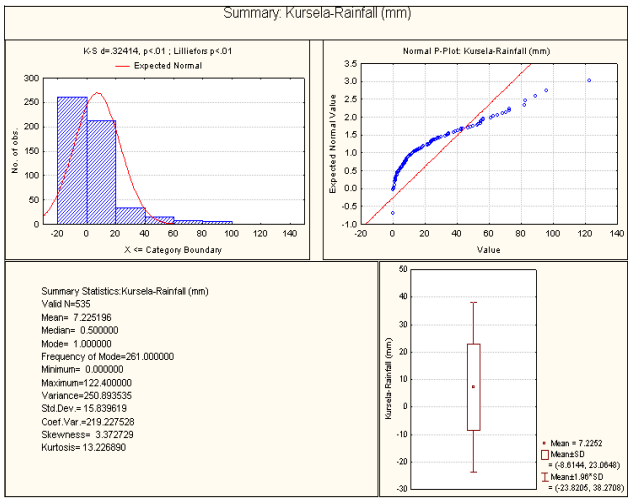

(i) Kursela Rainfall

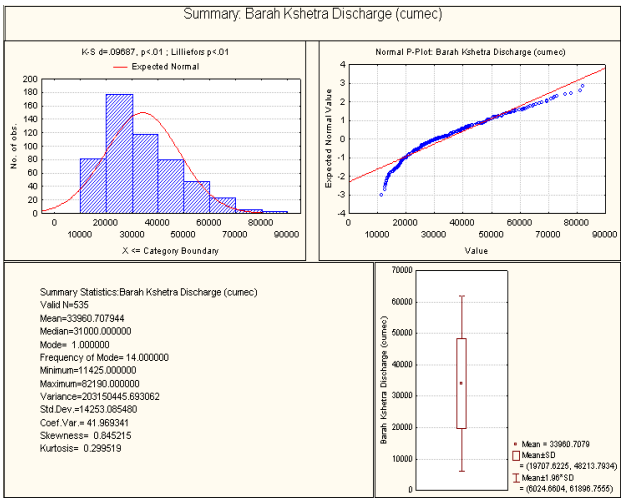

(j) Barahkshetra Discharge

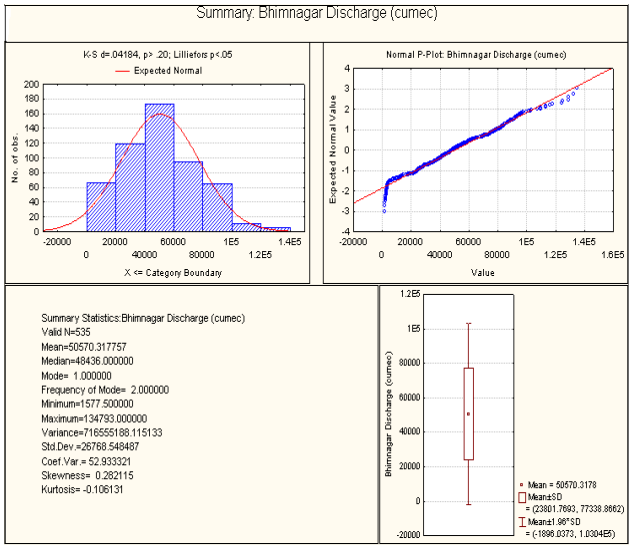

(k) Bhimnagar Discharge

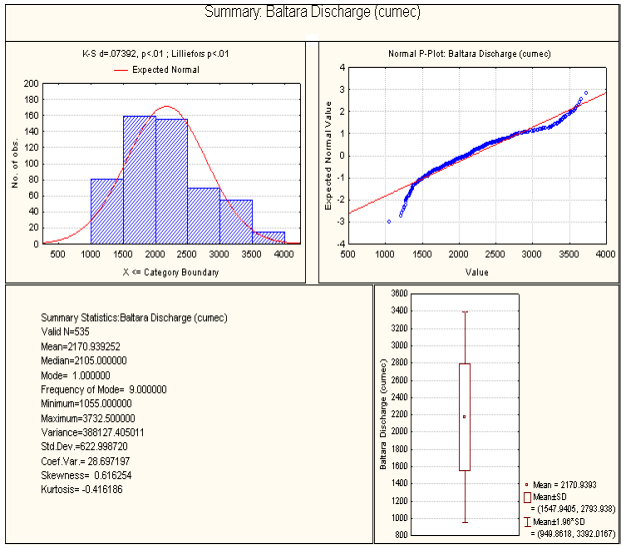

(l) Baltara Discharge

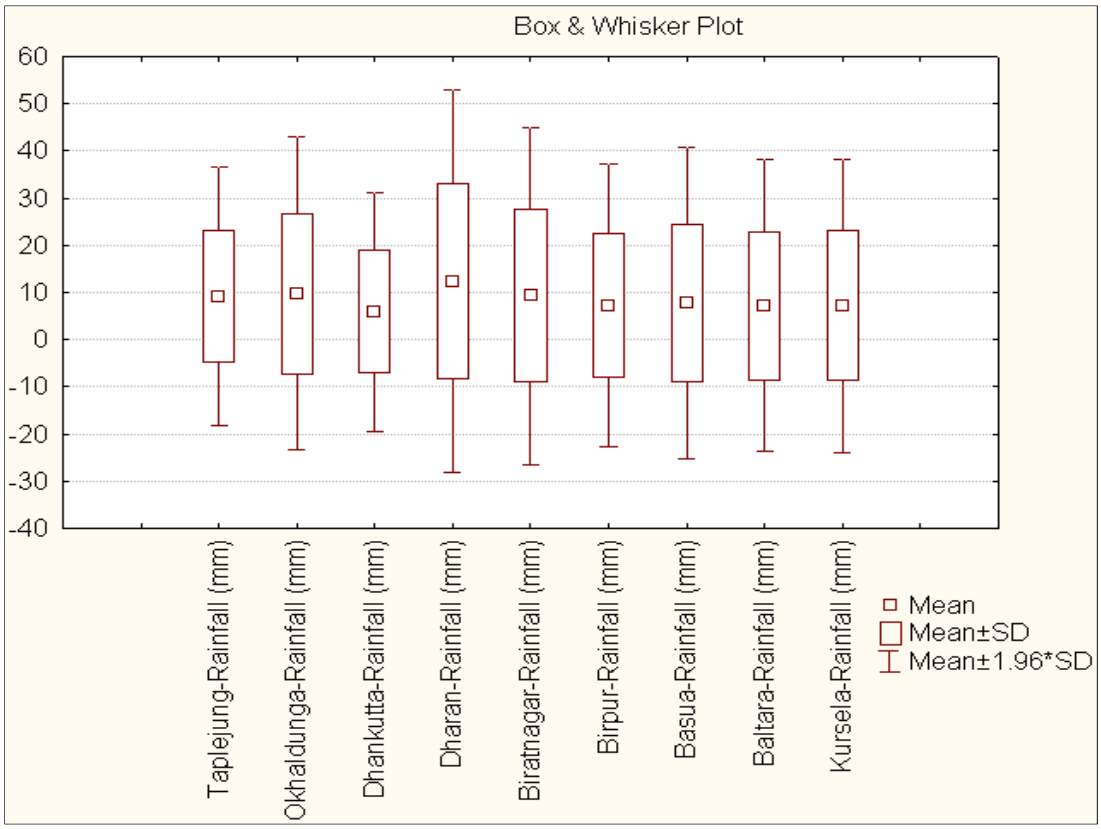

(m) Box & Whisker Plot for Rainfall Data

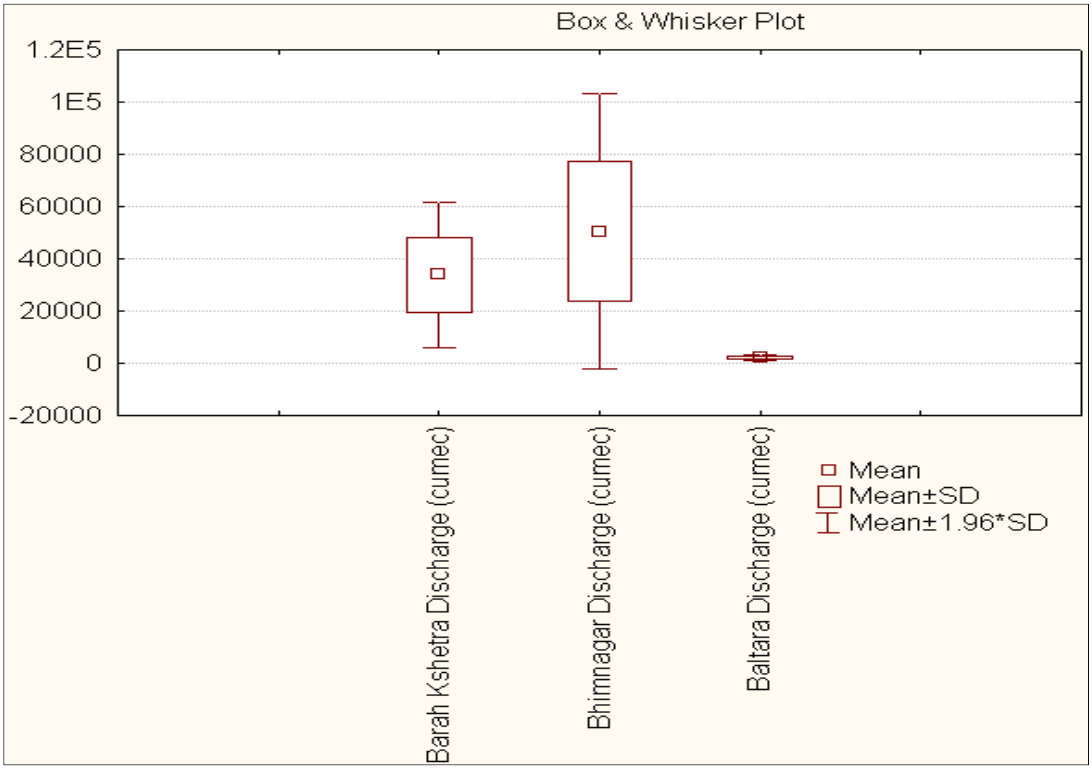

(n) Box & Whisker Plot for Discharge Data

APPENDIX-II

Rainfall-Runoff Relationship linear and nonlinear

(a) Rainfall Vs Runoff

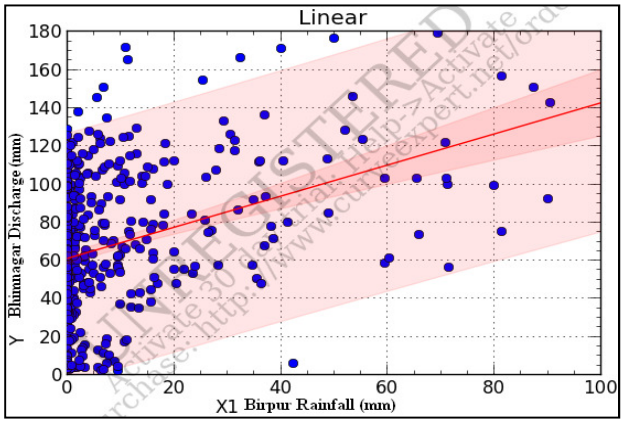

$y = 6.1292 + 8.1611x$, (r^2 =0.12)

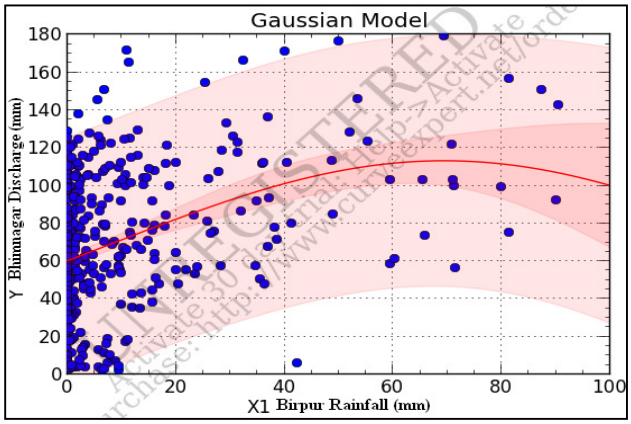

$y = 1.1324e^{\frac{-(x-6.9379)^2}{2*6.1807^2}}$, ($r^2$ =0.13)

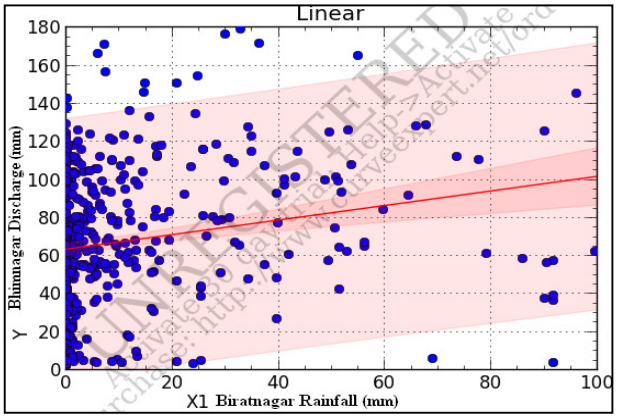

$y = 6.3672 + 3.8255x$, (r^2 =0.04)

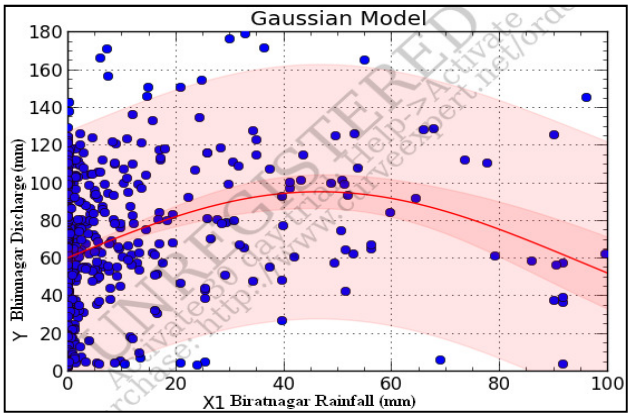

$y = 9.5546e^{\frac{-(x-4.6477)^2}{2*4.8711^2}}$, ($r^2$ =0.09)

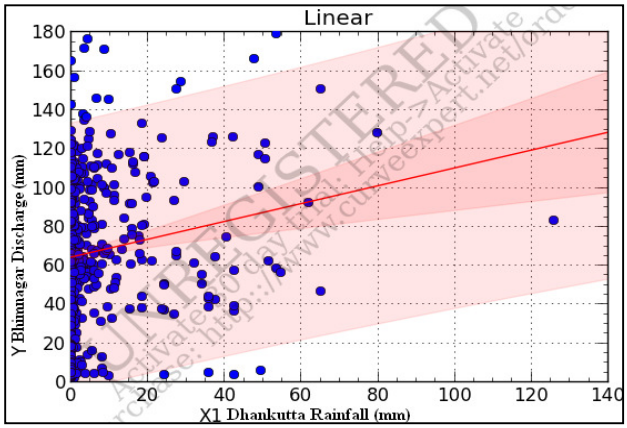

$y = 6.4503 + 4.5873x$, (r^2 =0.02)

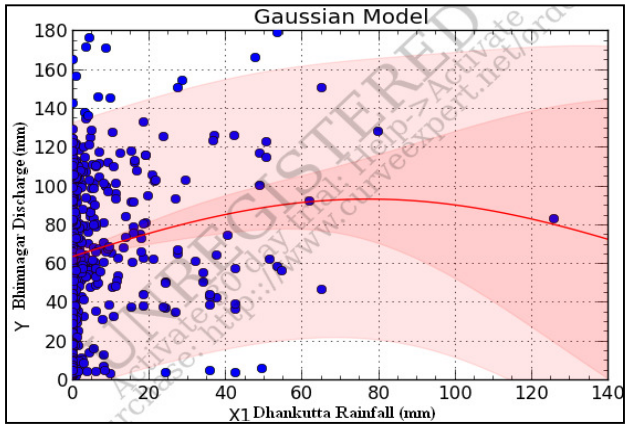

$y = 9.3521e^{\frac{-(x-7.7139)^2}{2*8.8598^2}}$, ($r^2$ =0.03)

(b) Arithmetic mean Rainfall Vs Runoff

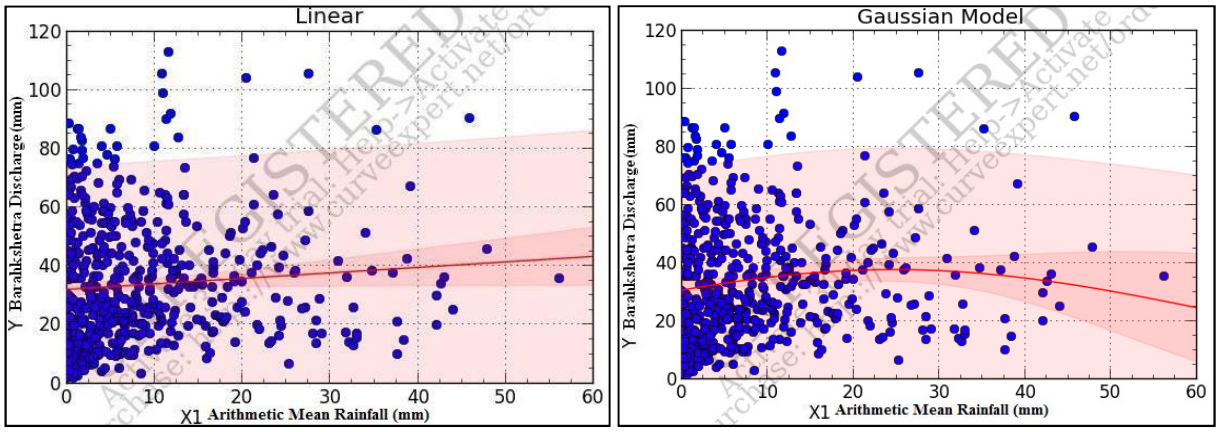

$y = 3.2051 + 1.8771x$, (r^2=0.007) $y = 3.7849e^{\frac{-(x-2.4633)^2}{2*3.8321^2}}$, ($r^2$=0.012)

(i) Barahkshetra

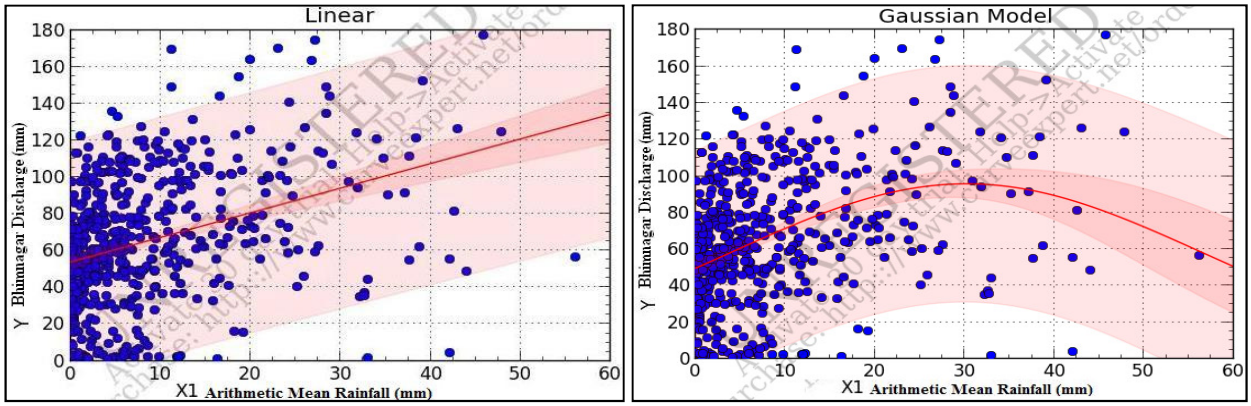

$y = 5.3812 + 1.3397x$, (r^2=0.13) $y = 9.5802e^{\frac{-(x-3.0199)^2}{2*2.6336^2}}$, ($r^2$=0.16)

(ii) Bhimnagar

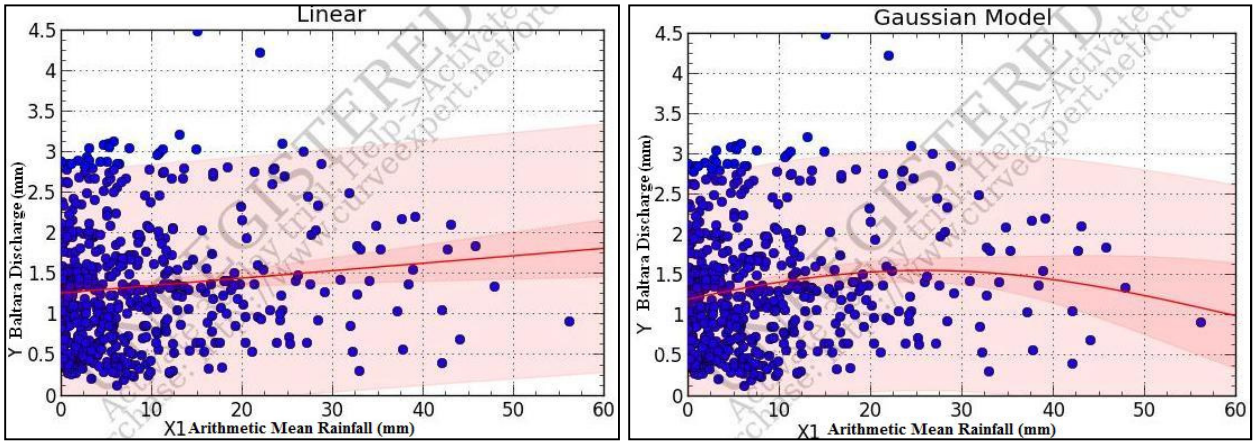

$y = 1.2662 + 9.1720x$, (r^2=0.013) $y = 1.5605e^{\frac{-(x-2.5884)^2}{2*3.5924^2}}$, ($r^2$=0.02)

(iii) Baltara

APPENDIX-III

Relationship between observed vs computed discharge for all the data sets (HEC-HMS)

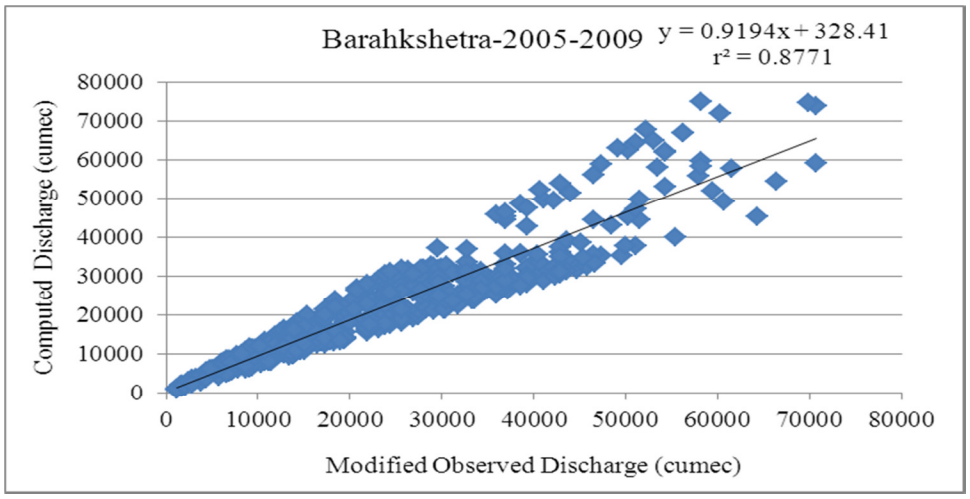

(a)

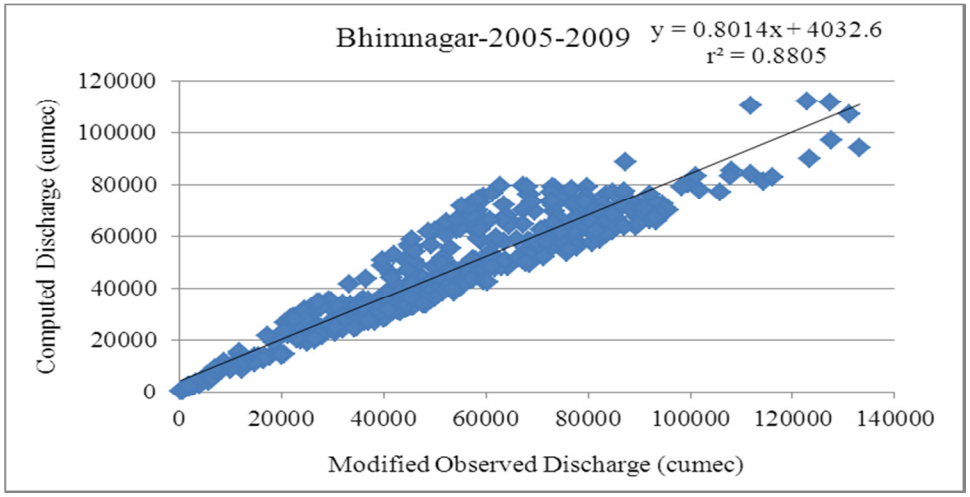

(b)

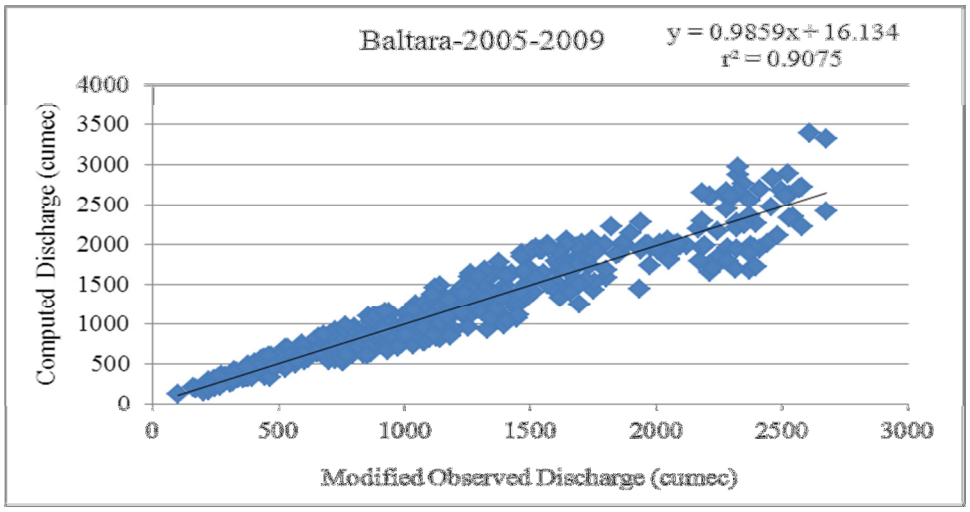

(c)

APPENDIX-IV

Equations for Linear/nonlinear inundation modeling

I. Baltara Discharge-Water Level-Inundated Area

(a) Linear

$y = 1.0808 + (-3.7500)x_1 + 8.5917x_2,$ (r^2=0.92)

(b) Equation for Full Cubic Model

$y = 3.7452 + (-1.8574)x_1 + (-1.7320)x_2 + 5.6276{x_1}^2 + (2.0015){x_2}^2 + 6.5832{x_1}^3 + (-5.2010){x_2}^3 +$

$1.3231x_1x_2 + (-2.4786){x_1}^2x_2 + 7.0424x_1{x_2}^2,$ (r^2=0.98)

II. Baltara Discharge-Rainfall-IA

(a) Linear

$y = (-6.7623) + (6.1014)x_1 + 3.3234x_2,$ (r^2=0.88)

(b) Equation for Full Cubic Model

$y = 6.1317 + 2.1194x_1 + (-1.0618)x_2 + 5.4831{x_1}^2 + 4.9588{x_2}^2 + (-1.6235){x_1}^3 + (-5.5921){x_2}^3 +$

$(-3.9481)x_1x_2 + 1.0484{x_1}^2x_2 + 5.0951)x_1{x_2}^2,$ (r^2=0.93)

III. Baltara-Discharge-SM-IA

(a) Linear

$y = (7.6421) + 1.7853x_1 + 3.3342x_2,$ (r^2=0.88)

(b) Equation for Full Cubic Model

$y = 1.6035 + 5.4930x_1 + (-1.1272)x_2 + (-2.4735){x_1}^2 + 1.7367{x_2}^2 + 2.7489{x_1}^3 + (-1.4980){x_2}^3 +$
$5.0702x_1x_2 + (-5.6330){x_1}^2x_2 + (-6.4818)x_1{x_2}^2,$ (r^2=0.98)